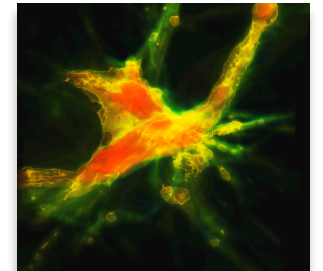
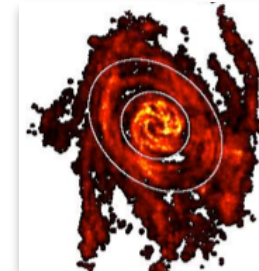
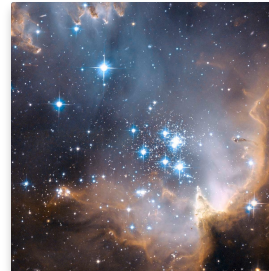
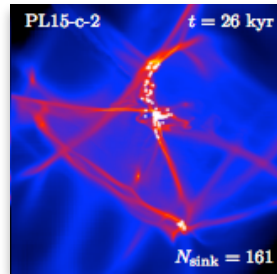
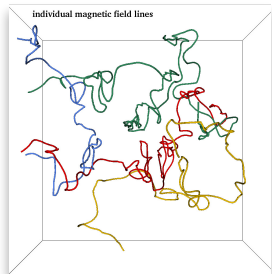


# ISM Dynamics and Star Formation



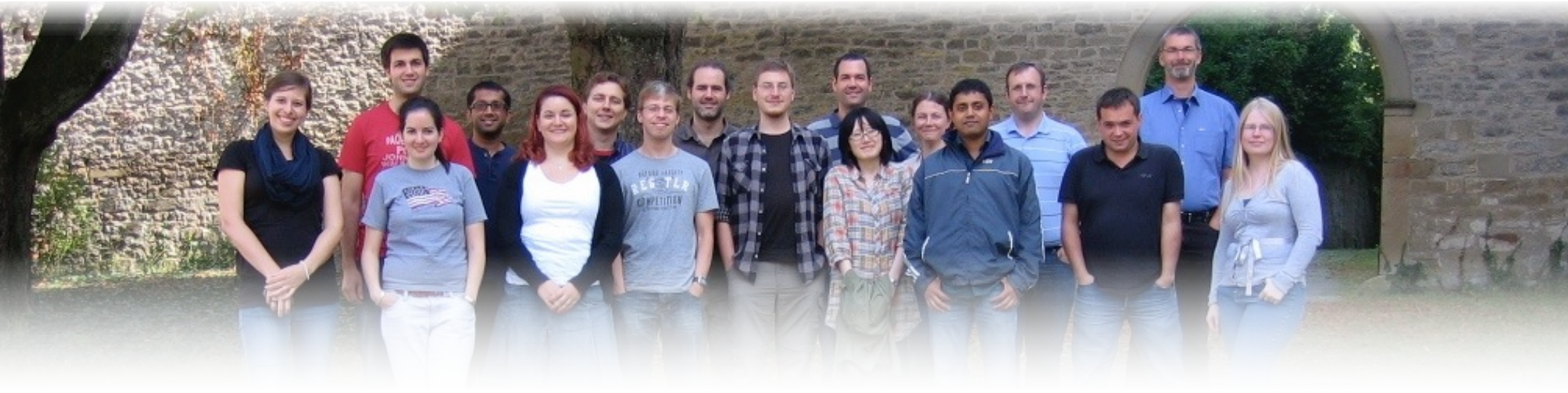
**Ralf Klessen**



Zentrum für Astronomie der Universität Heidelberg  
Institut für Theoretische Astrophysik



# thanks to ...



... people in the star formation group at Heidelberg University:

Christian Baczynski, Erik Bertram, Frank Bigiel, Andre Bubel, Diane Cormier, Volker Gaibler, Simon Glover, Dimitriou Gouliermis, Tilman Hartwig, Juan Ibanez, Christoph Klein, Lukas Konstandin, Mei Sasaki, Jennifer Schober, Rahul Shetty, Rowan Smith, László Szűcs

... former group members:

Robi Banerjee, Ingo Berentzen, Paul Clark, Christoph Federrath, Philipp Girichidis, Thomas Greif, Milica Micic, Thomas Peters, Dominik Schleicher, Stefan Schmeja, Sharanya Sur, ...

... many collaborators abroad!



Deutsche  
Forschungsgemeinschaft  
**DFG**



**BADEN-  
WÜRTTEMBERG**  
STIFTUNG  
Wir stiften Zukunft



European  
Research  
Council

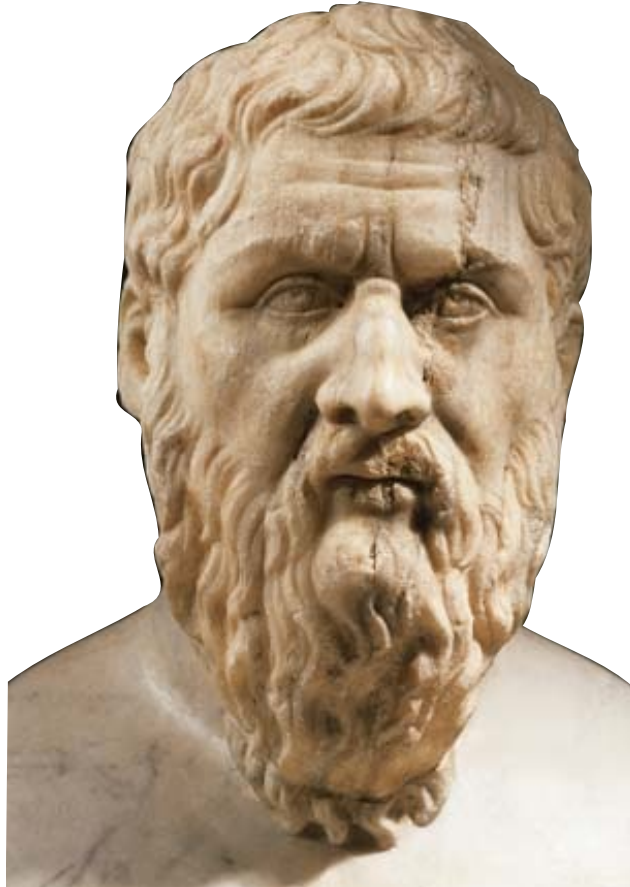


# agenda

- introductory remarks
  - relation between measurement and underlying physics
- applications / controversies / puzzles
  - global star formation relations  
*are we sure we see universal dependencies?*
  - molecular gas  
*are we sure we see all  $H_2$  gas?*
  - filaments  
*are they real (ly everywhere)?*



Prolegomena

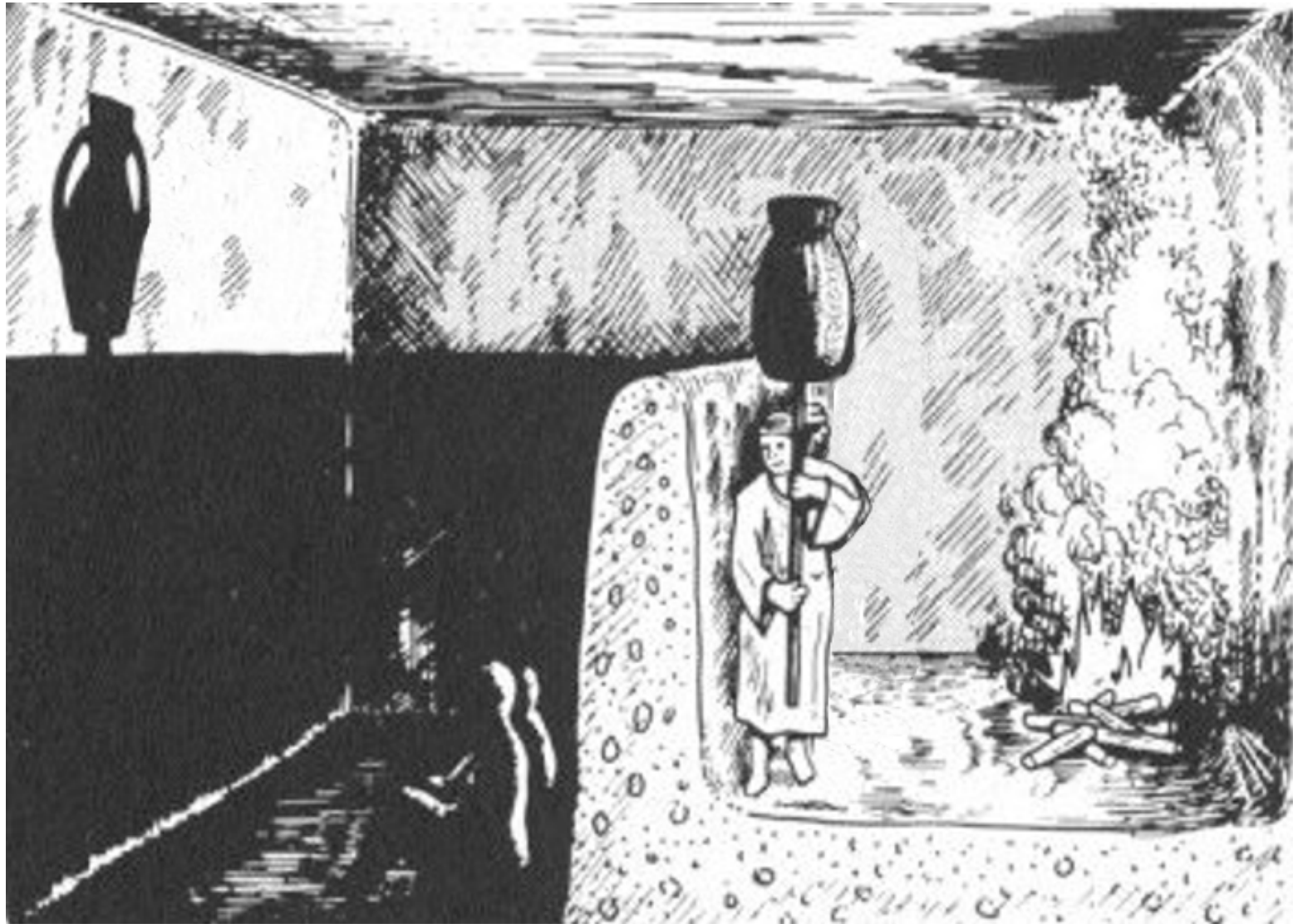


Platon

428/427–348/347 BC

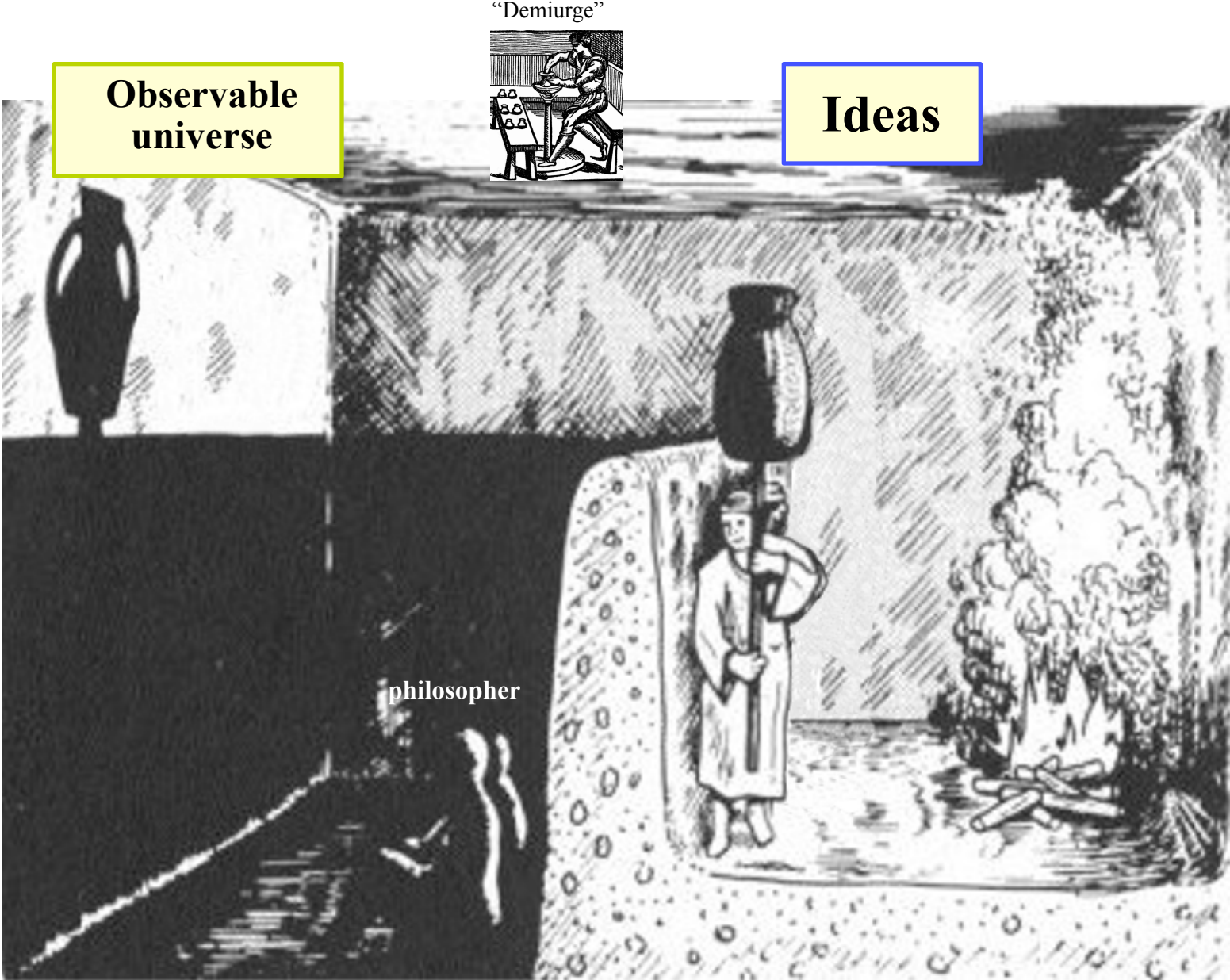


## Plato's allegory of the cave\*



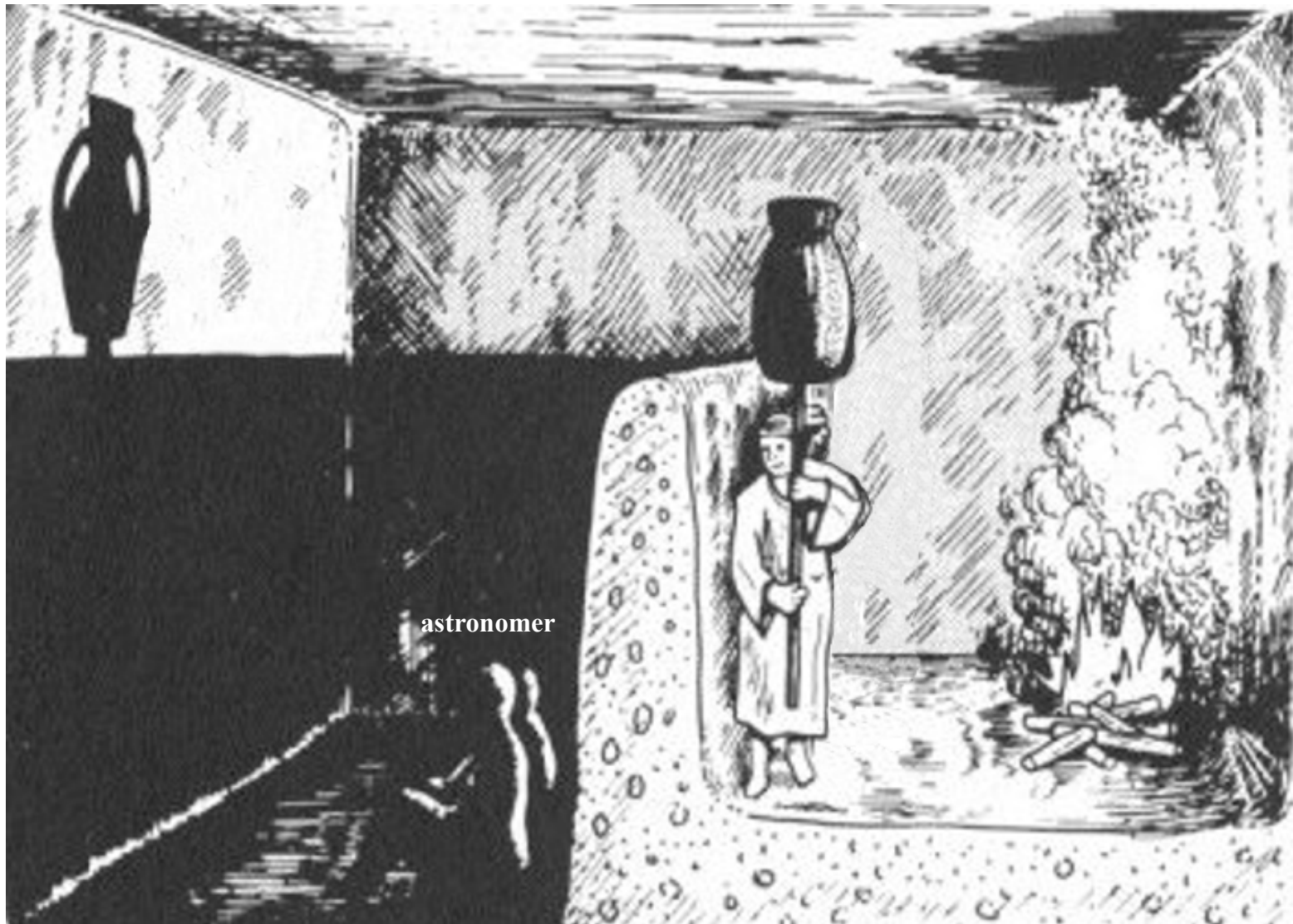
\* The Republic  
(514a-520a)

**Plato's allegory of the cave\***



\* The Republic (514a-520a)

## Plato's allegory of the cave\* ↔ Astronomical observations



\* The Republic  
(514a-520a)




**Plato's allegory of the cave\* ↔ Astronomical observations**


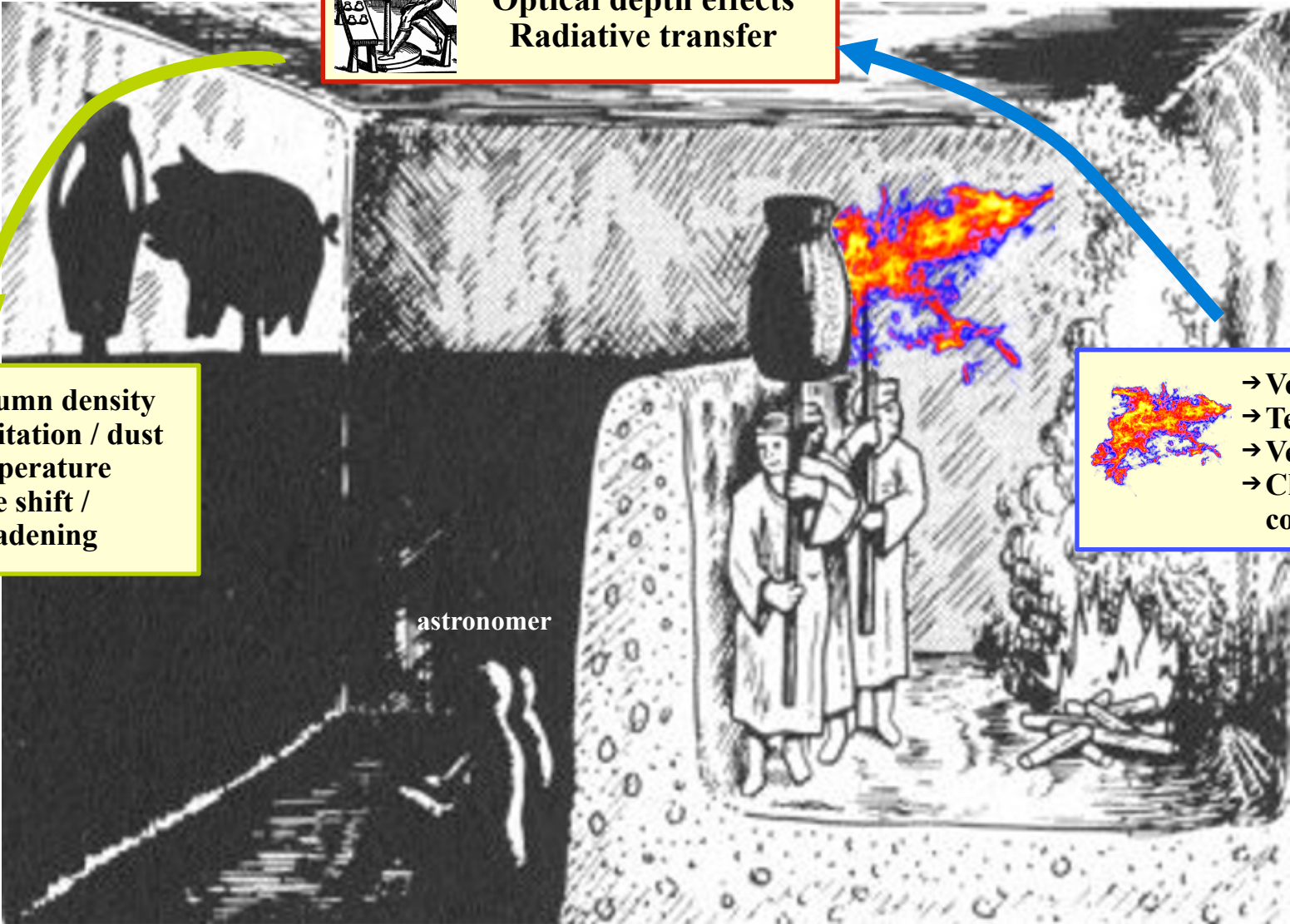


\* The Republic (514a-520a)

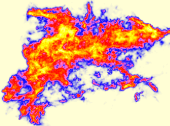
# Plato's allegory of the cave\* ↔ Astronomical observations



Projection effects  
Optical depth effects  
Radiative transfer



→ Column density  
→ Excitation / dust temperature  
→ Line shift / broadening



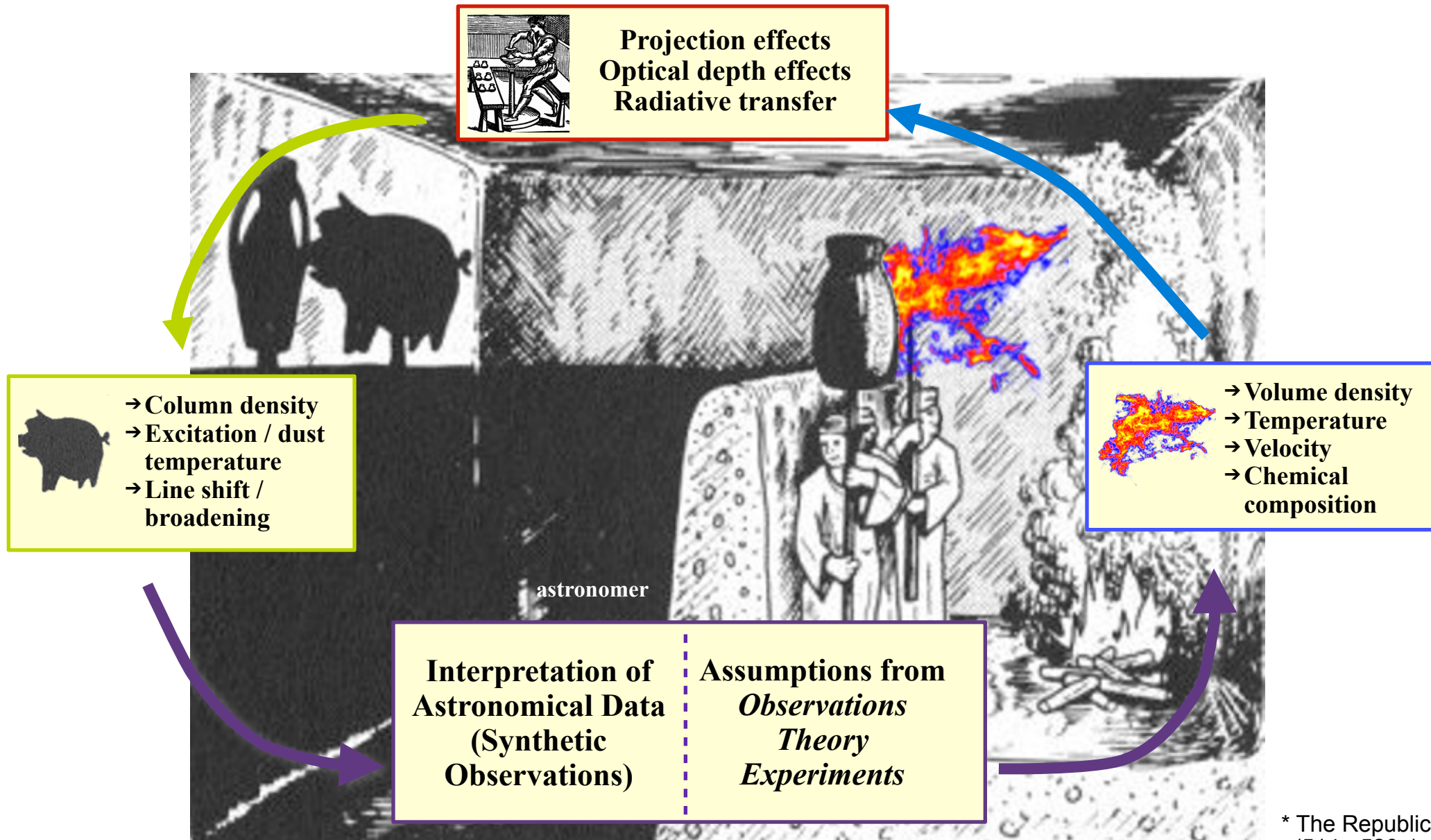
→ Volume density  
→ Temperature  
→ Velocity  
→ Chemical composition

astronomer

\* The Republic (514a-520a)



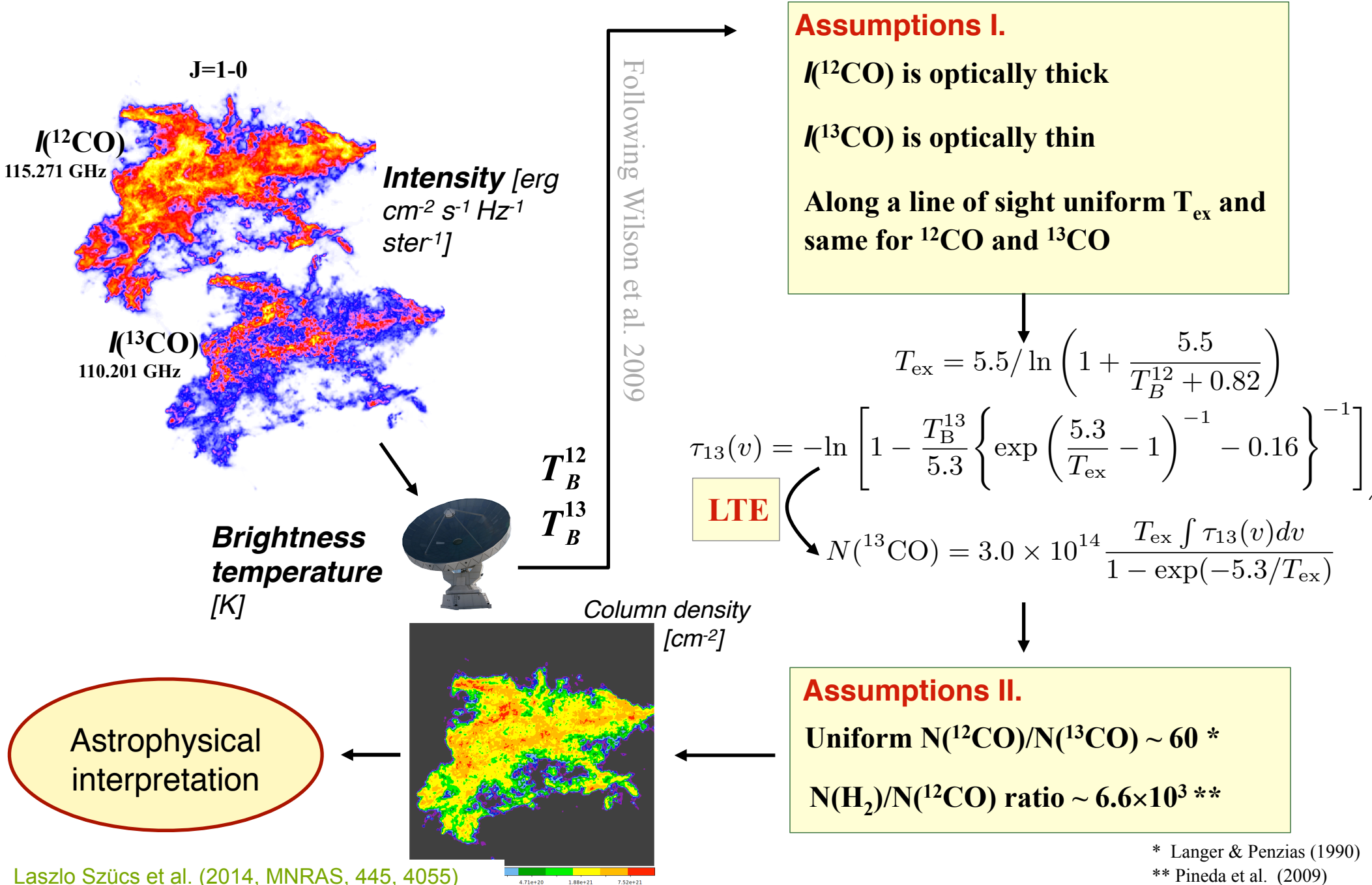
# Plato's allegory of the cave\* ↔ Astronomical observations



\* The Republic (514a-520a)



# Example: from CO emission to total column density





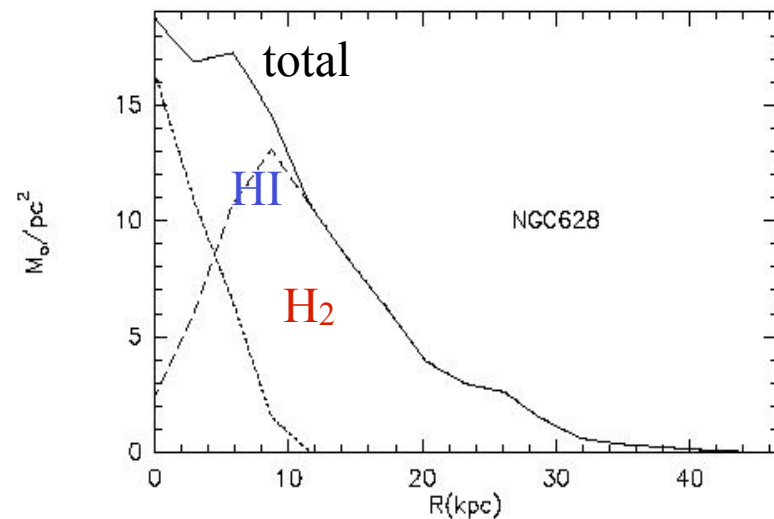
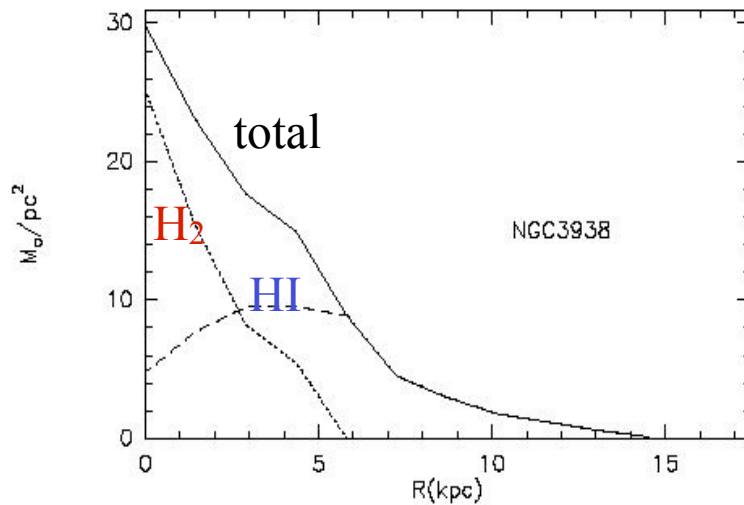
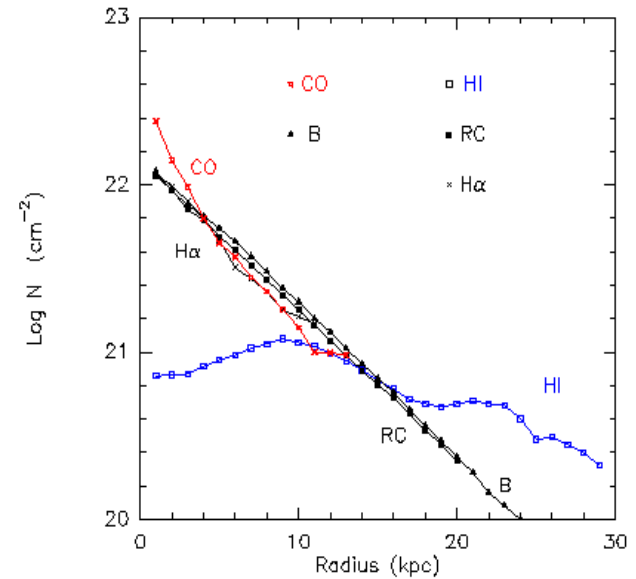


global SF relations



# 1. radial distribution in spirals

- HI versus H<sub>2</sub>:
  - H<sub>2</sub> is restricted to the optical disk
  - while the HI extends 2 - 4 x optical radius
- HI hole or depression in the centers, sometimes compensated by H<sub>2</sub>
- often H<sub>2</sub> is exponential like stars, HI does *not* follow in most cases

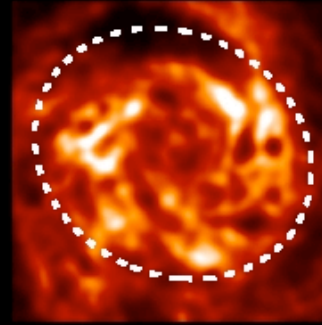
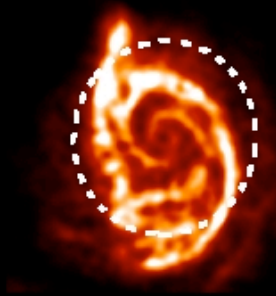
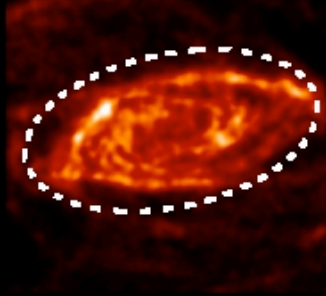
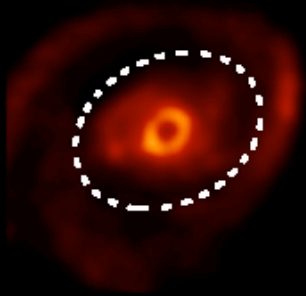


NGC 4736

NGC 5055

NGC 5194

NGC 6946



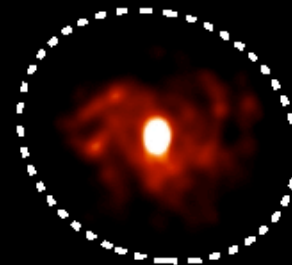
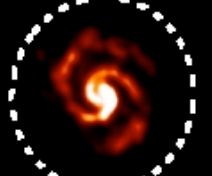
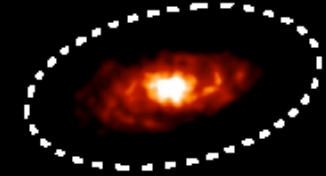
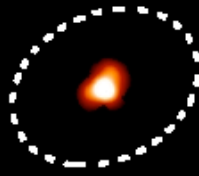
atomic  
hydrogen

NGC 4736

NGC 5055

NGC 5194

NGC 6946



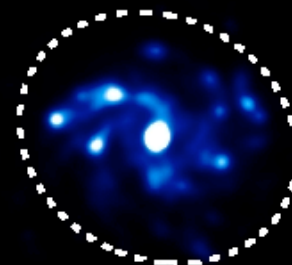
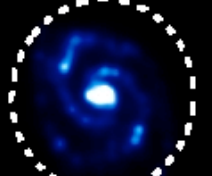
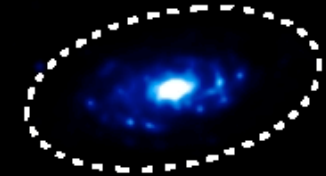
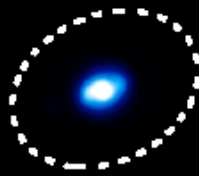
molecular  
hydrogen

NGC 4736

NGC 5055

NGC 5194

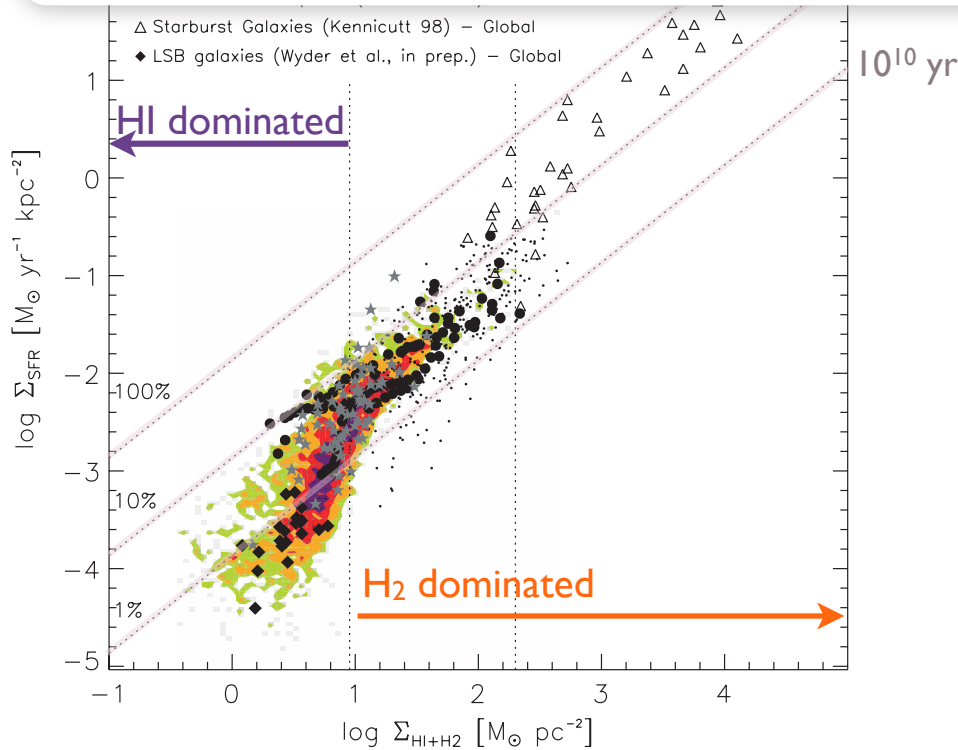
NGC 6946



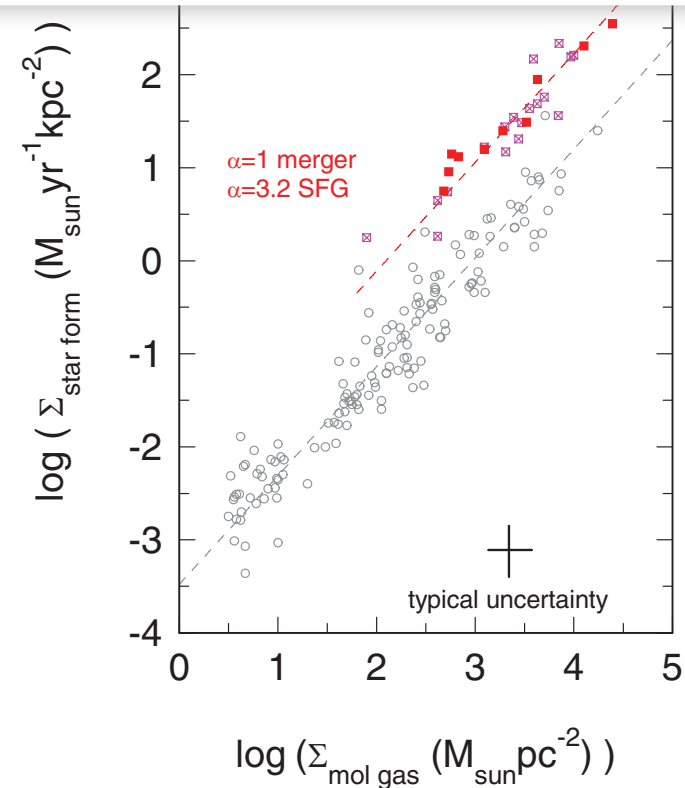
star  
formation

- HI gas more extended
- H2 and SF well correlated

## 2. correlation with star formation



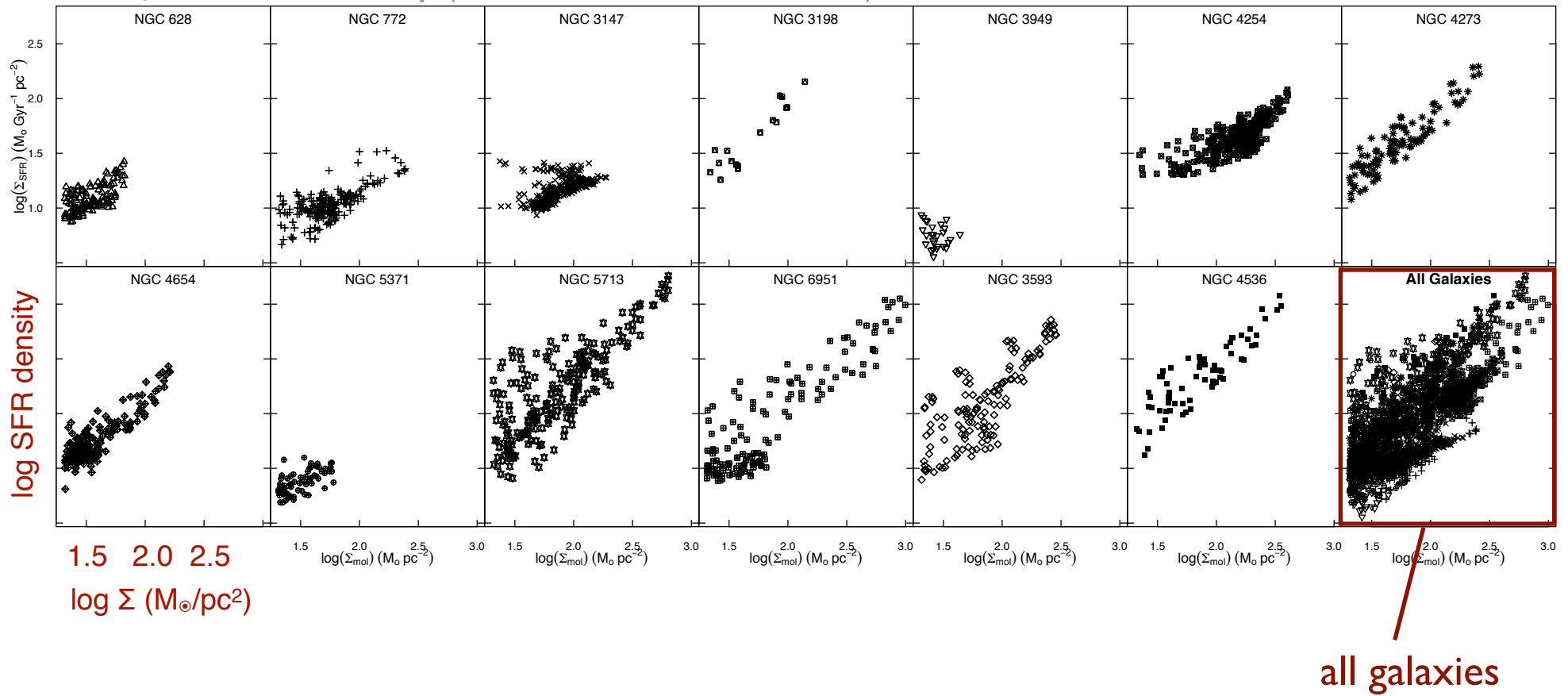
Bigiel et al. (2008, AJ, 136, 2846)



Genzel et al. (2010, MNRAS, AJ, 407, 2091)

- standard model: roughly linear relation between H
- standard model: roughly constant depletion time: few  $\times 10$
- super linear relation between total gas and SFR

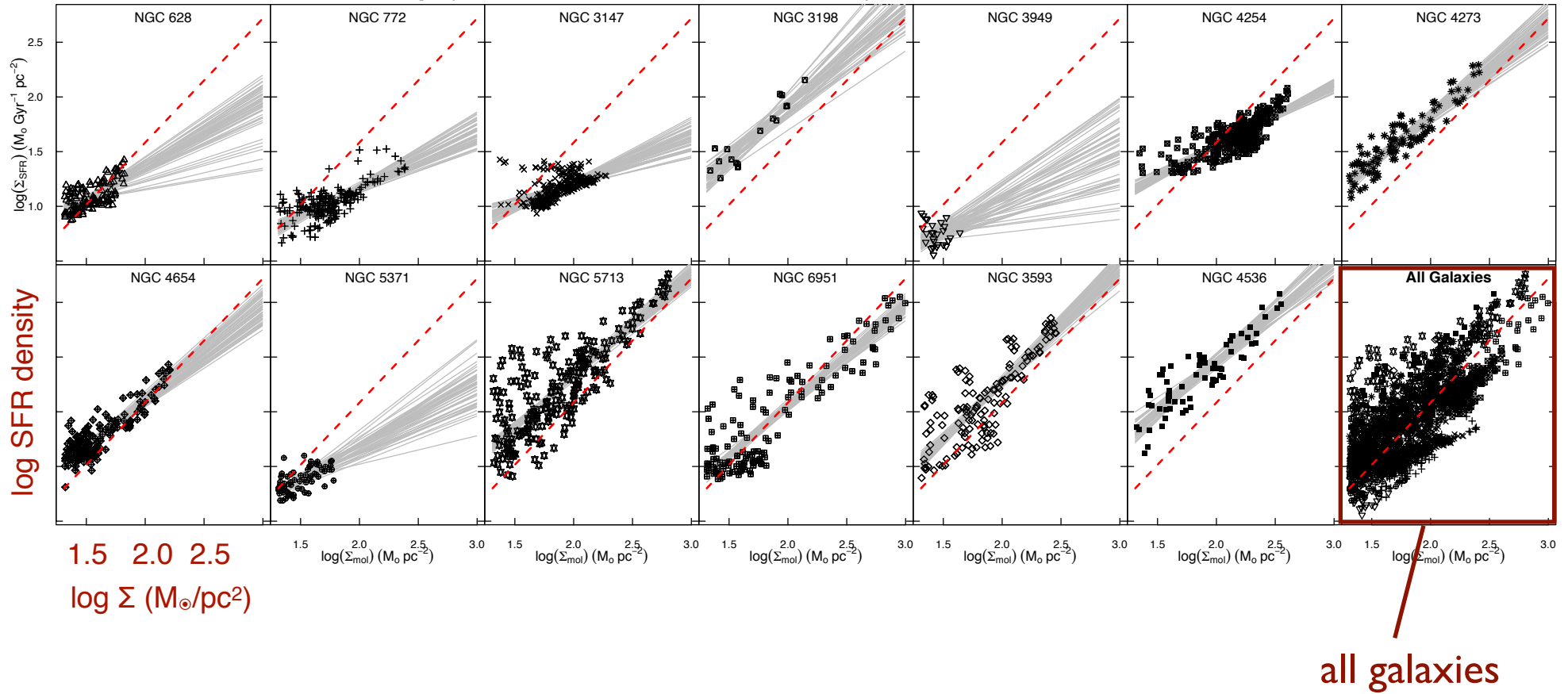
data from STING survey (Rahman et al. 2011, 2012)



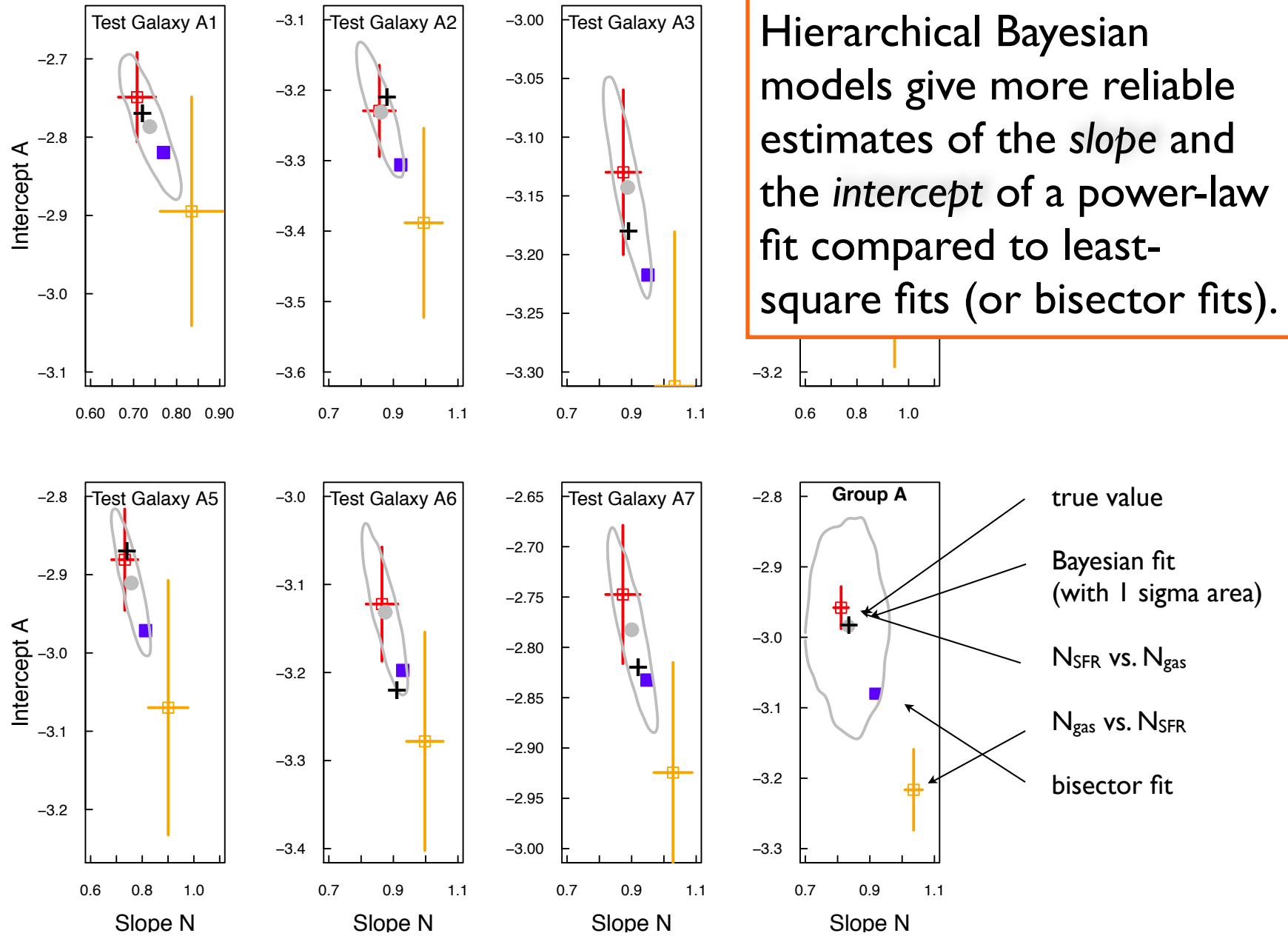
- QUIZ: do you see a universal



data from STING survey (Rahman et al. 2011, 2012)

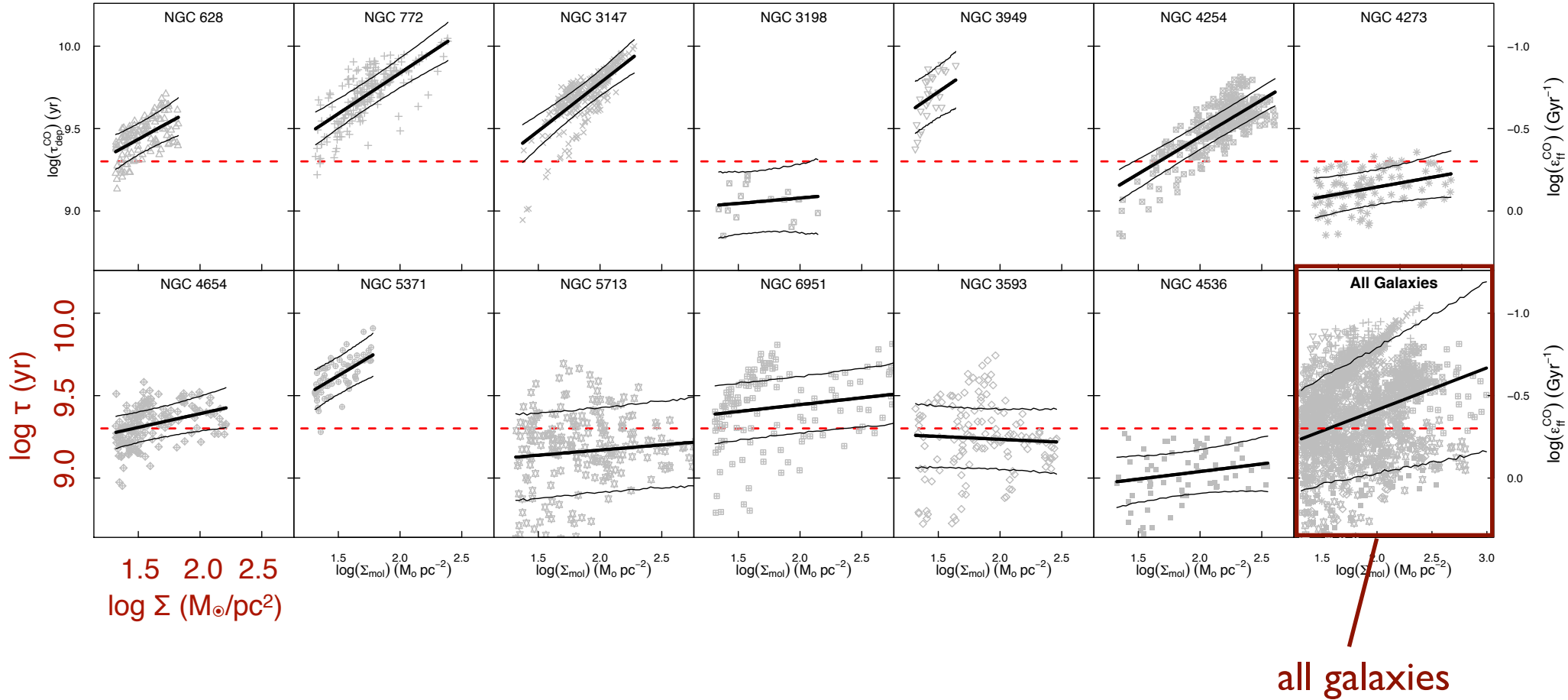


- QUIZ: do you see a universal
- ANSWER: - probably not  
- in addition, the relation often is sublinear



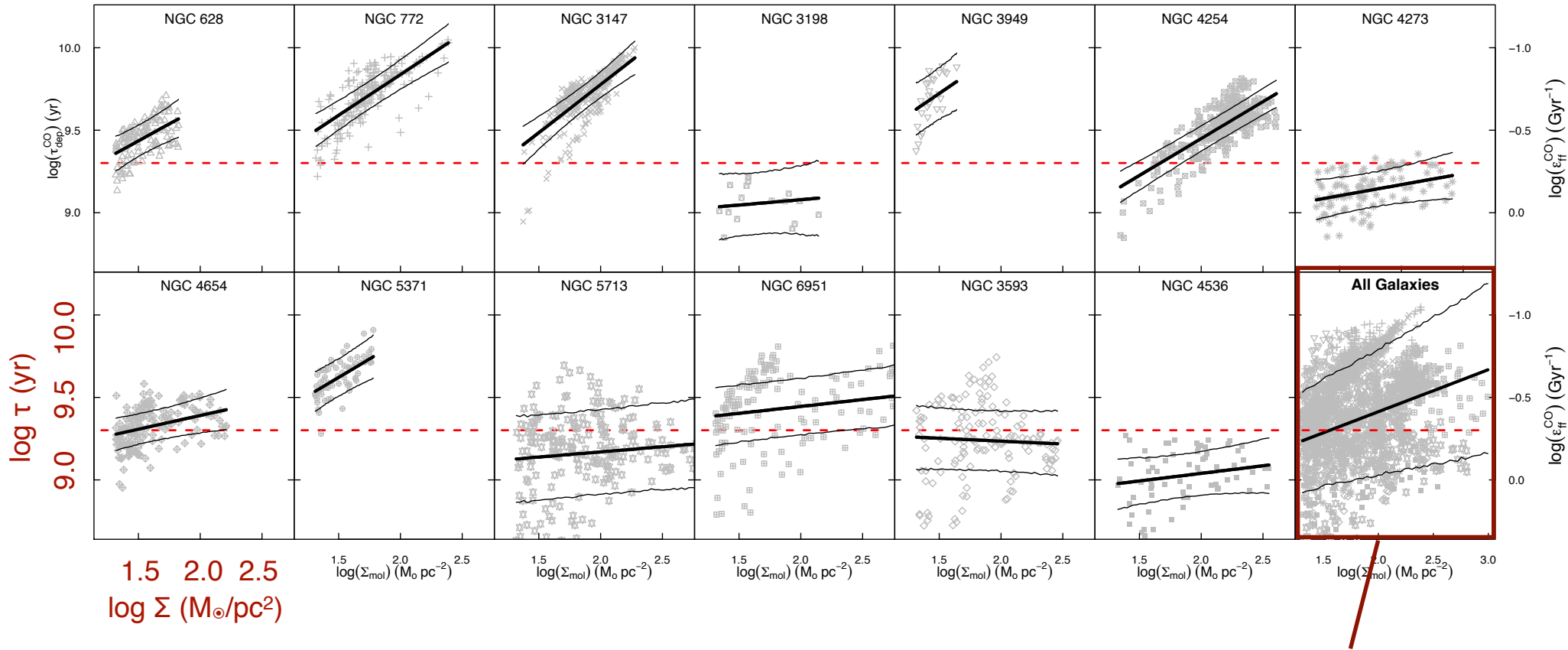
**Figure 1.** Slope and intercept of test galaxies in Group A. Black cross shows the true values. Red and orange squares show the  $OLS(\Sigma_{SFR}|\Sigma_{mol})$  and  $OLS(\Sigma_{mol}|\Sigma_{SFR})$  results, with their  $1\sigma$  uncertainties, respectively. The gray circles indicate the estimate provided by the median of hierarchical Bayesian posterior result, and the contours mark the  $1\sigma$  deviation. The filled blue squares mark the bisector estimates. The last panel on the bottom row shows the group parameters and fit estimates.

data from STING survey (Rahman et al. 2011, 2012)



Hierarchical Bayesian model for STING galaxies indicate *varying depleting times*.

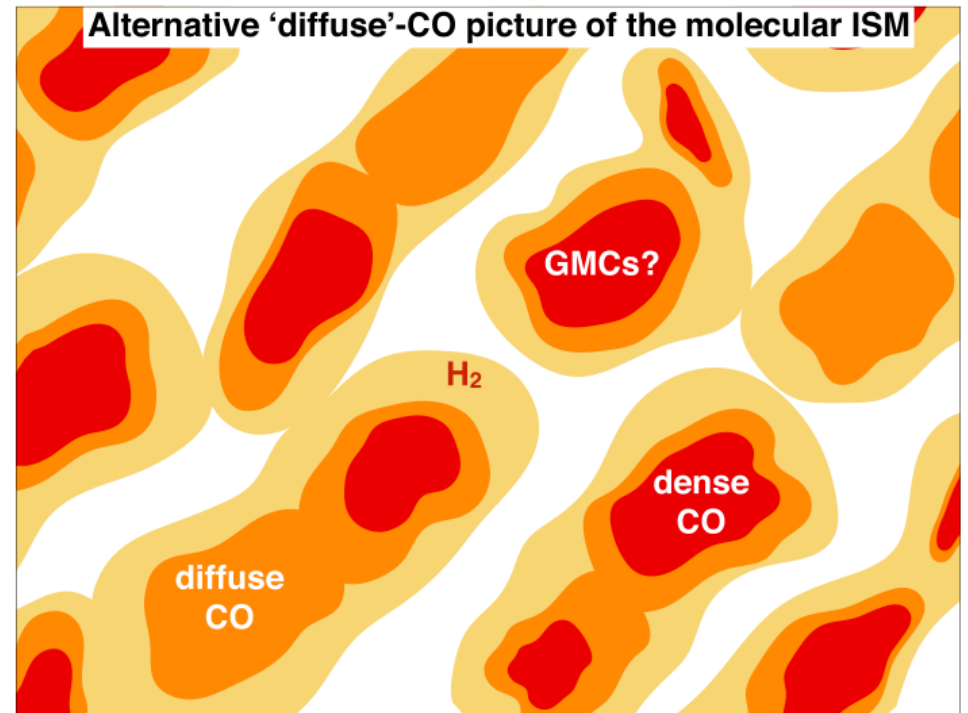
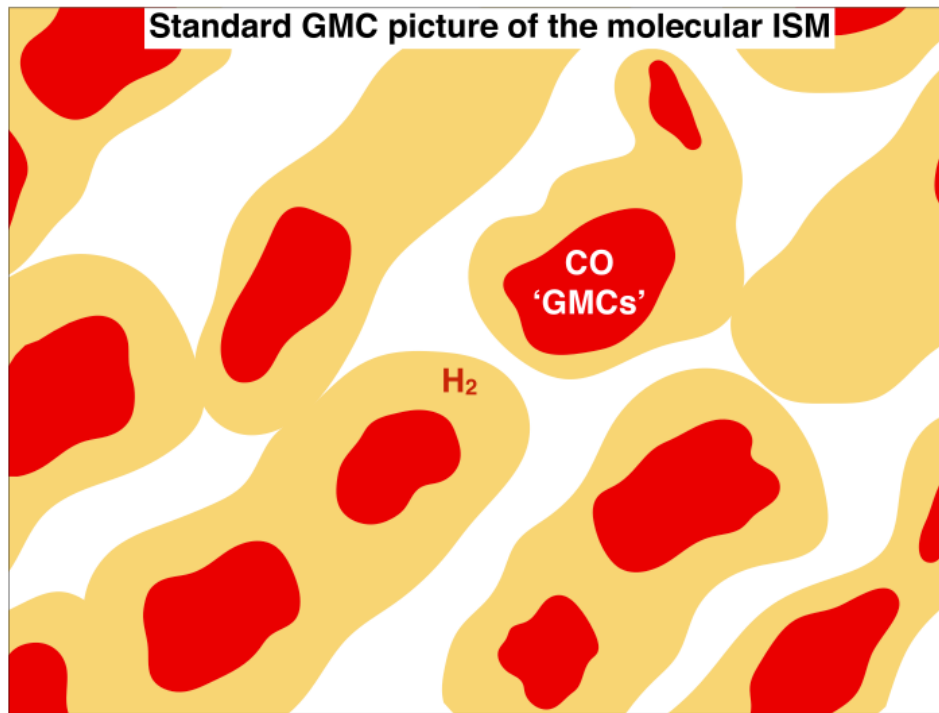
data from STING survey (Rahman et al. 2011, 2012)



*physical origin of this behavior?*

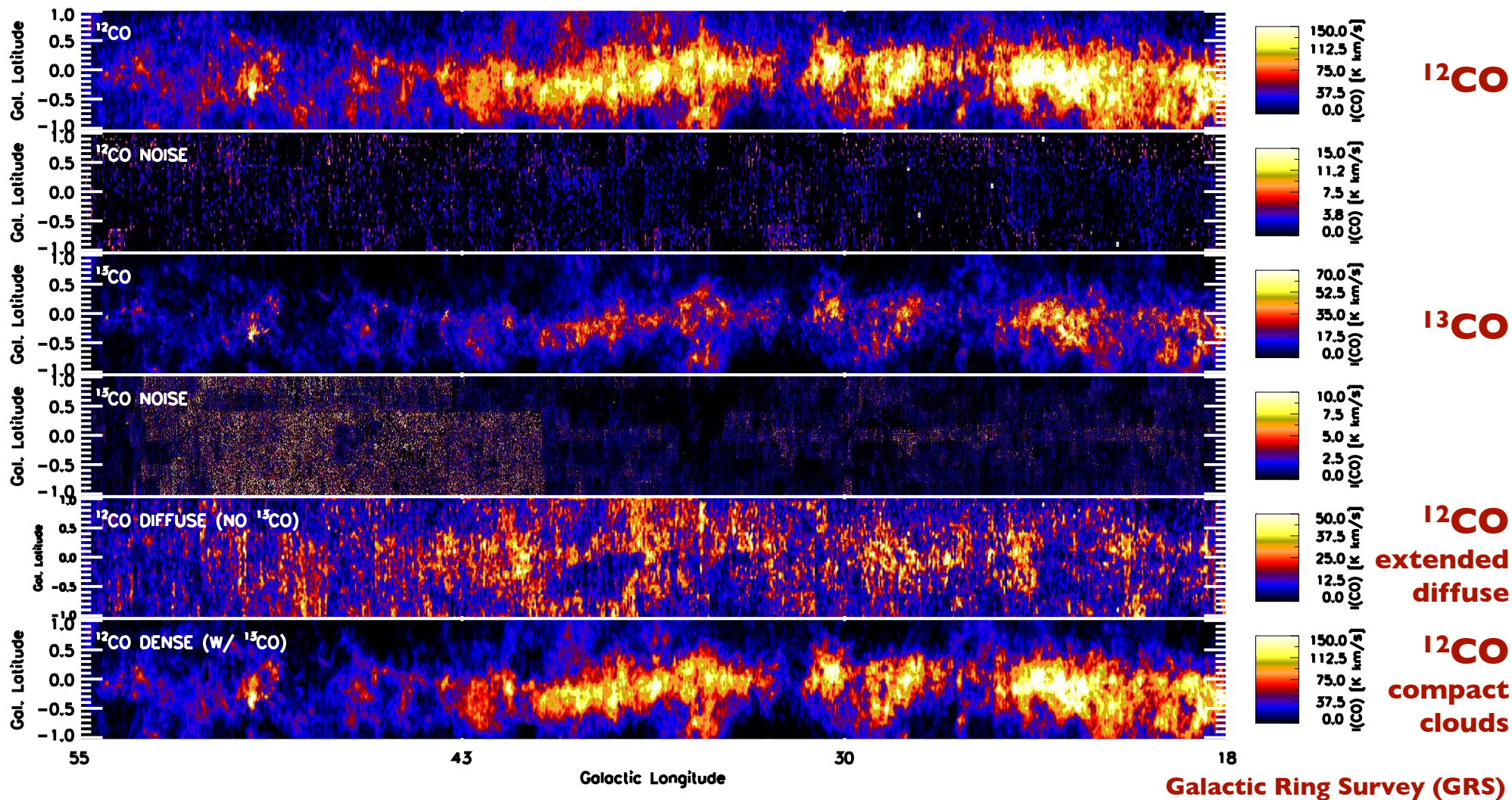
- maybe strong shear in dense arms (example M51, Meidt et al. 2013)...
- maybe non-star forming H densities (recall H





*in addition:*

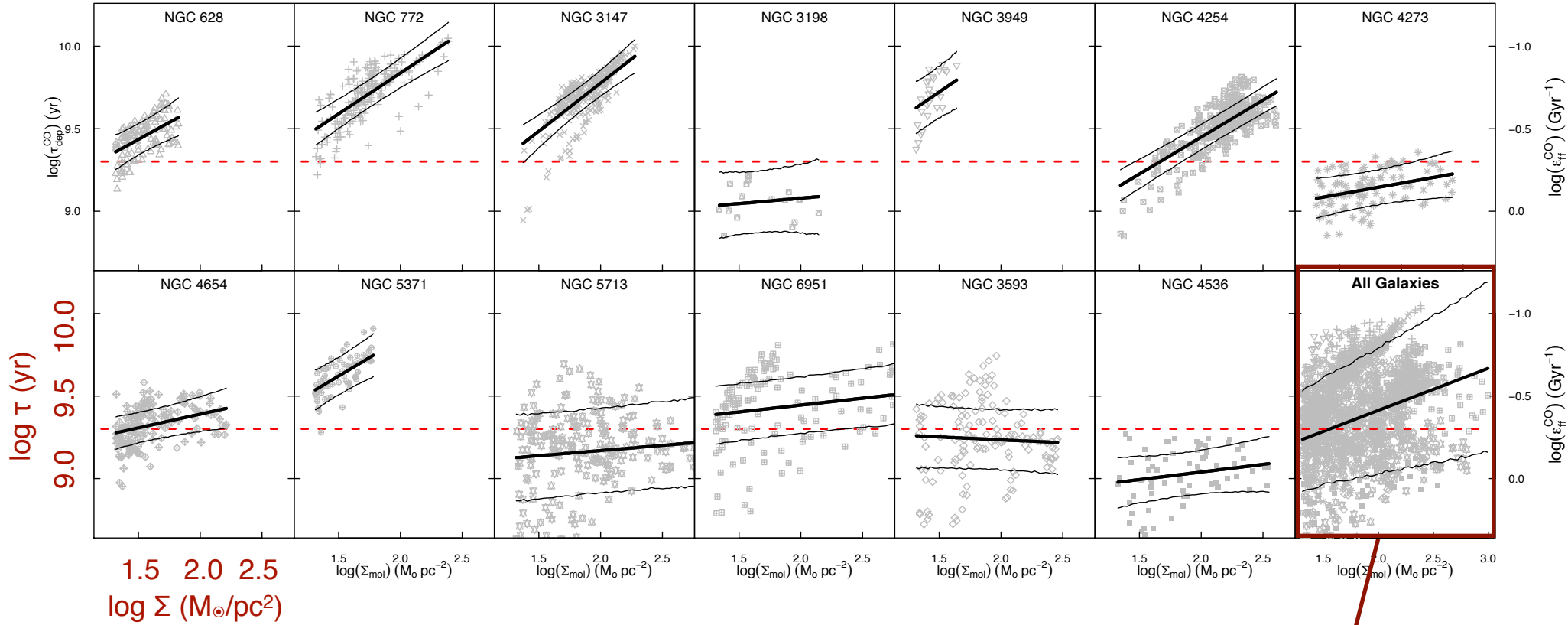
- maybe a large fraction of H<sub>2</sub> dense clouds, but in a diffuse state!



*in addition:*

- comparison of tracing all the gas (including the more diffuse component)

data from STING survey (Rahman et al. 2011, 2012)



all galaxies

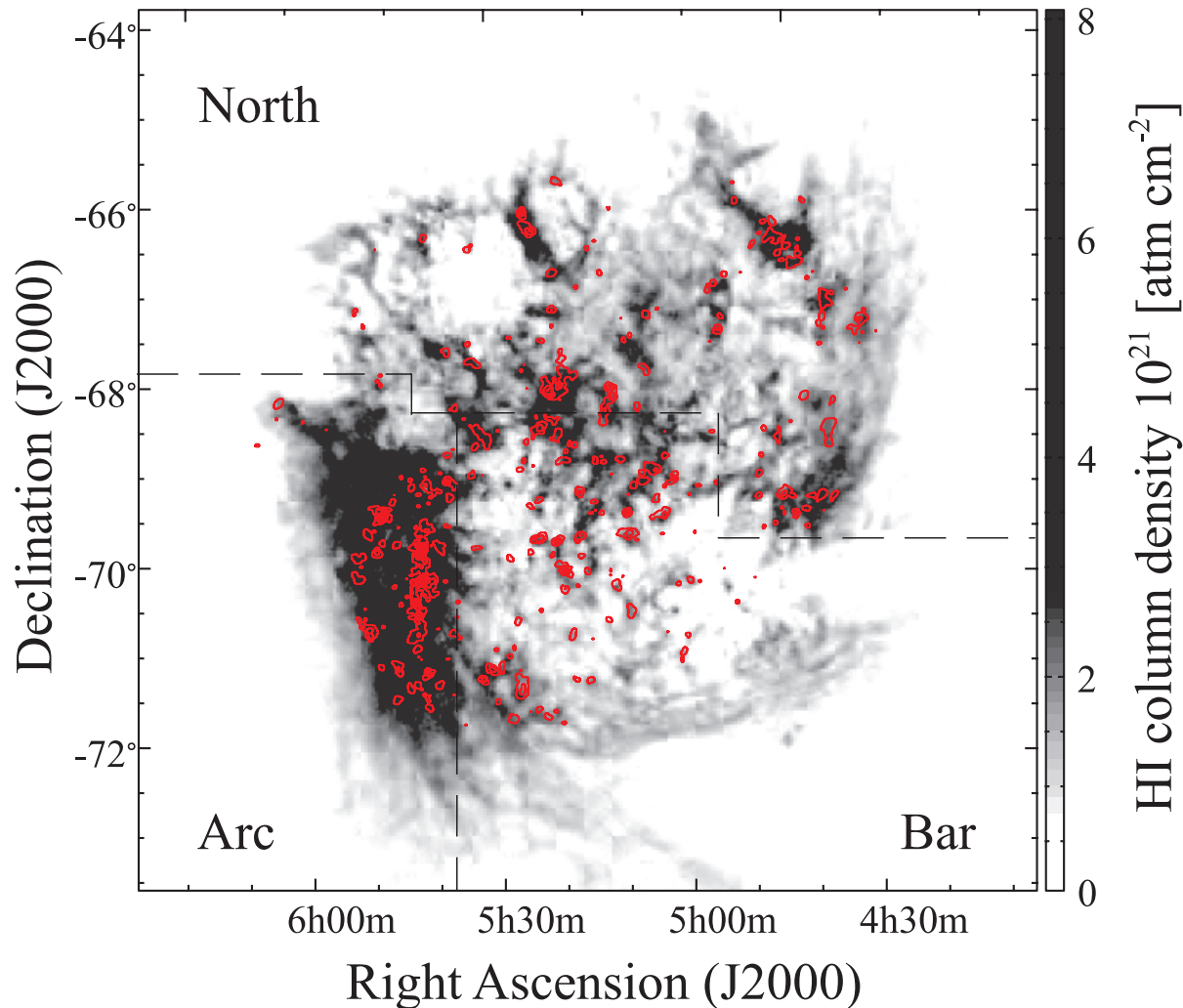
*physical origin of this behavior?*

- maybe strong shear in dense arms (example M51, Meidt et al. 2013)...
- maybe non-star forming  $H$  densities (recall  $H$ )

molecular cloud  
formation



# molecular cloud formation

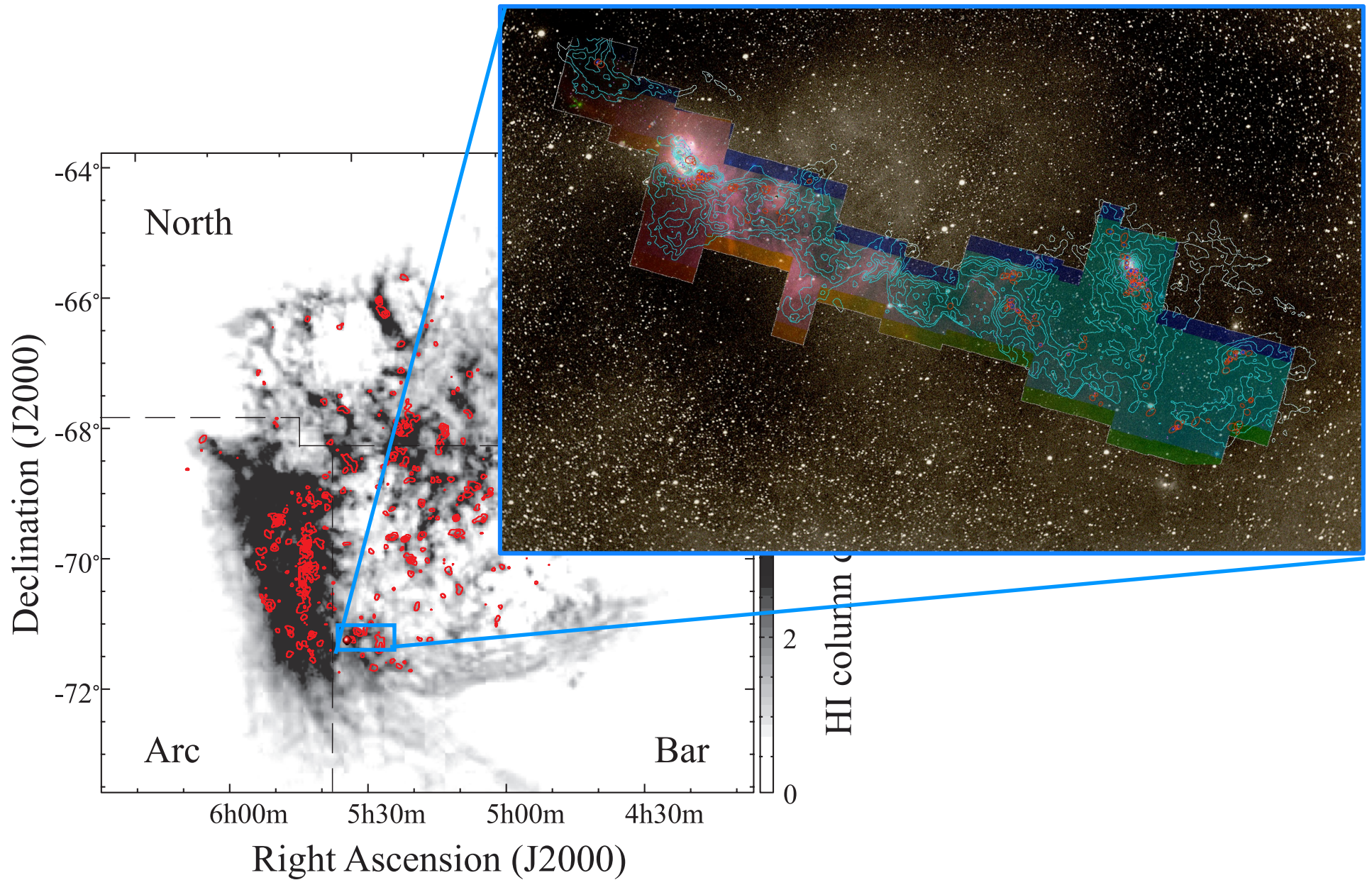


## Idea:

Molecular clouds form at *stagnation points* of large-scale convergent flows, mostly triggered by global (or external) perturbations. Their internal turbulence is driven by accretion, i.e. by the process of cloud formation

- molecular clouds grow in mass
- this is inferred by looking at molecular clouds in different evolutionary phases in the LMC (Fukui et al. 2008, 2009)

zooming in ...



# position-position-velocity structure of the Perseus cloud

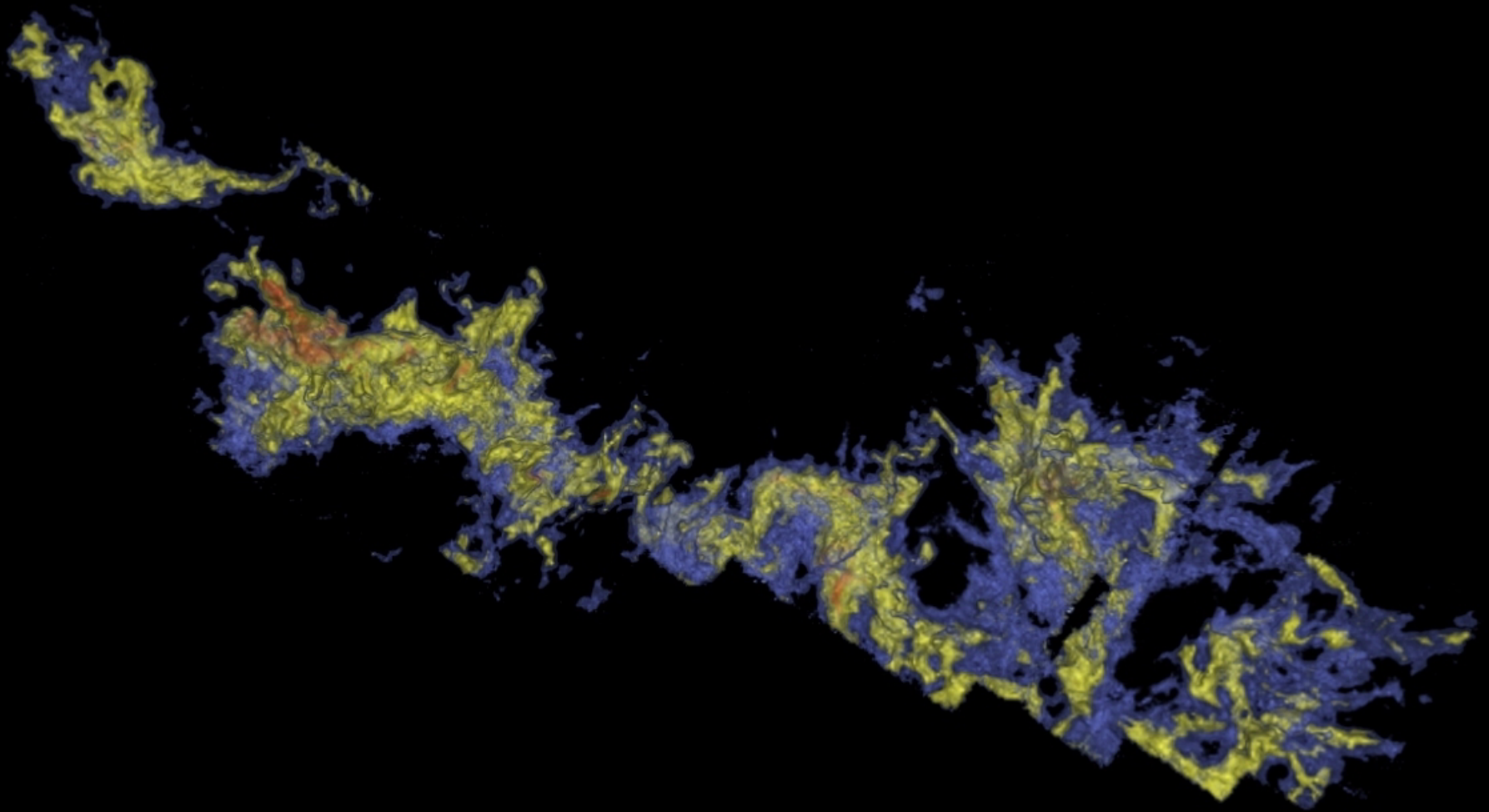
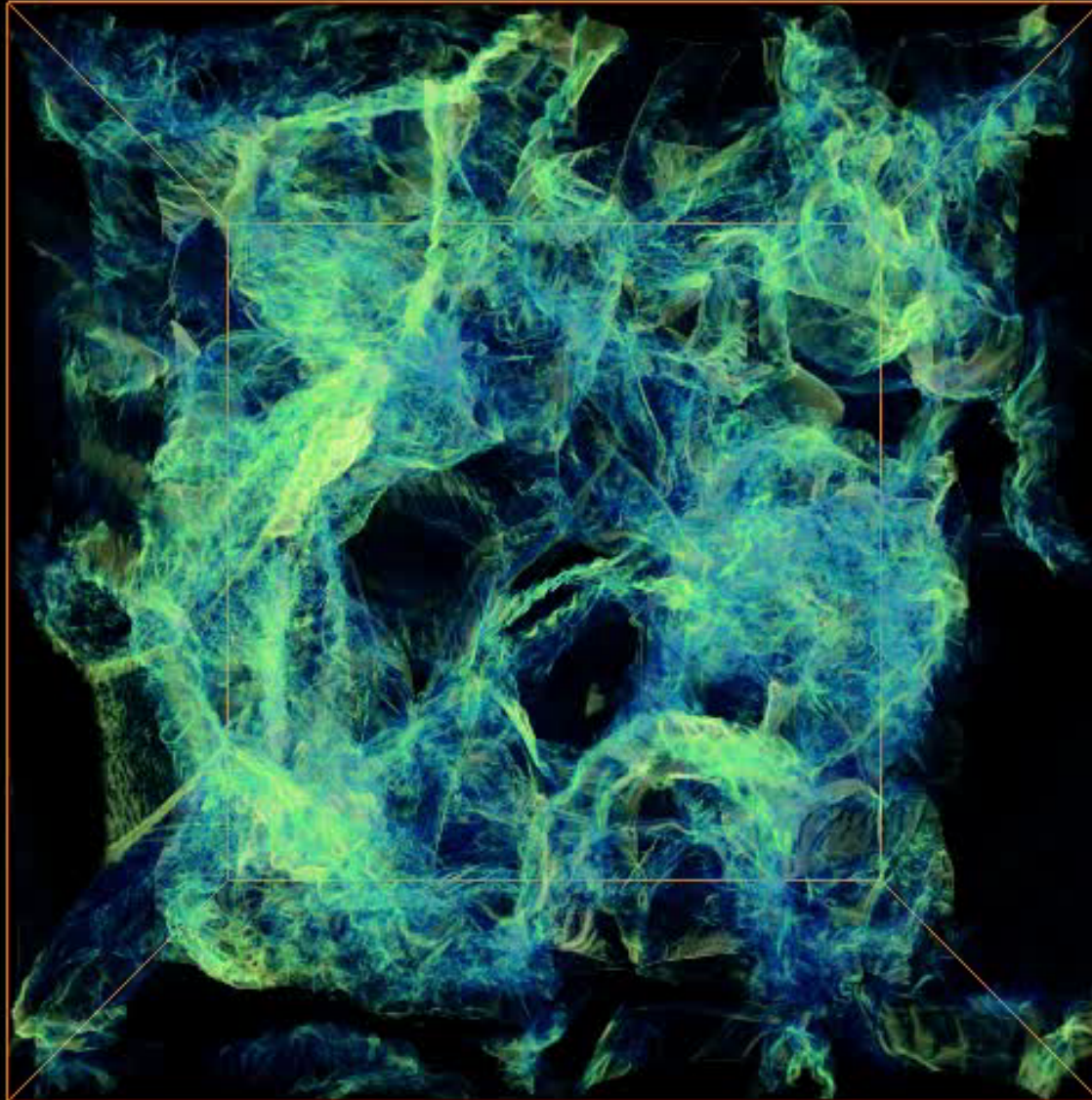


image from Alyssa Goodman: COMPLETE survey



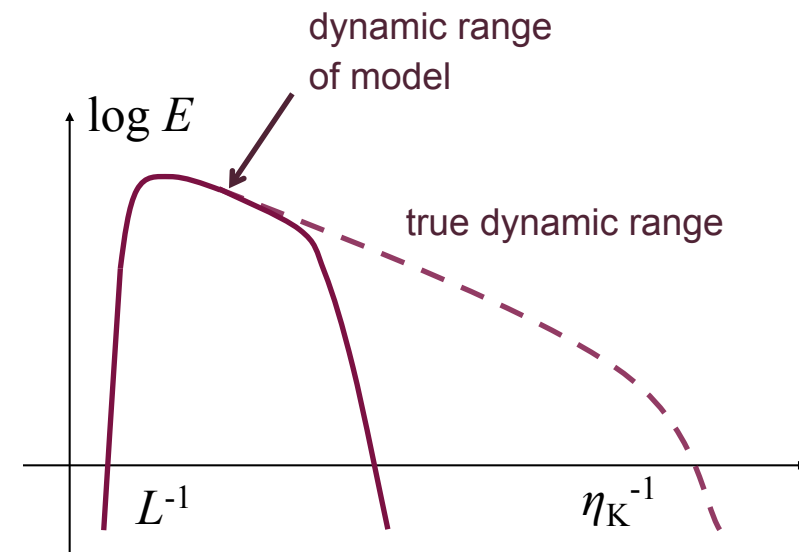


Schmidt et al. (2009, A&A, 494, 127)



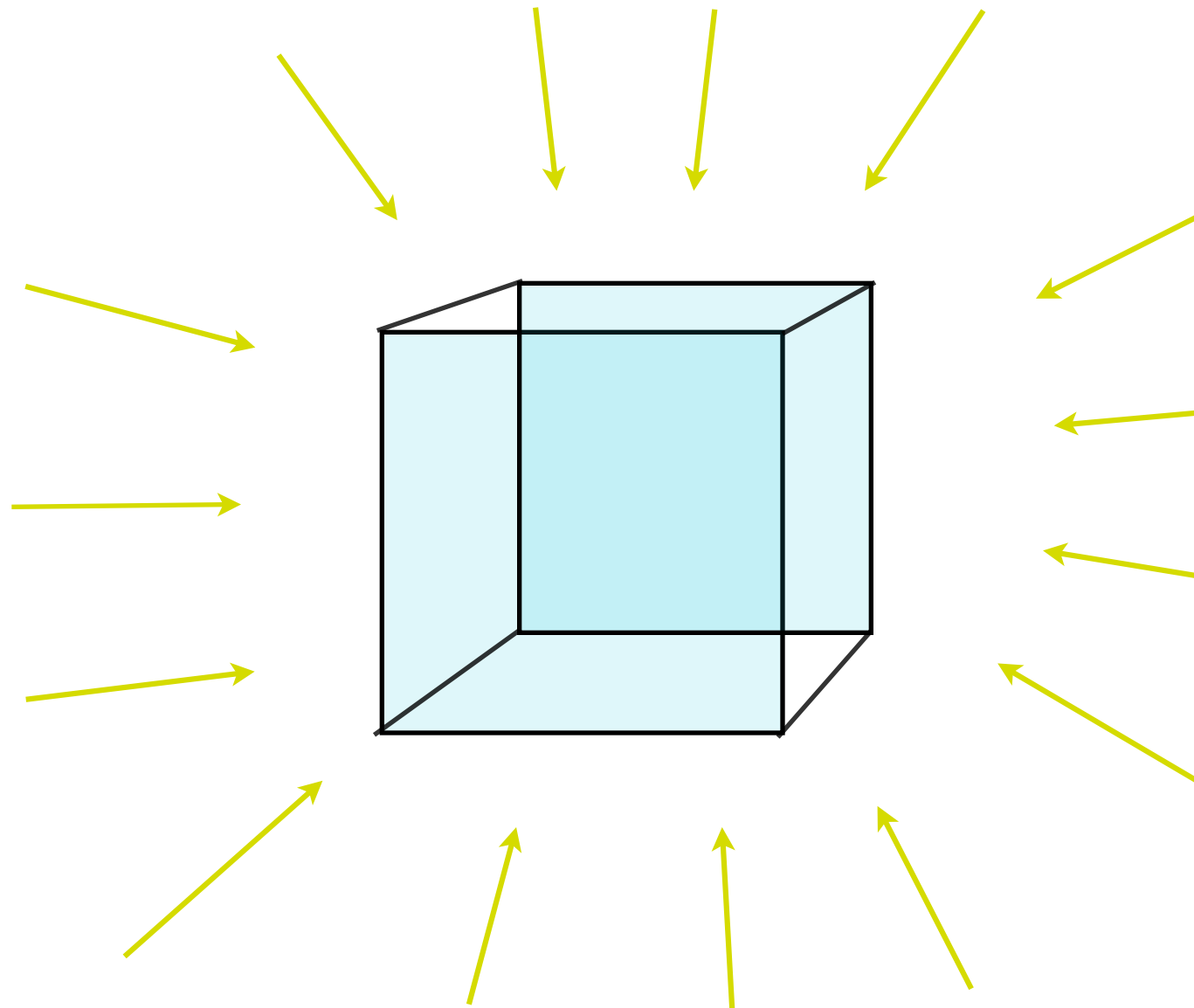
# caveat of numerical simulations

- most astrophysical turbulence simulations use an **LES** approach to model the flow
- principal problem: only large scale flow properties
  - Reynolds number:  $Re = LV/\nu$  ( $Re_{nature} \gg Re_{model}$ )
  - dynamic range much smaller than true physical one
  - need **subgrid model** (often only dissipation)
  - but what to do for more complex when processes on subgrid scale determine large-scale dynamics (chemical reactions, nuclear burning, etc)
  - Turbulence is “space filling” --> difficulty for AMR (don't know what criterion to use for refinement)
- how **large** a Reynolds number do we need to catch basic dynamics right?



including detailed  
chemistry

# experimental set-up



- Arepo and FLASH
- stochastic forcing (Ornstein-Uhlenbeck)
- self-gravity
- time-dependent chemistry (DVODE, standard variable-coefficient ordinary differential equation solver)
- cooling & heating processes
- gives you mathematically well defined boundary conditions
- > good for statistical studies
- gives external radiation with TreeCol (a new approximative scheme to calculate column densities from the gravity solver)

# chemical model 0

- 32 chemical species

- 17 in instantaneous equilibrium:

$H^-$ ,  $H_2^+$ ,  $H_3^+$ ,  $CH^+$ ,  $CH_2^+$ ,  $\tilde{O}H^+$ ,  $H_2O^+$ ,  $\tilde{H}_3O^+$ ,  $CO^+$ ,  $HOC^+$ ,  $O^-$ ,  $C^-$  and  $O_2^+$

- 19 full non-equilibrium evolution

$e^-$ ,  $H^+$ ,  $H$ ,  $H_2$ ,  $He$ ,  $He^+$ ,  $C$ ,  $C^+$ ,  $O$ ,  $O^+$ ,  $OH$ ,  $H_2O$ ,  $CO$ ,

$C_2$ ,  $O_2$ ,  $HCO^+$ ,  $CH$ ,  $CH_2$  and  $CH_3^+$

- 218 reactions

- various heating and cooling processes



# chemical model 1

Process

Reference(s)

## Cooling:

|   |  |
|---|--|
| C fine structure lines                      | Atomic data – Silva & Viegas (2002)<br>Collisional rates (H) – Abrahamsson, Krems & Dalgarno (2007)<br>Collisional rates (H <sub>2</sub> ) – Schroder et al. (1991)<br>Collisional rates (e <sup>-</sup> ) – Johnson et al. (1987)<br>Collisional rates (H <sup>+</sup> ) – Roueff & Le Bourlot (1990)             |
| C <sup>+</sup> fine structure lines         | Atomic data – Silva & Viegas (2002)<br>Collisional rates (H <sub>2</sub> ) – Flower & Launay (1977)<br>Collisional rates (H, T < 2000 K) – Hollenbach & McKee (1989)<br>Collisional rates (H, T > 2000 K) – Keenan et al. (1986)<br>Collisional rates (e <sup>-</sup> ) – Wilson & Bell (2002)                     |
| O fine structure lines                      | Atomic data – Silva & Viegas (2002)<br>Collisional rates (H) – Abrahamsson, Krems & Dalgarno (2007)<br>Collisional rates (H <sub>2</sub> ) – see Glover & Jappsen (2007)<br>Collisional rates (e <sup>-</sup> ) – Bell, Berrington & Thomas (1998)<br>Collisional rates (H <sup>+</sup> ) – Pequignot (1990, 1996) |
| H <sub>2</sub> rovibrational lines          | Le Bourlot, Pineau des Forêts & Flower (1999)  |
| CO and H <sub>2</sub> O rovibrational lines | Neufeld & Kaufman (1993); Neufeld, Lepp & Melnick (1995)   |
| OH rotational lines                         | Pavlovski et al. (2002)  |
| Gas-grain energy transfer                   | Hollenbach & McKee (1989)  |
| Recombination on grains                     | Wolfire et al. (2003)  |
| Atomic resonance lines                      | Sutherland & Dopita (1993)   |
| H collisional ionization                    | Abel et al. (1997)   |
| H <sub>2</sub> collisional dissociation     | See Table B1   |
| Compton cooling                             | Cen (1992)   |

## Heating:

|   |   |
|---|---|
| Photoelectric effect                    | Bakes & Tielens (1994); Wolfire et al. (2003) |
| H <sub>2</sub> photodissociation        | Black & Dalgarno (1977)                       |
| UV pumping of H <sub>2</sub>            | Burton, Hollenbach & Tielens (1990)           |
| H <sub>2</sub> formation on dust grains | Hollenbach & McKee (1989)                     |
| Cosmic ray ionization                   | Goldsmith & Langer (1978)                     |





# chemical model 2

Table B1.

| No. | Rea |
|-----|-----|
| 1   | H + |

|    |                                   |    |   |  |    |
|----|-----------------------------------|----|---|--|----|
| 14 | $H^- + H \rightarrow H + H + e^-$ | 88 | $H_2 + He^+ \rightarrow He + H_2^+$     | $k_{88} = 7.2 \times 10^{-15}$                               | 63 |
| 36 | $CH + H_2$                        | 89 | $H_2 + He^+ \rightarrow He + H + H^+$   | $k_{89} = 3.7 \times 10^{-14} \exp\left(\frac{35}{T}\right)$ | 63 |
| 37 | $CH + C$                          | 90 | $CH + H^+ \rightarrow CH^+ + H$         | $k_{90} = 1.9 \times 10^{-9}$                                | 28 |
| 38 | $CH + O$                          | 91 | $CH_2 + H^+ \rightarrow CH_2^+ + H$     | $k_{91} = 1.4 \times 10^{-9}$                                | 28 |
| 39 | $C + O$                           | 92 | $Cl_2 + H^+ \rightarrow Cl_2^+ + H$     | $k_{92} = 5 \times 10^{-10}$                                 | 28 |
| 40 | $CH_2 + O$                        | 93 | $C_2 + e^- \rightarrow C + C$           | $k_{93} = 6 \times 10^{-9}$                                  | 28 |
| 41 | $CH_2 + O$                        | 94 | $OH + H^+ \rightarrow OH^+ + H$         | $k_{94} = 2.1 \times 10^{-9}$                                | 28 |
| 42 | $C_2 + O \rightarrow$             | 95 | $OH + He^+ \rightarrow O^+ + He + H$    | $k_{95} = 1.1 \times 10^{-9}$                                | 28 |
|    |                                   | 96 | $H_2O + H^+ \rightarrow H_2O^+ + H$     | $k_{96} = 6.9 \times 10^{-9}$                                | 64 |
|    |                                   | 97 | $H_2O + He^+ \rightarrow OH + He + H^+$ | $k_{97} = 2.04 \times 10^{-10}$                              | 65 |
|    |                                   | 98 | $H_2O + He^+ \rightarrow OH^+ + He + H$ | $k_{98} = 2.04 \times 10^{-10}$                              | 65 |

Table B2. List of photochemical reactions included in our chemical model

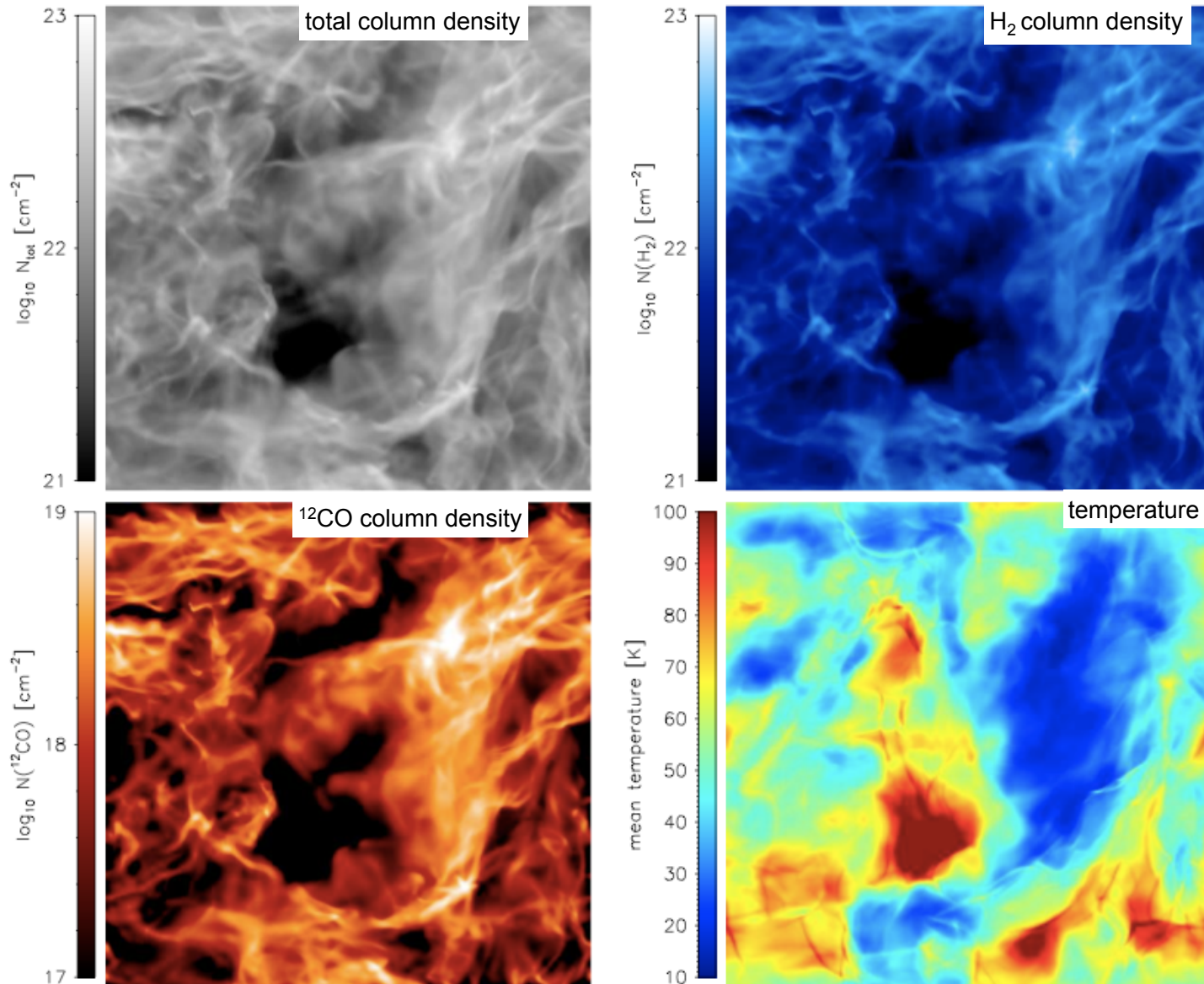
| No. | Reaction                               | Optically thin rate ( $s^{-1}$ ) | $\gamma$ | Ref. |  |                |
|-----|--|----------------------------------|----------|------|--|----------------|
| 166 | $H^- + \gamma \rightarrow H + e^-$     | $R_{166} = 7.1 \times 10^{-7}$   | 0.5      | 1    |  |                |
| 167 | $H_2^+ + \gamma \rightarrow H + H^+$   | $R_{167} = 1.1 \times 10^{-9}$   | 1.9      | 2    |  |                |
| 168 | $H_2 + \gamma \rightarrow H + H$       | $R_{168} = 5.6 \times 10^{-11}$  | See §2.2 | 3    |  |                |
| 169 | $H_3^+ + \gamma \rightarrow H_2 + H^+$ | $R_{169} = 4.9 \times 10^{-13}$  | 1.8      | 4    |  |                |
| 170 | $H_3^+ + \gamma \rightarrow H_2^+ + H$ | $R_{170} = 4.9 \times 10^{-13}$  | 2.3      | 4    |  |                |
| 171 | $C + \gamma \rightarrow C^+ + e^-$     | $R_{171} = 2.1 \times 10^{-10}$  | 2.0      | 5    | $25 \times 10^{-15}$   | 81             |
| 172 | $C^- + \gamma \rightarrow$             |                                  |          |      | $0 \times 10^{-17}$  | 82             |
| 173 | $CH + \gamma \rightarrow$              |                                  |          |      | $0 \times 10^{-17}$  | 82             |
| 174 | $CH + \gamma \rightarrow$              |                                  |          |      | $36 \times 10^{-18} \left(\frac{T}{300}\right)^{0.35} \exp\left(-\frac{161.3}{T}\right)$ | 83             |
| 175 | $CH^+ + \gamma \rightarrow$            |                                  |          |      | $1 \times 10^{-19}$  | 84             |
| 176 | $CH_2 + \gamma \rightarrow$            |                                  |          |      | $0.9 \times 10^{-17} \left(\frac{T}{300}\right)^{0.33} \exp\left(-\frac{1629}{T}\right)$ | $T \leq 300$ K |
| 177 | $CH_2 + \gamma \rightarrow$            |                                  |          |      | $46 \times 10^{-16} T^{-0.5} \exp\left(-\frac{4.93}{T^{2/3}}\right)$                     | $T > 300$ K    |
| 178 | $CH_3^+ + \gamma \rightarrow$          |                                  |          |      | $0 \times 10^{-16} \left(\frac{T}{300}\right)^{-0.2}$                                    |                |
| 179 | $CH_3^+ + \gamma \rightarrow$          |                                  |          |      | $5 \times 10^{-18}$  | $T \leq 300$ K |
| 180 | $CH_3^+ + \gamma \rightarrow$          |                                  |          |      | $14 \times 10^{-18} \left(\frac{T}{300}\right)^{-0.15} \exp\left(\frac{68}{T}\right)$    | $T > 300$ K    |

Table B3. List of reactions included in our chemical model that involve cosmic rays or cosmic-ray induced UV emission

| No. | Reaction  | Rate ( $s^{-1} \zeta_H^{-1}$ )                 | Ref.     |
|-----|---|--|----------|
| 199 | $H + c.r. \rightarrow H^+ + e^-$                | $R_{199} = 1.0$                                | —        |
| 200 | $He + c.r. \rightarrow He^+ + e^-$              | $R_{200} = 1.1$                                | 1        |
| 201 | $H_2 + c.r. \rightarrow H^+ + H + e^-$          | $R_{201} = 0.037$                              | 1        |
| 202 | $H_2 + c.r. \rightarrow H + H$                  | $R_{202} = 0.22$                               | 1        |
| 203 | $H_2 + c.r. \rightarrow H^+ + H^-$              | $R_{203} = 6.5 \times 10^{-4}$                 | 1        |
| 204 | $H_2 + c.r. \rightarrow H_2^+ + e^-$            | $R_{204} = 2.0$                                | 1        |
| 205 | $C + c.r. \rightarrow C^+ + e^-$                | $R_{205} = 3.8$                                | 1        |
| 206 | $O + c.r. \rightarrow O^+ + e^-$                | $R_{206} = 5.7$                                | 1        |
| 207 | $CO + c.r. \rightarrow CO^+ + e^-$              | $R_{207} = 6.5$                                | 1        |
| 208 | $C + \gamma_{c.r.} \rightarrow C^+ + e^-$       | $R_{208} = 2800$                               | 2        |
| 209 | $CH + \gamma_{c.r.} \rightarrow C + H$          | $R_{209} = 4000$                               | 3        |
| 210 | $CH^+ + \gamma_{c.r.} \rightarrow C^+ + H$      | $R_{210} = 960$                                | 3        |
| 211 | $CH_2 + \gamma_{c.r.} \rightarrow CH_2^+ + e^-$ | $R_{211} = 2700$                               | 1        |
| 212 | $CH_2 + \gamma_{c.r.} \rightarrow CH + H$       | $R_{212} = 2700$                               | 1        |
| 213 | $C_2 + \gamma_{c.r.} \rightarrow C + C$         | $R_{213} = 1300$                               | 3        |
| 214 | $OH + \gamma_{c.r.} \rightarrow O + H$          | $R_{214} = 2800$                               | 3        |
| 215 | $H_2O + \gamma_{c.r.} \rightarrow OH + H$       | $R_{215} = 5300$                               | 3        |
| 216 | $O_2 + \gamma_{c.r.} \rightarrow O + O$         | $R_{216} = 4100$                               | 3        |
| 217 | $O_2 + \gamma_{c.r.} \rightarrow O_2^+ + e^-$   | $R_{217} = 640$                                | 3        |
| 218 | $CO + \gamma_{c.r.} \rightarrow C + O$          | $R_{218} = 0.21 T^{1/2} x_{H_2} x_{CO}^{-1/2}$ | 4        |
| 197 | $O_2 + \gamma \rightarrow O + O$                | $R_{197} = 7.0 \times 10^{-10}$                | 7        |
| 198 | $CO + \gamma \rightarrow C + O$                 | $R_{198} = 2.0 \times 10^{-10}$                | See §2.2 |

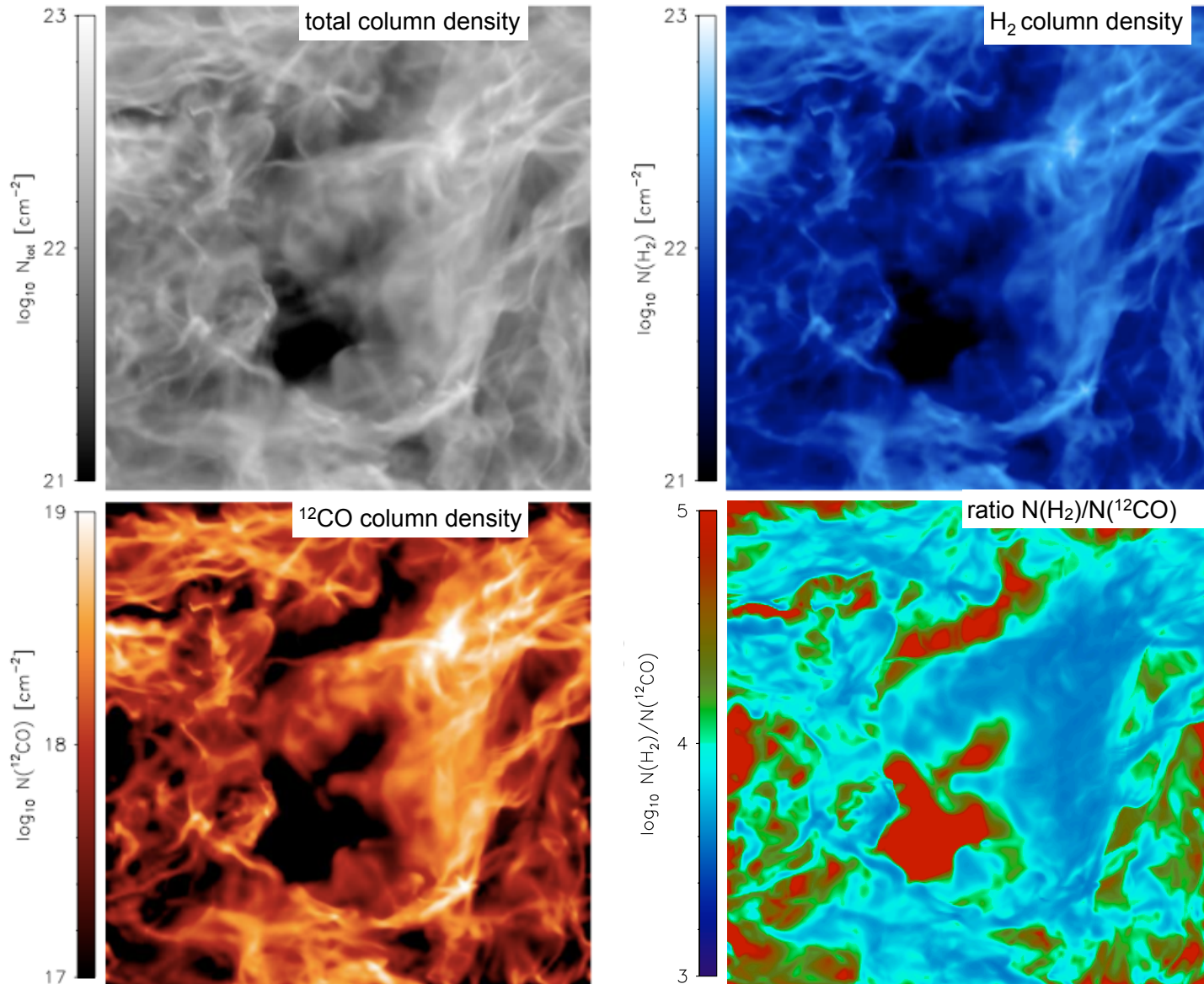
|    |                |     |                                |                                 |    |
|----|----------------|-----|--------------------------------|---------------------------------|----|
| 86 | $HCO^+ + C$    | 140 | $O^- + C \rightarrow CO + e^-$ | $k_{140} = 5.0 \times 10^{-10}$ | 28 |
| 87 | $HCO^+ + H_2O$ |     | $\rightarrow CO + H_3O^+$      | $k_{87} = 2.5 \times 10^{-9}$   | 28 |

# effects of chemistry



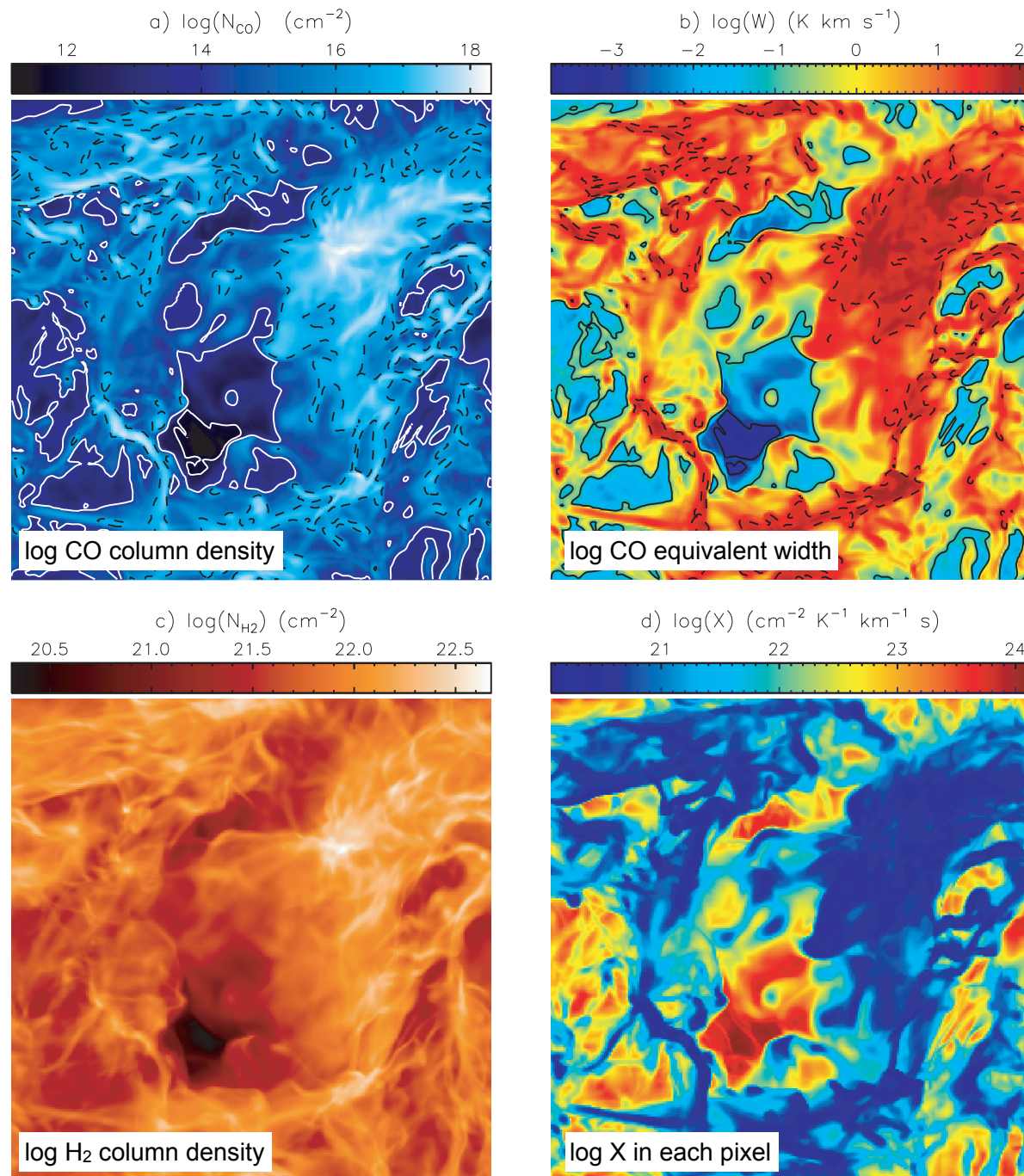
(Glover et al. 2010)

# effects of chemistry



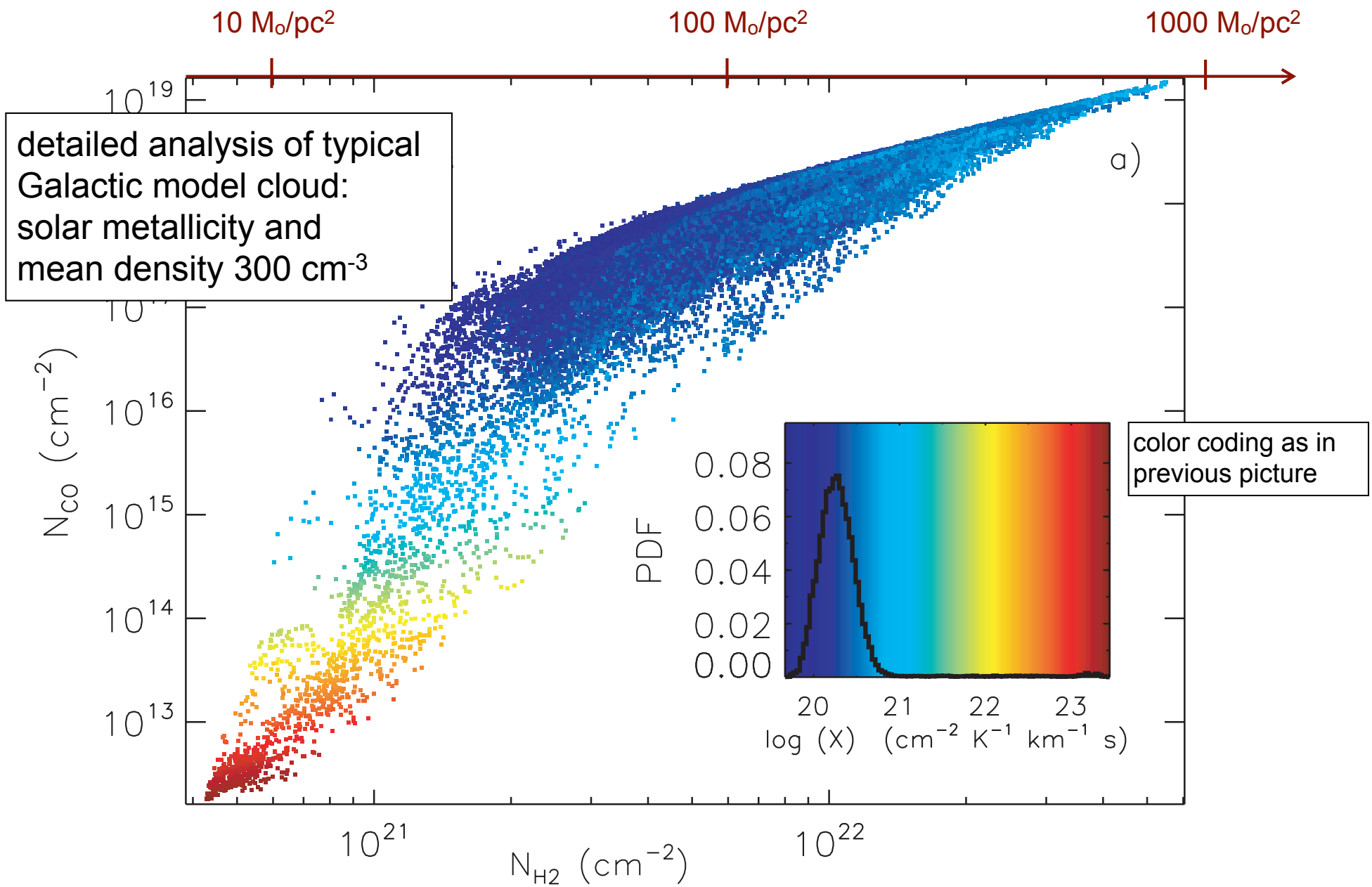
(Glover et al. 2010)





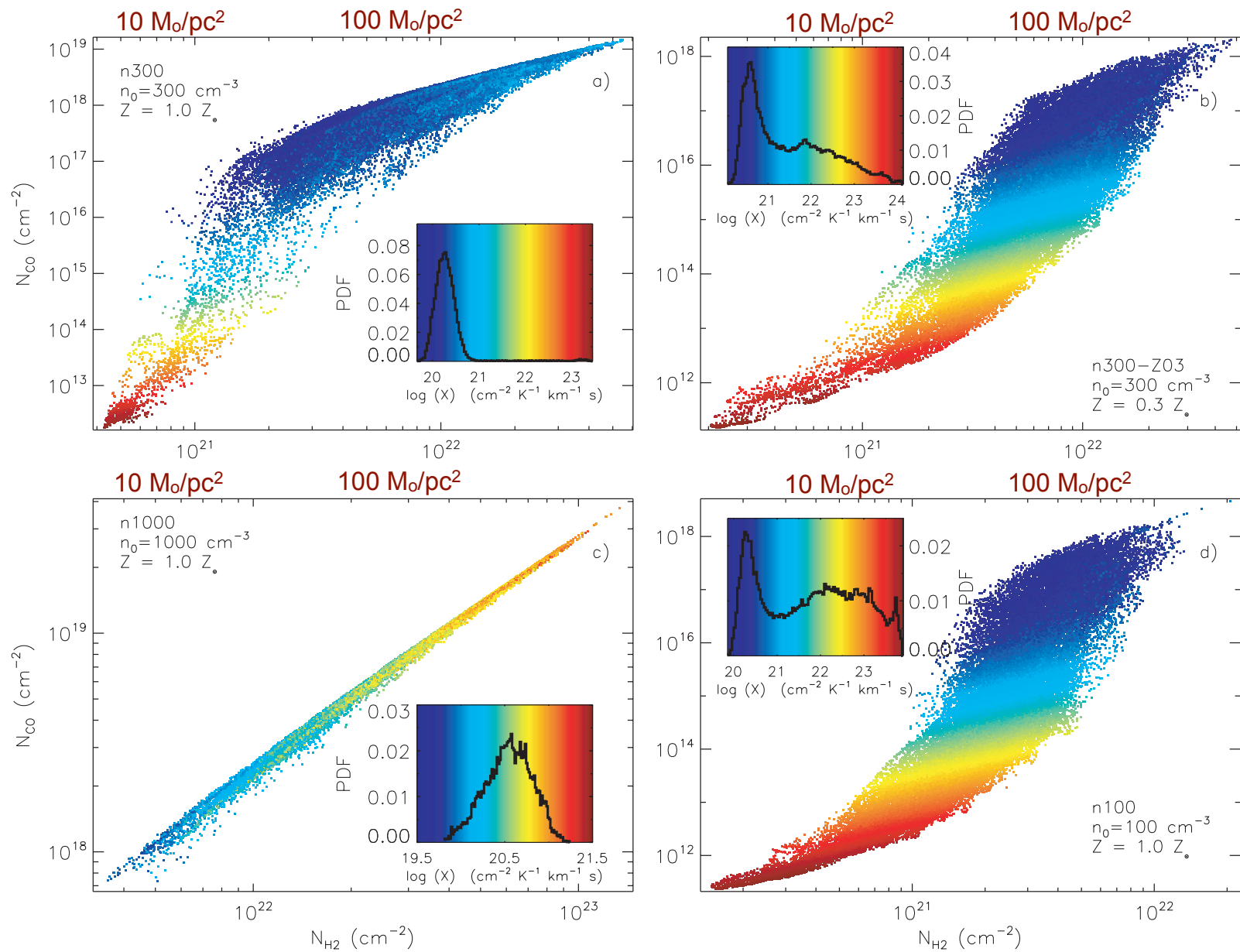
(Shetty, Glover, Dullemond, Klessen 2011)

**Figure 4.** Images of (a)  $N_{\text{CO}}$ , (b)  $W$ , (c)  $N_{\text{H}_2}$  and (d) the  $X$  factor of model n300-Z03. Each side has a length of 20 pc. In (a) and (b), solid contours indicate  $\log(N_{\text{CO}}) = 12, 14$  and  $\log(W) = -3, -1$ ; dashed contours are  $\log(N_{\text{CO}}) = 16.5$  and  $\log(W) = 1.5$  (see the text and Fig. 2d).



(Shetty, Glover, Dullemond, Klessen 2011)

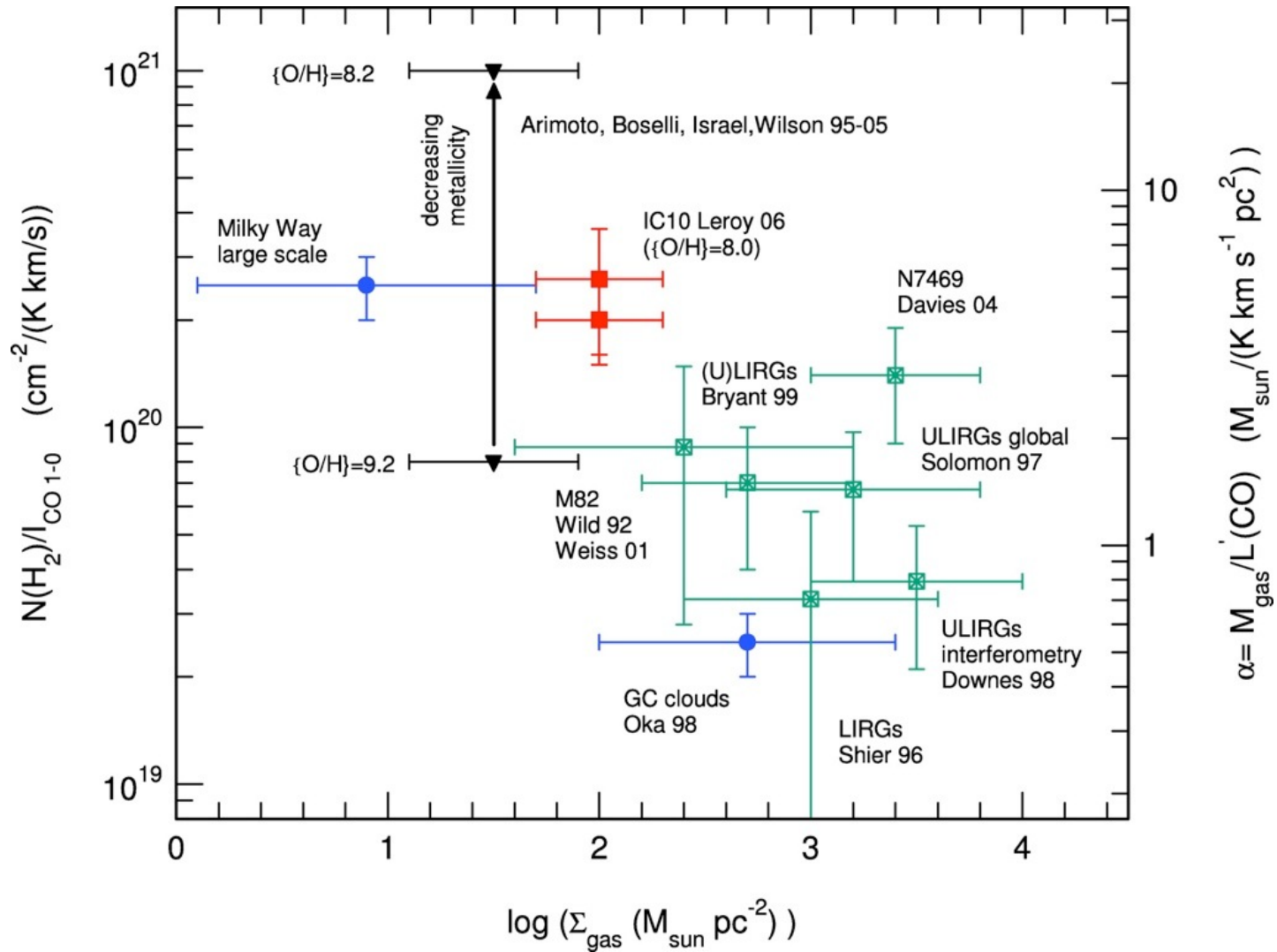




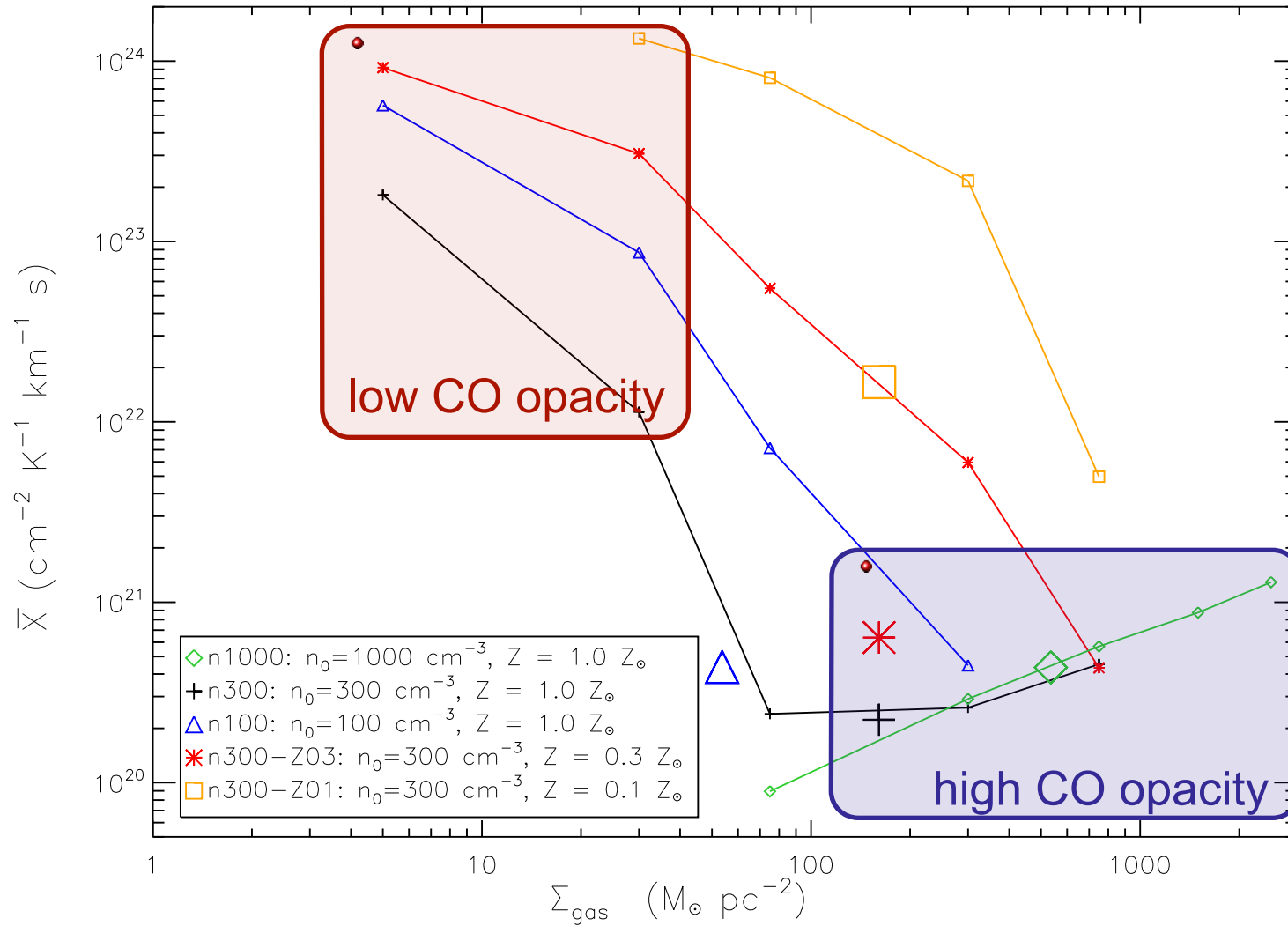
(Shetty, Glover, Dullemond, Klessen 2011)

**Figure 5.** X factor for four models.  $N_{\text{CO}}$  is plotted as a function of  $N_{\text{H}_2}$ . The colour of each point indicates the X factor. Inset figures show the colour scale and PDF of the X factor. The corresponding maps of  $N_{\text{H}_2}$ ,  $N_{\text{CO}}$  and the X factor from model n300-Z03 are shown in Fig. 4.

# observed x-factor

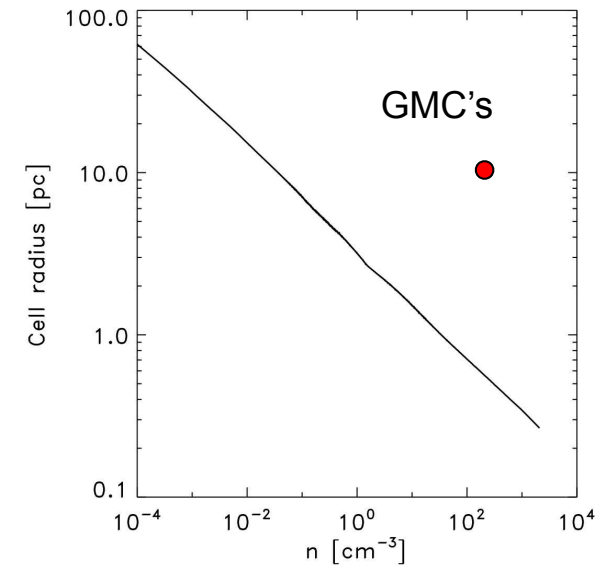
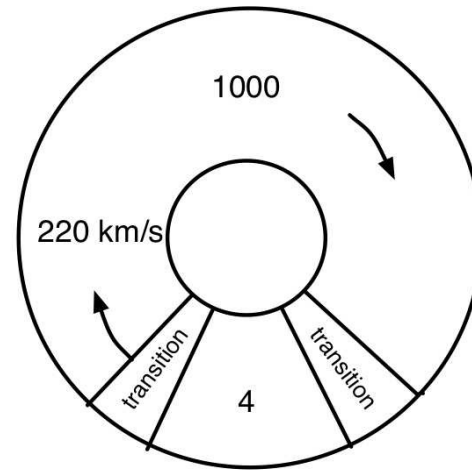
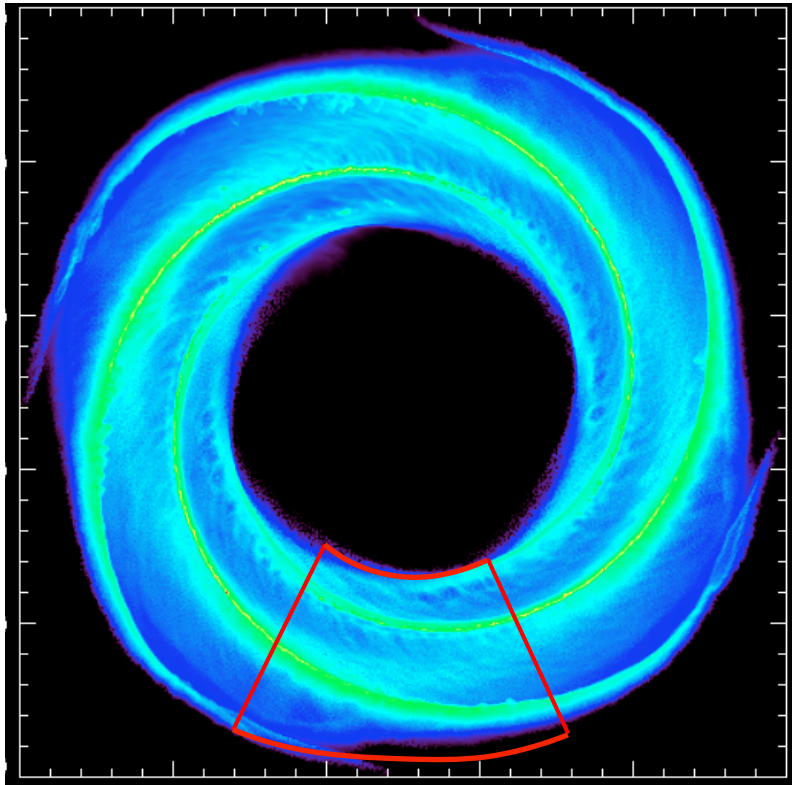


# derived x-factor



CO-dark gas

# modeling molecular cloud formation

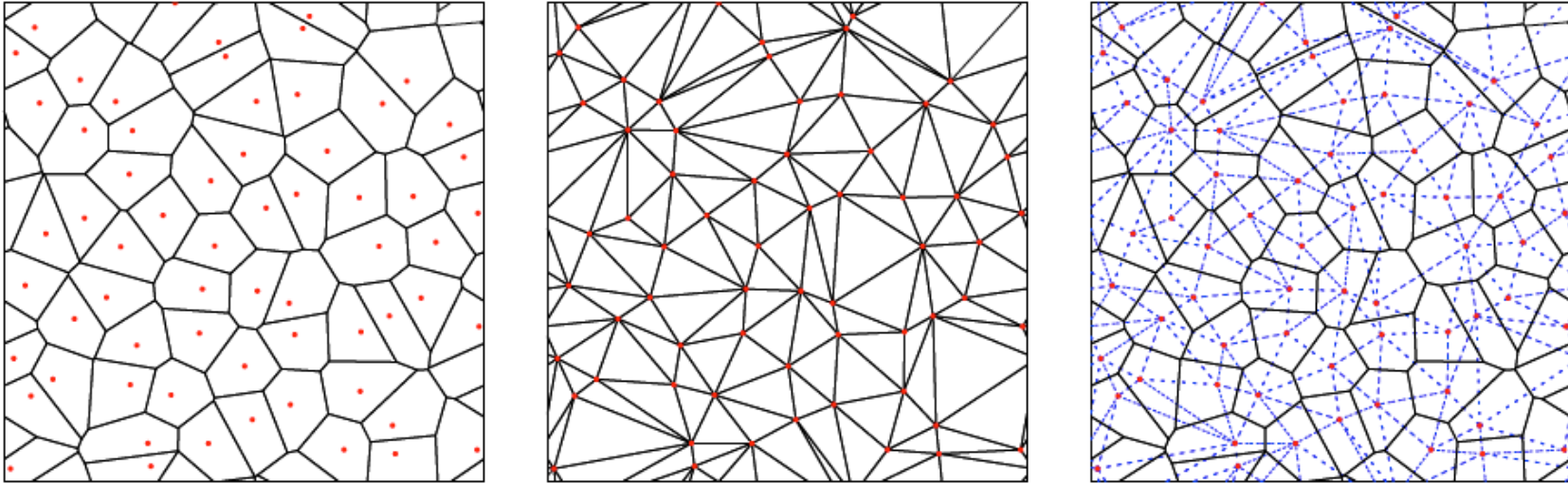


- Arepo moving mesh code (*Springel 2010*)
- time dependent chemistry (*Glover et al. 2007*)  
gives heating & cooling in a 2 phase medium
- two layers of refinement with mass resolution down to 4  $M_{\odot}$  in full Galaxy simulation
- UV field and cosmic rays
- TreeCol (*Clark et al. 2012*)
- external spiral potential (*Dobbs & Bonnell 2006*)
- no gas self-gravity, SN, or magnetic fields yet

| Simulation   | Surface Density<br>$M_{\odot} \text{ pc}^{-2}$ | Radiation Field<br>$G_0$ |
|--------------|--|--------------------------|
| Milky Way    | 10   | 1                        |
| Low Density  | 4  | 1                        |
| Strong Field | 10   | 10                       |
| Low & Weak   | 4  | 0.1                      |

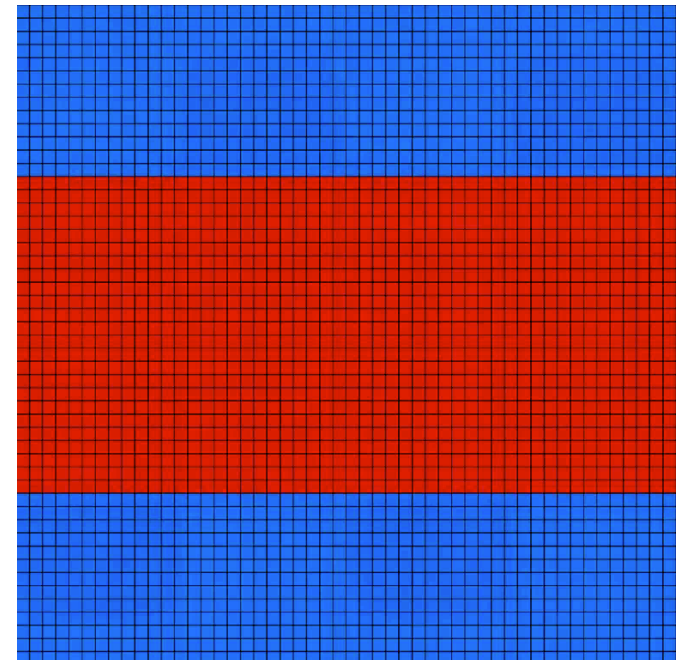


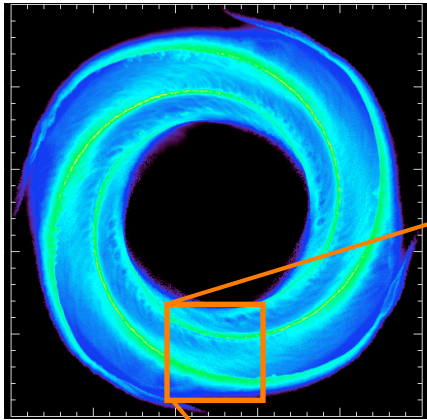
# numerical method



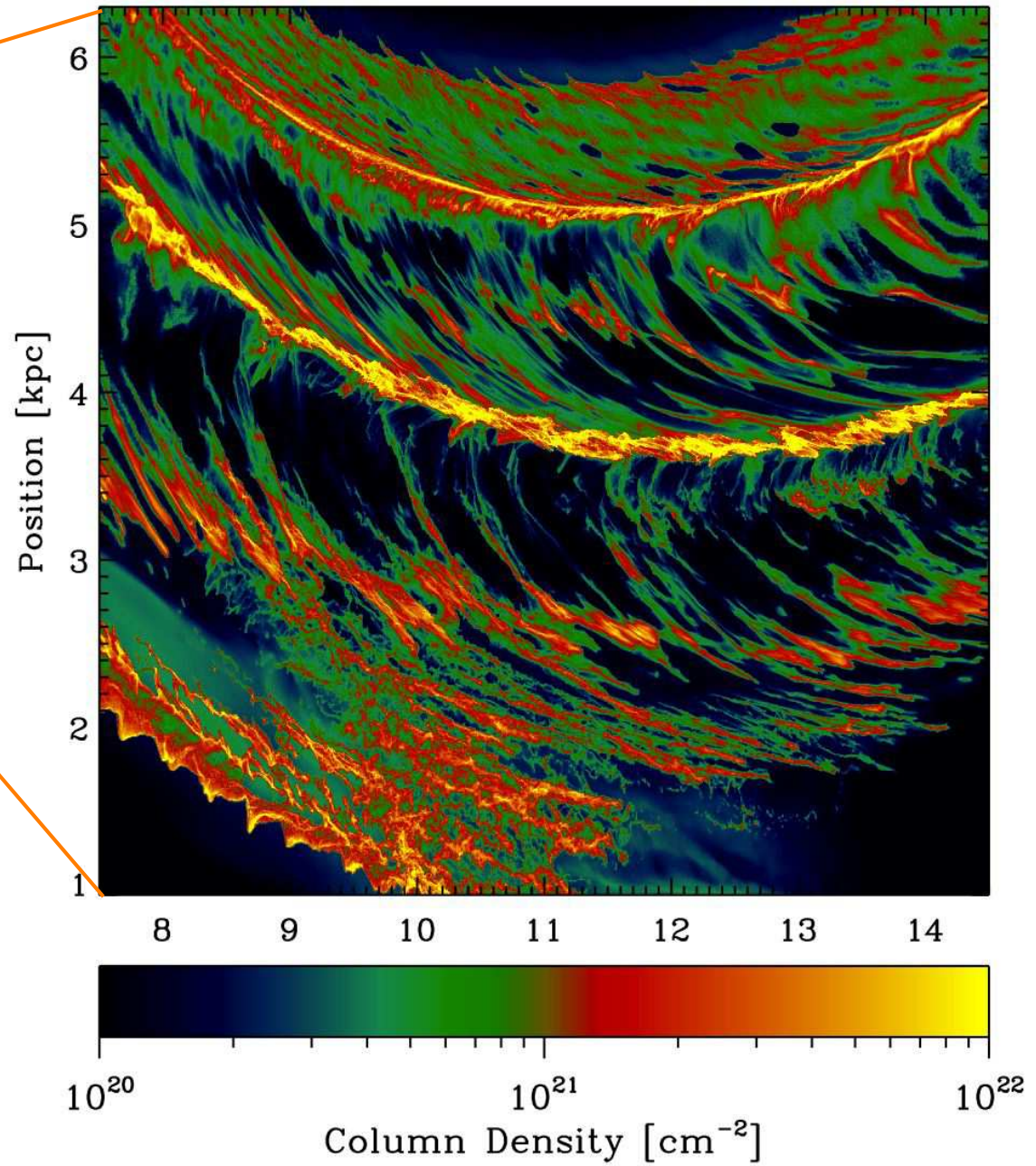
*moving mesh code **Arepo**:*

- semi-Lagrangian
- flexible refinement
- fluid instabilities and no artificial clumping  
(Agertz et al. 2007)
- can also handle sub-sonic turbulence  
(Bauer & Springel 2012)
- no preferred geometry

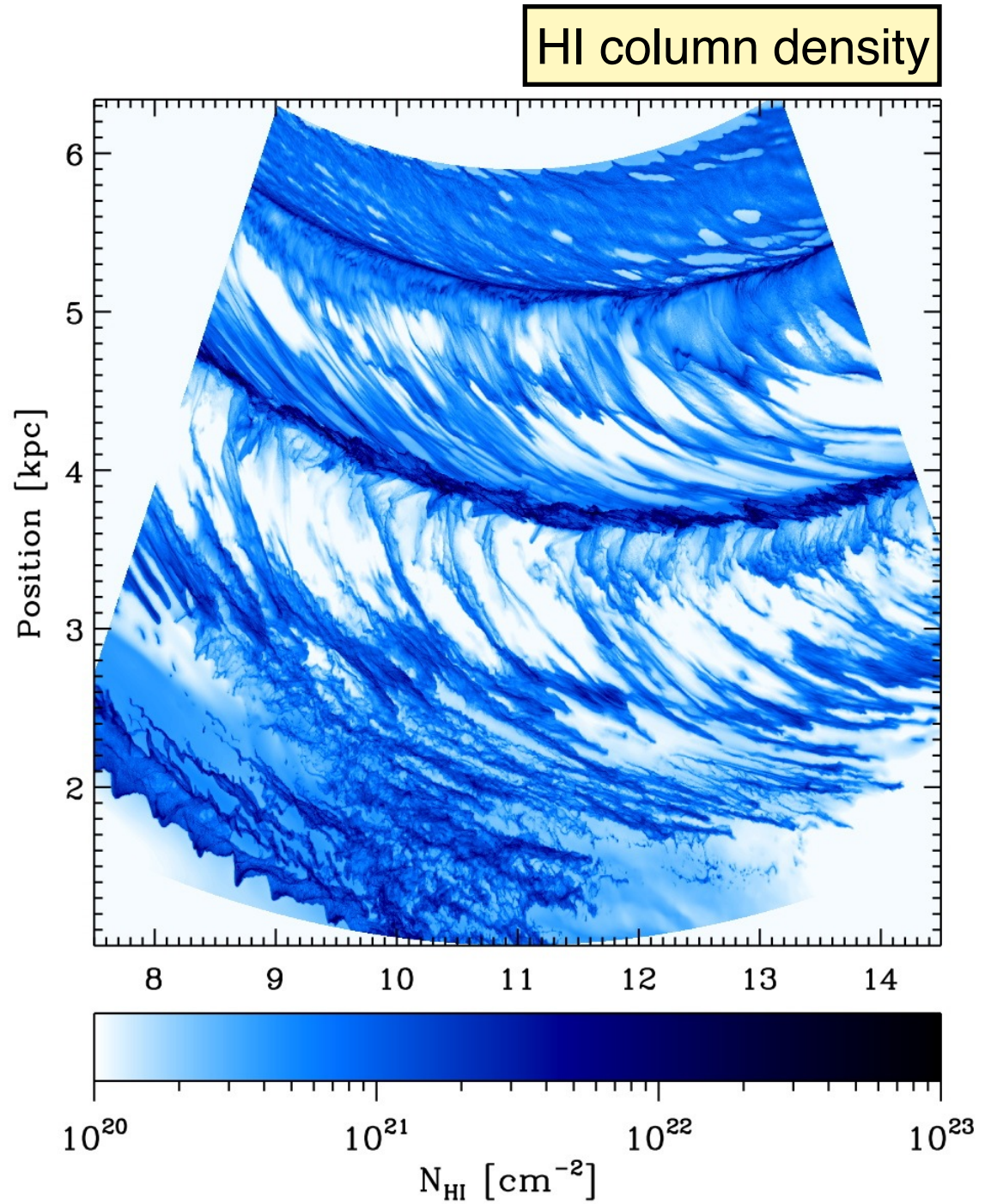
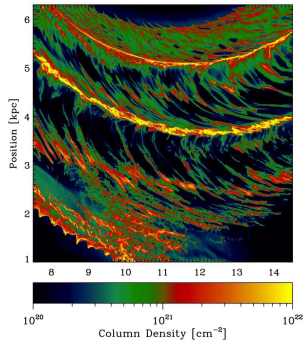




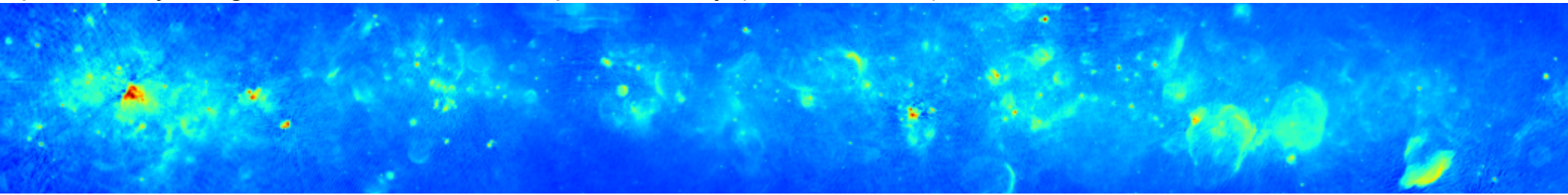
total column density



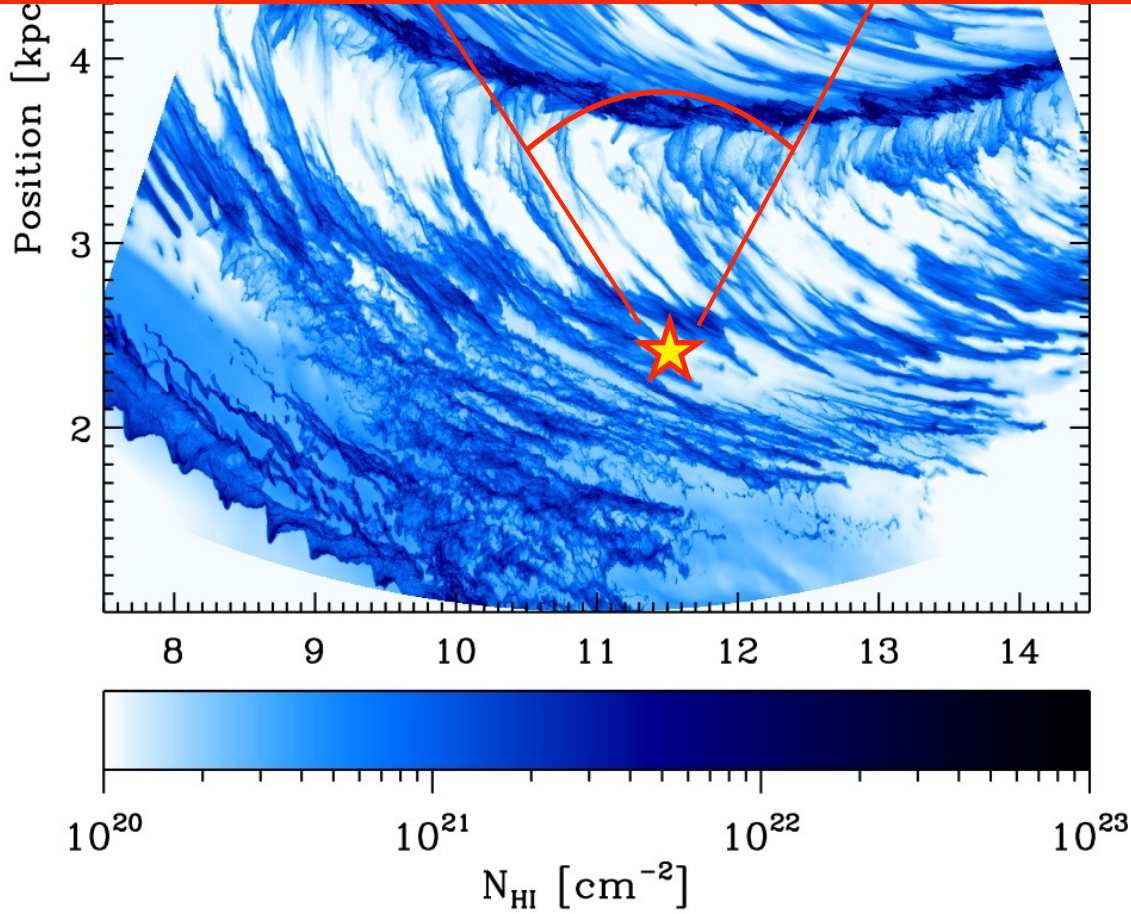




preliminary image from THOR Galactic plane survey (PI H. Beuther): continuum emission around 21 cm



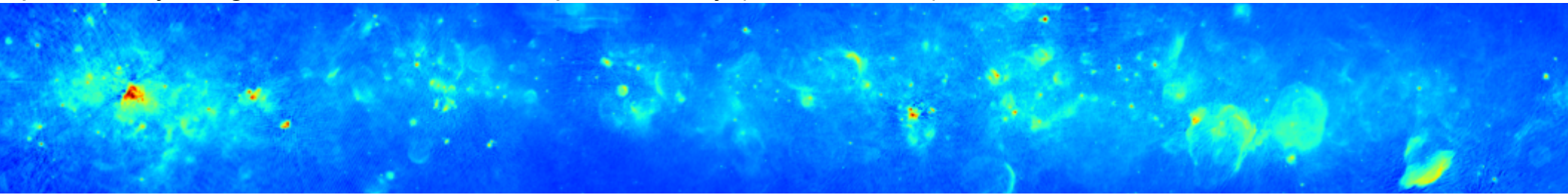
next step: produce all sky maps at various positions in the model galaxy (use RADMC-3D)



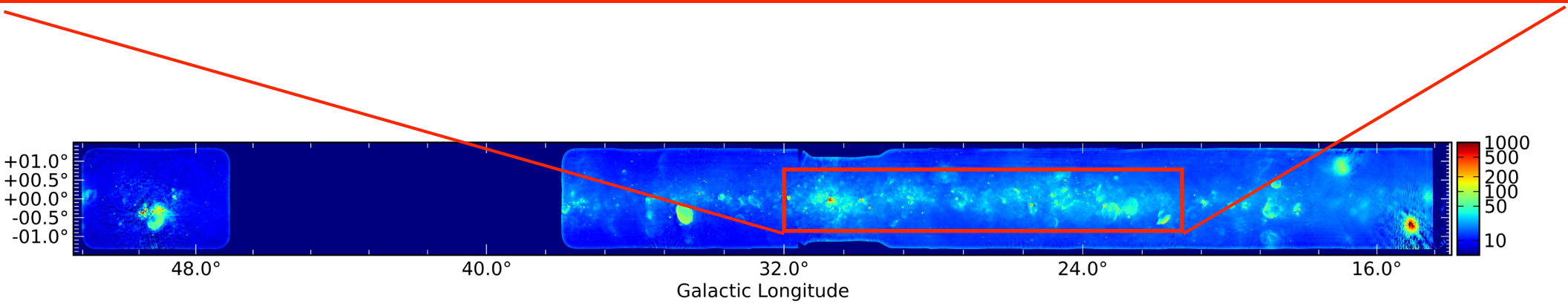
(Smith et al., 2014, MNRAS, 441, 1628)



preliminary image from THOR Galactic plane survey (PI H. Beuther): continuum emission around 21 cm



next step: produce all sky maps at various positions in the model galaxy (use RADMC-3D)

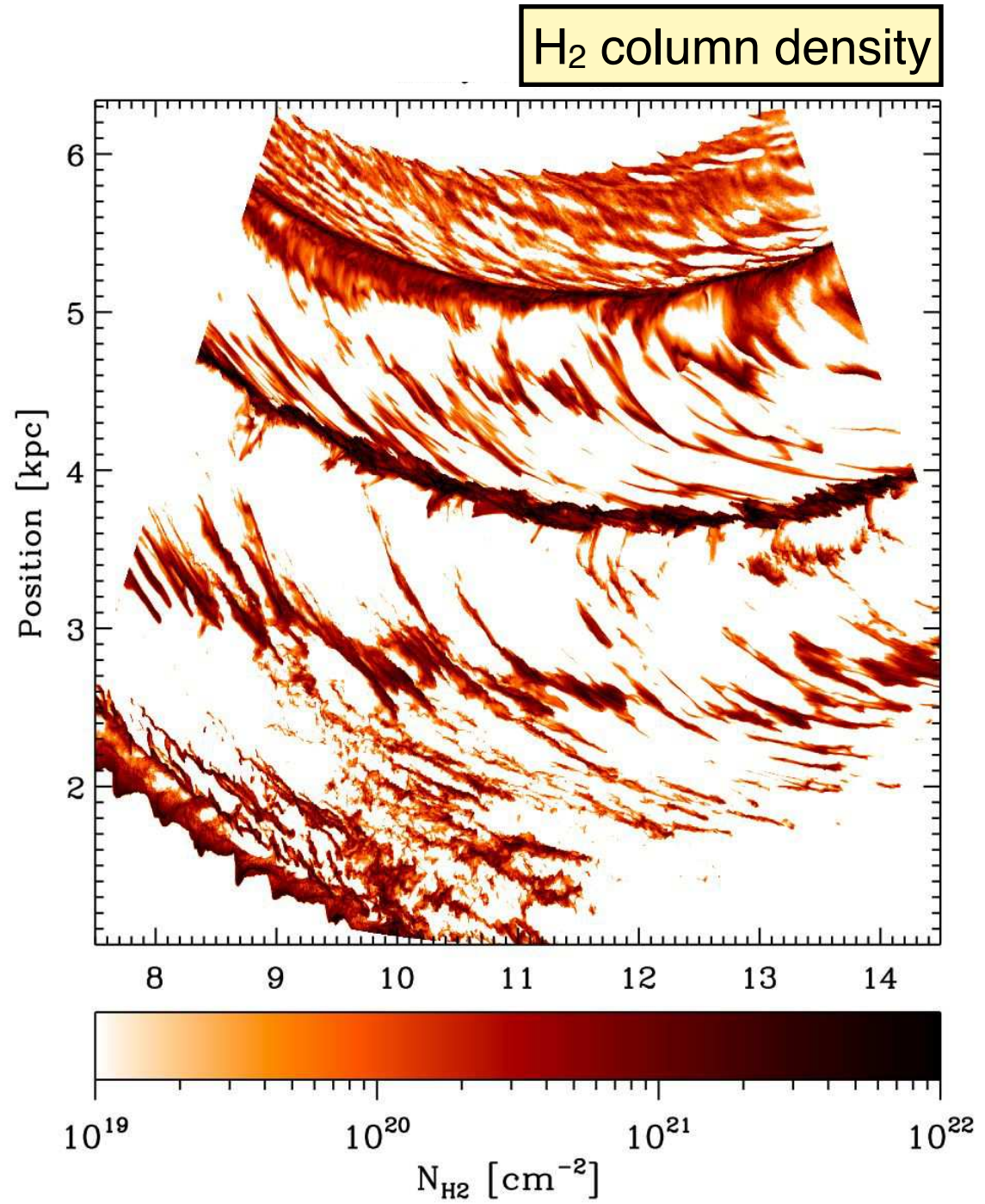
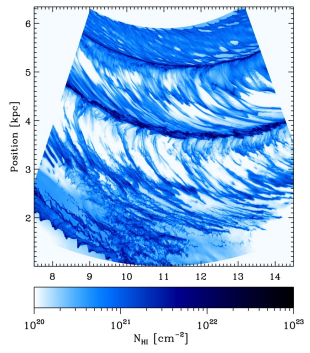
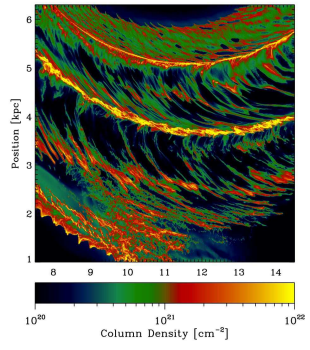


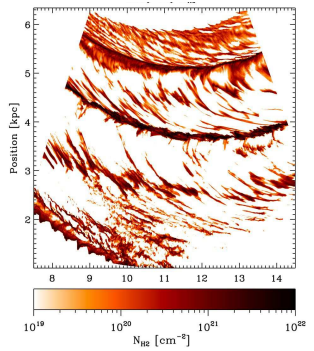
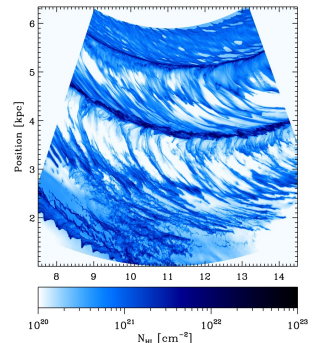
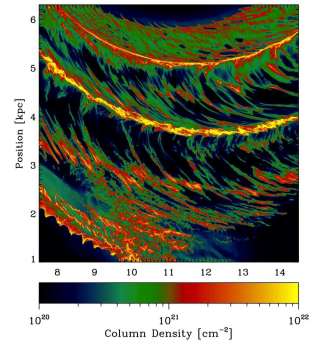
The **HI/OH/Recombination**  
line survey of the Milky Way

**THOR**

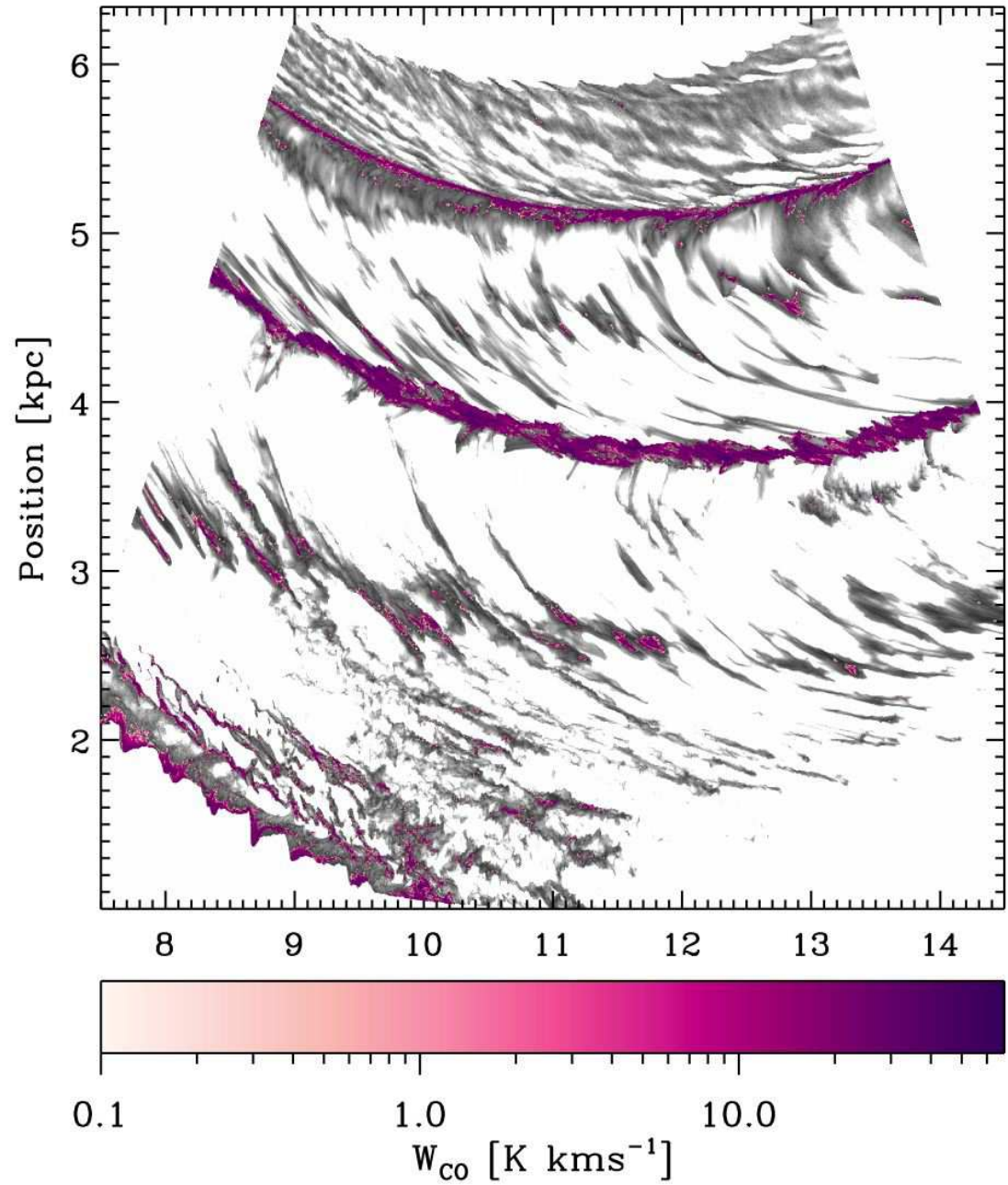
<http://www.mpia.de/thor/Overview.html>





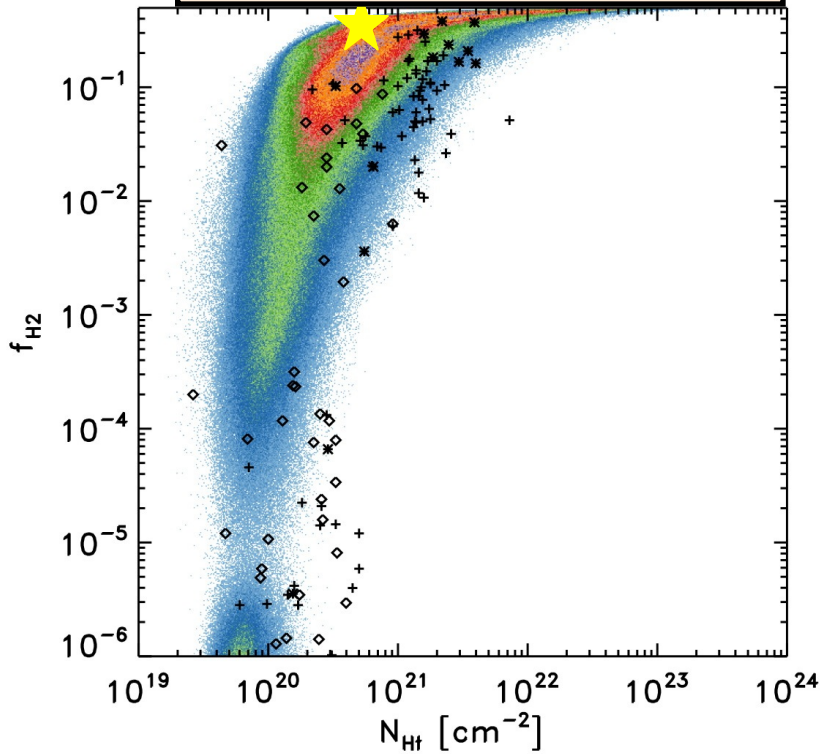


# CO column density

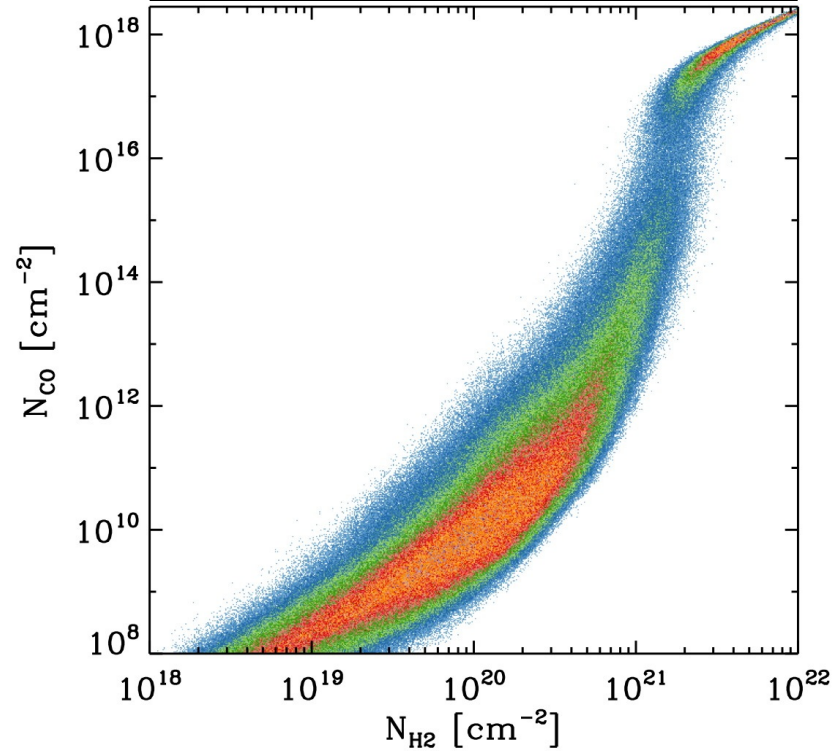




H<sub>2</sub> fraction vs. column density N



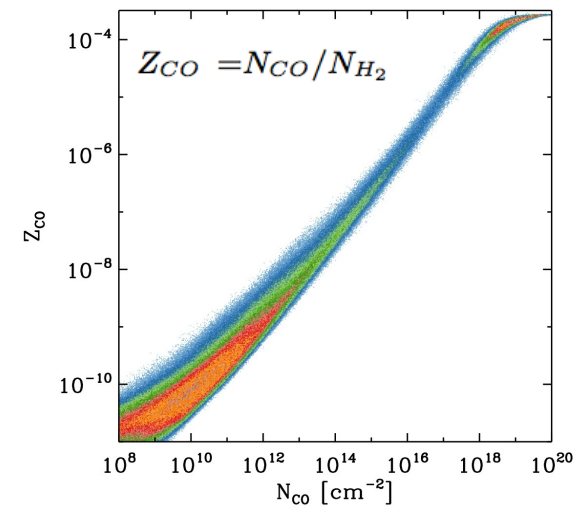
CO col. density vs. H<sub>2</sub> col. density



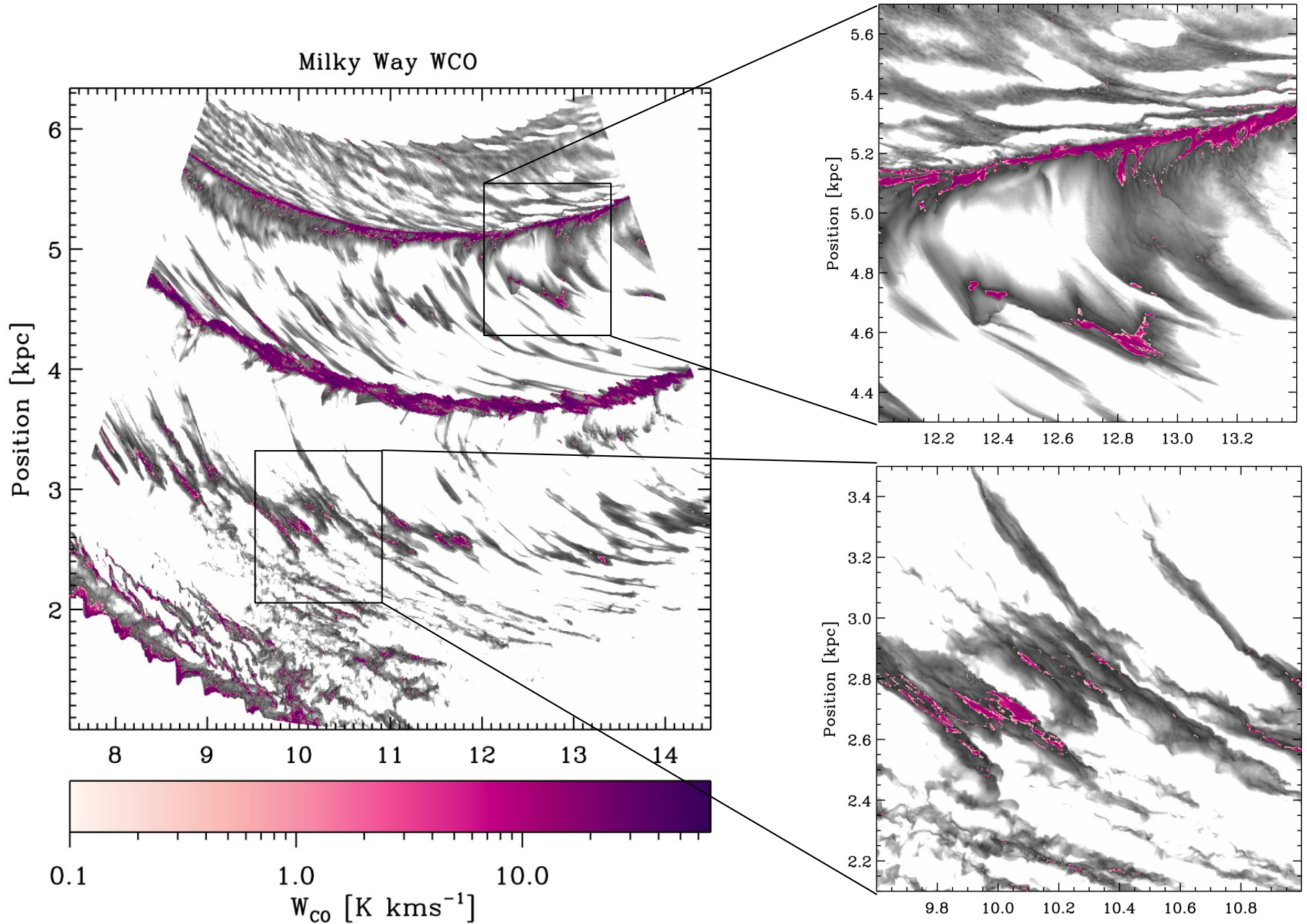
H<sub>2</sub> forms above column densities of  $10^{20}$  cm<sup>-2</sup>

CO columns jump after  $N_{H_2} \sim 10^{21}$  cm<sup>-2</sup>

$$\log(Z_{CO} [cm^{-2}]) = -18.1 \log(N_{CO} [cm^{-2}]) + 0.8.$$

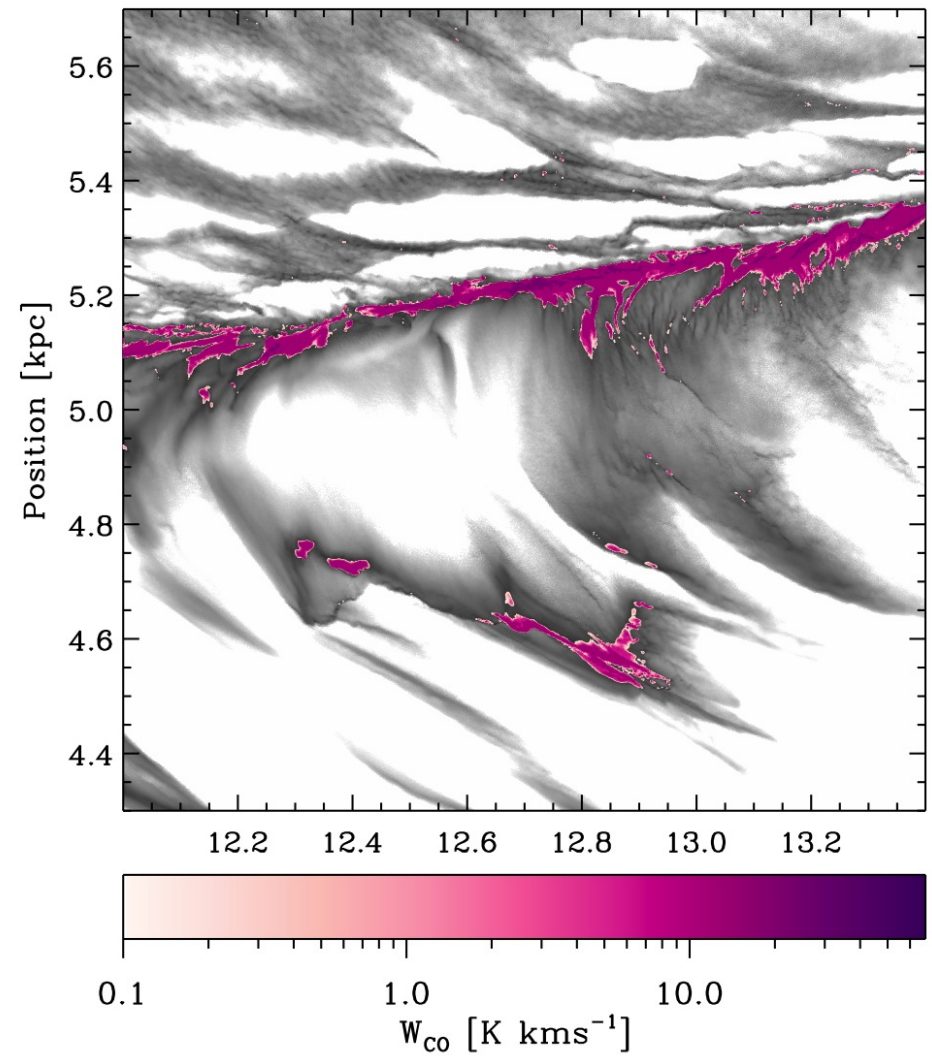
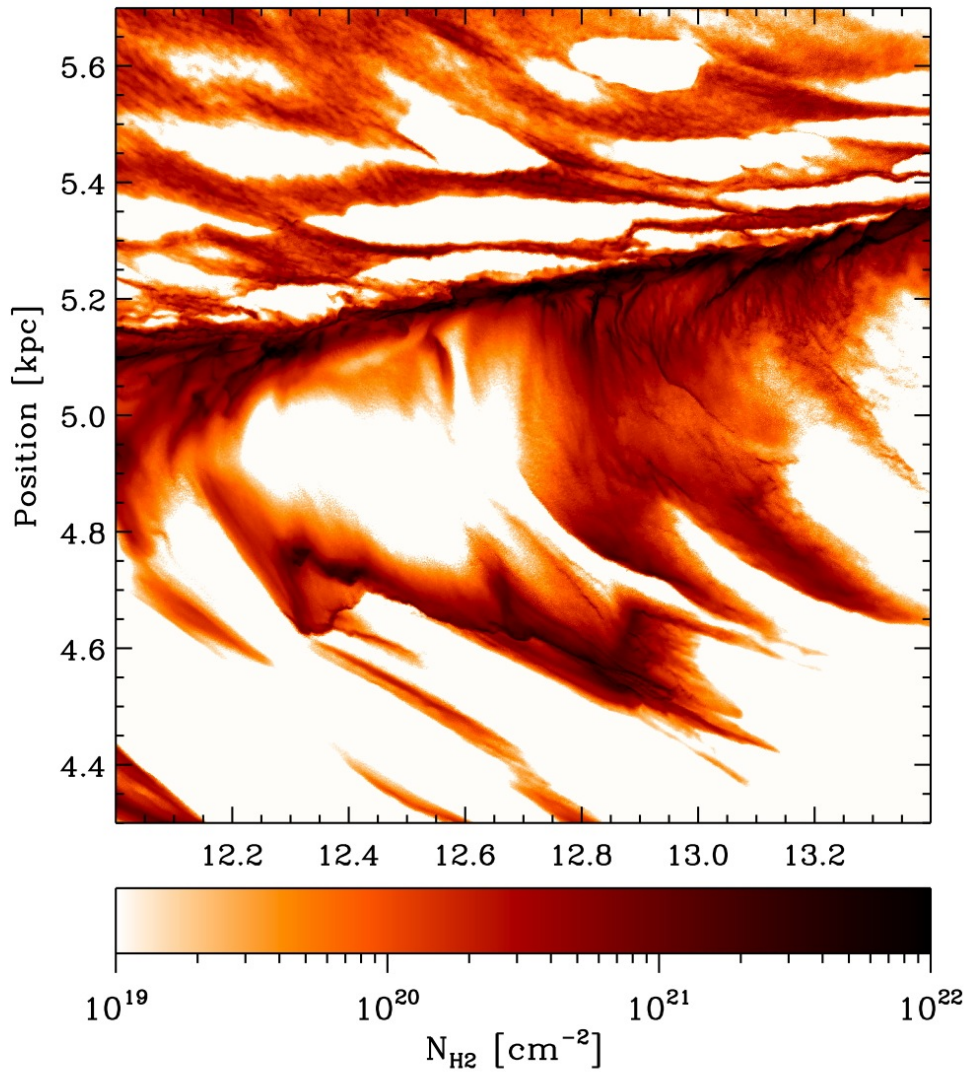


# details of CO emission



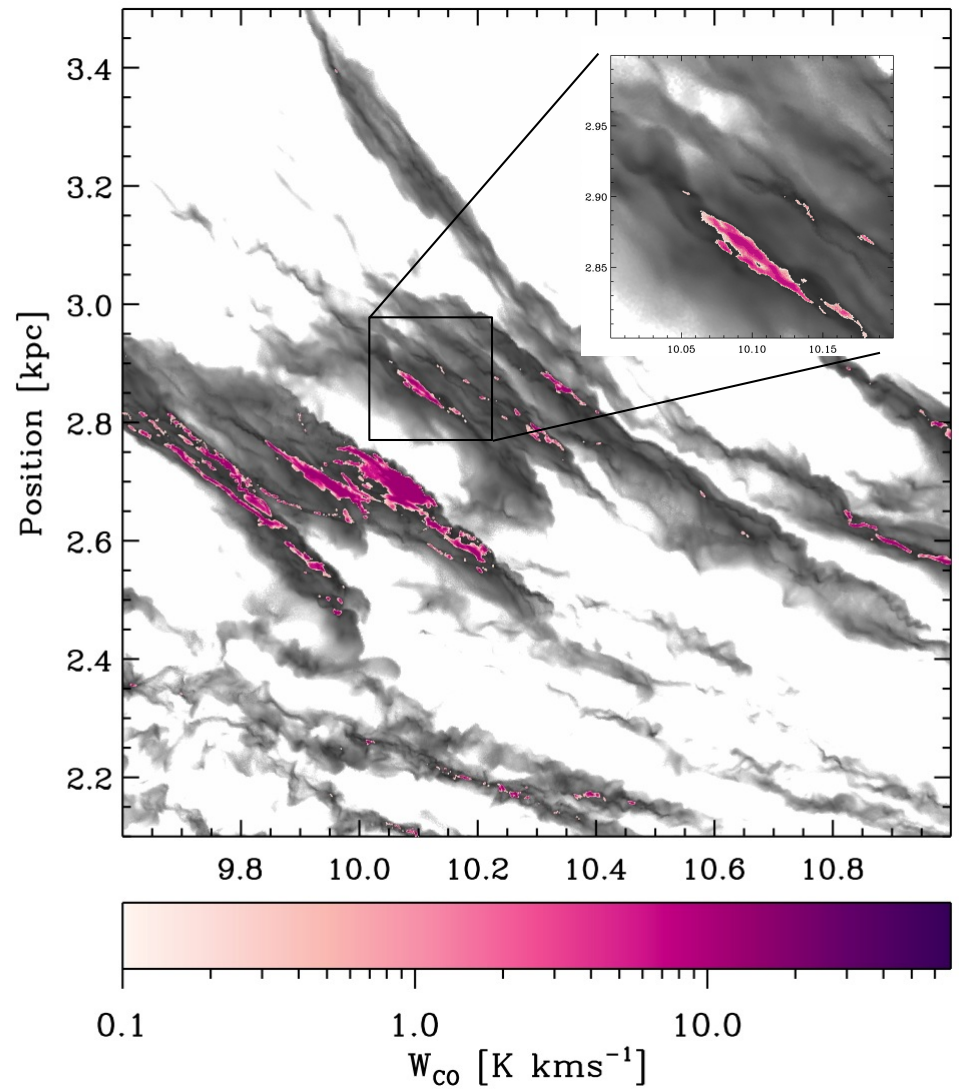
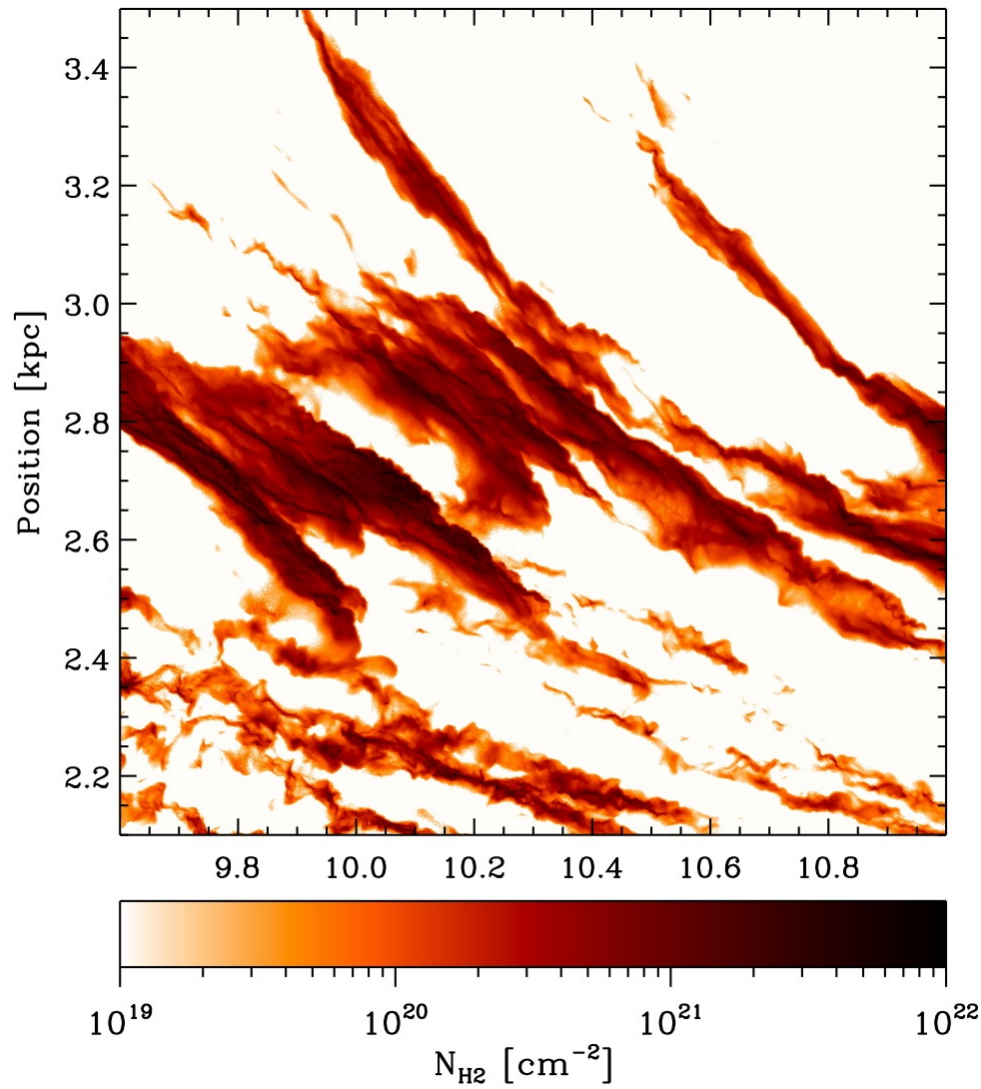


# relation between CO and H<sub>2</sub>



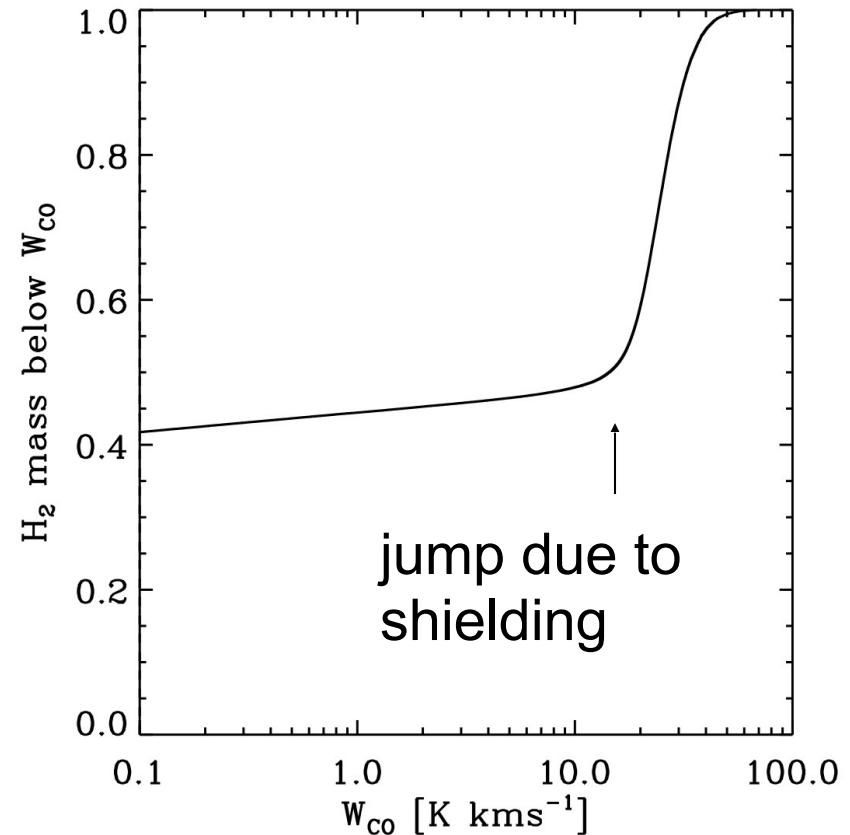
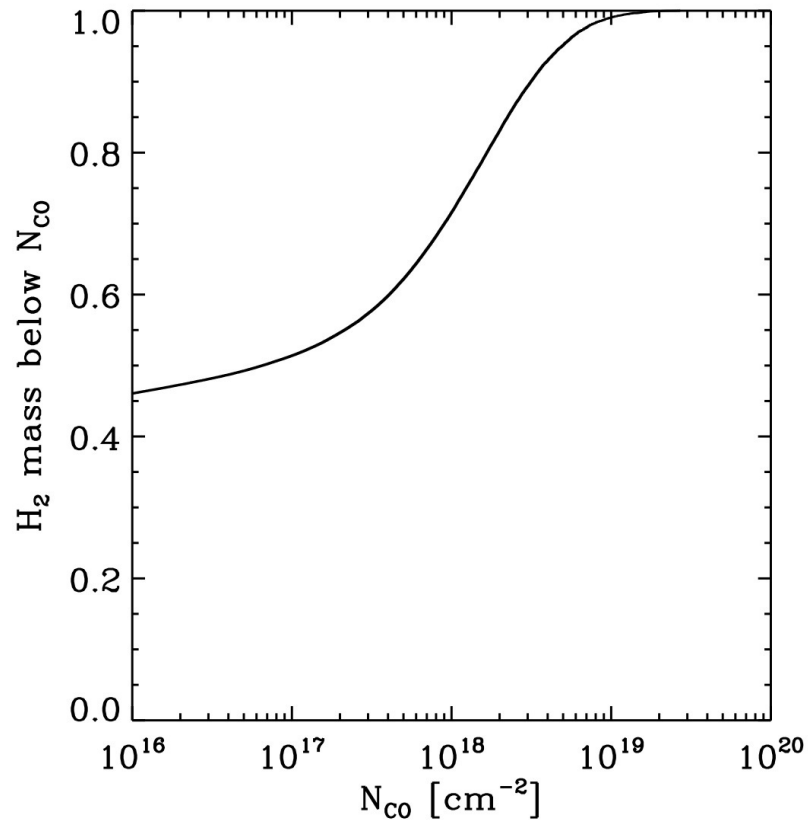


# relation between CO and H<sub>2</sub>



Filamentary molecular clouds in inter-arm regions are likely only the observable parts of much larger structures.

# dark gas fraction



46% molecular gas below CO column densities of  $10^{16}$  cm<sup>-2</sup>

42% has an integrated CO emission of less than 0.1 K kms<sup>-1</sup>

$$f_{\text{DG}} = 0.42$$

$$X_{\text{CO}} = 2.2 \times 10^{20} \text{ cm}^{-2} \text{K}^{-1} \text{km}^{-1} \text{s}$$

# dark gas fraction

## *Observational estimates:*

Grenier et al. (2005)  $f_{\text{DG}} = 0.33\text{-}0.5$

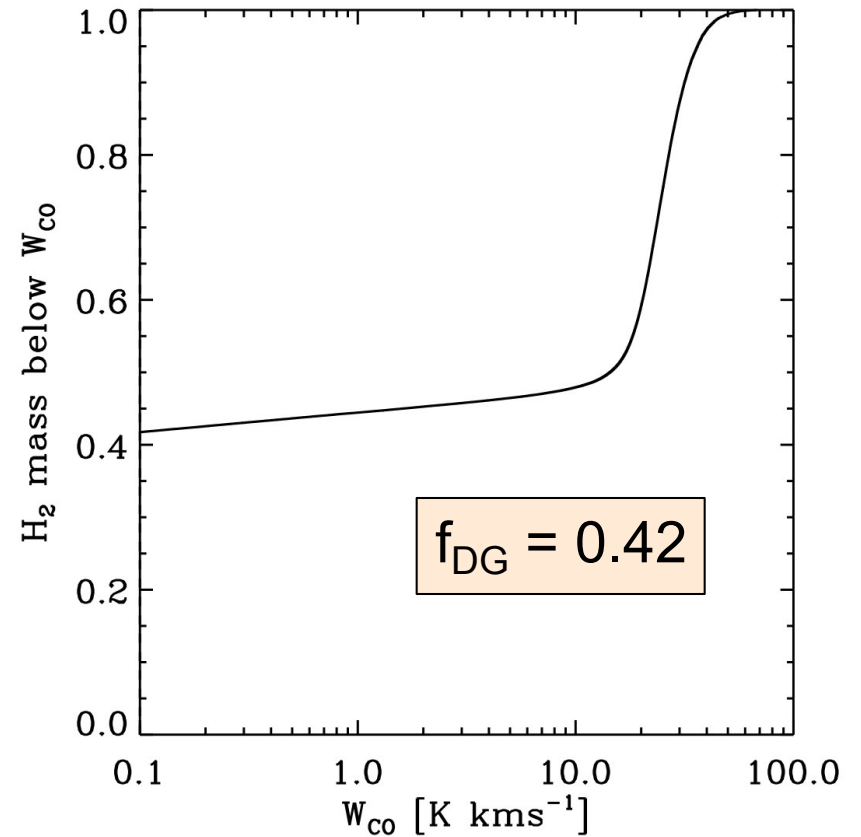
Planck coll. (2011)\*  $f_{\text{DG}} = 0.54$

Paradis et al. (2012)\*  $f_{\text{DG}} = 0.62$

(inner  $f_{\text{DG}} = 0.71$ , outer  $f_{\text{DG}} = 0.43$ )

Pineda et al. (2013)  $f_{\text{DG}} = 0.3$

Roman-Duval et al.  
(in prep.)  $f_{\text{DG}} \sim 0.5$



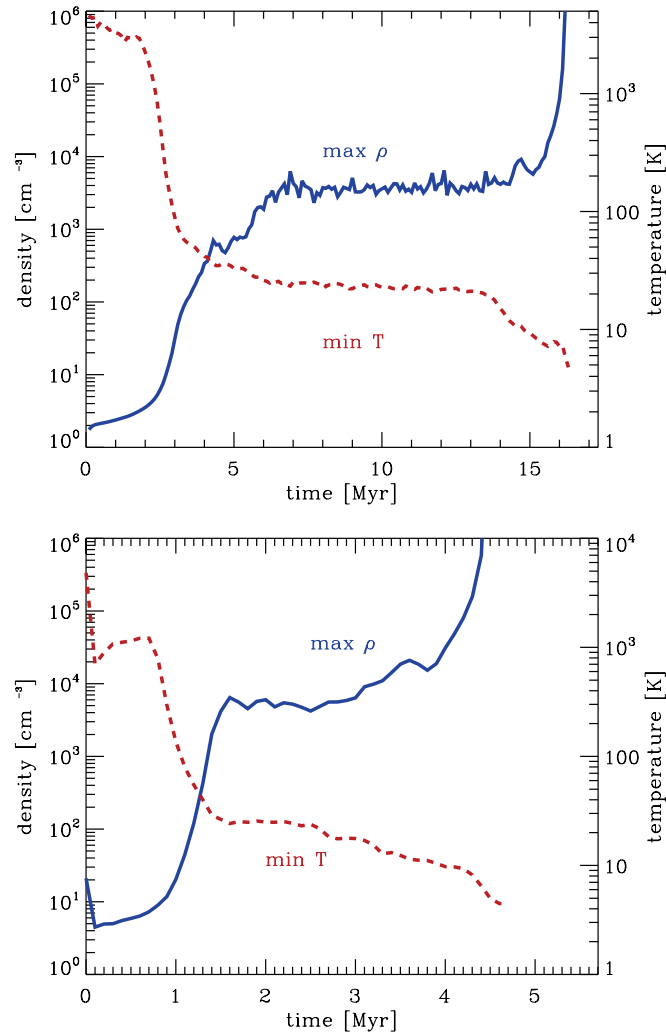
\* dust methods have large uncertainties.

# is there CO-dark H<sub>2</sub> gas?

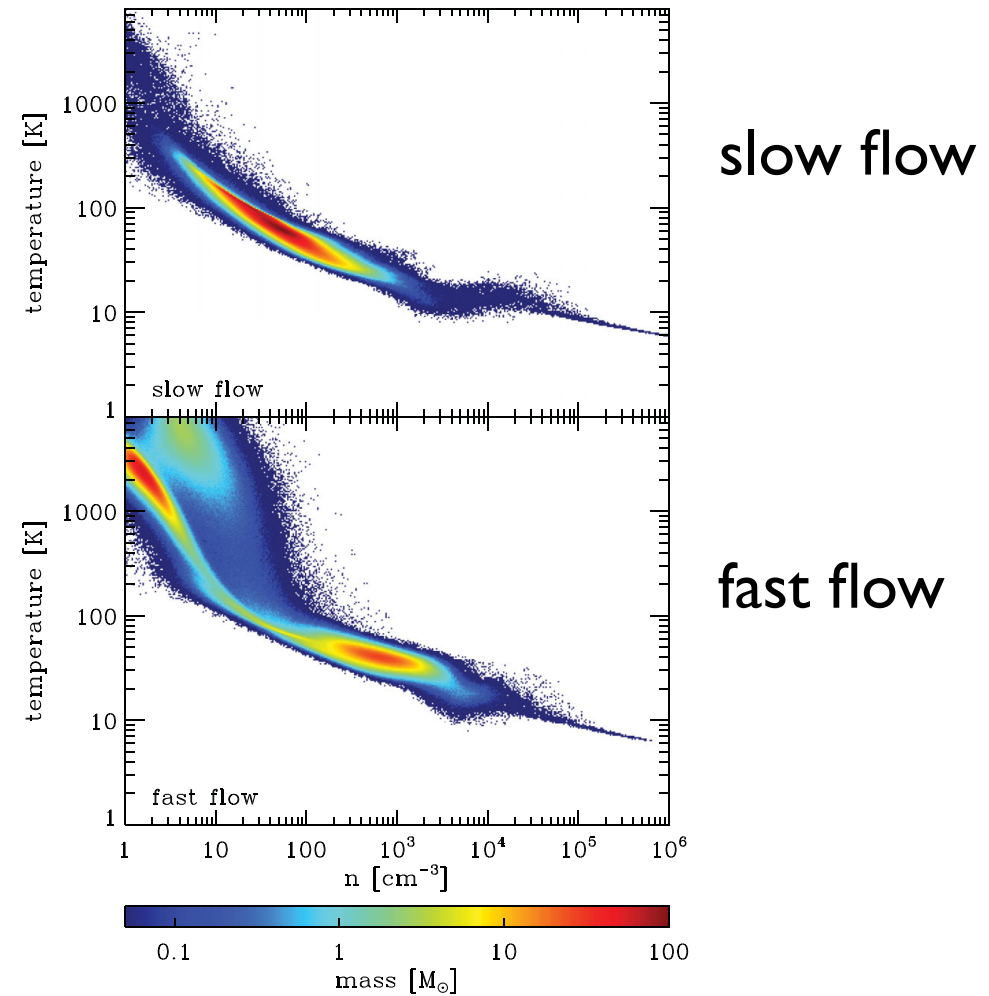
- there is increasing evidence, that a significant fraction of the H<sub>2</sub> gas in galaxies is not traced by CO (e.g. Pringle, Allen, Lubov 2001, Hosokawa & Inutsuka 2007, Clark et al. 2012)
- 3D simulations of colliding HI gas forming molecular clouds at the stagnation region performed by Paul Clark in Heidelberg
  - SPH (also with FLASH)
  - full fledged CO chemistry
  - TREECOL for calculating extinction
  - 'standard' dust model
  - sink particles to account for local collapse (star formation)
  - two models: slow and fast flow



# further evidence form detailed colliding flow calculations



**Figure 3.** Evolution with time of the maximum density (blue, solid line) and minimum temperature (red, dashed line) in the slow flow (top panel) and the fast flow (bottom panel). Note that at any given instant, the coldest SPH particle is not necessarily the densest, and so the lines plotted are strictly independent of one another.

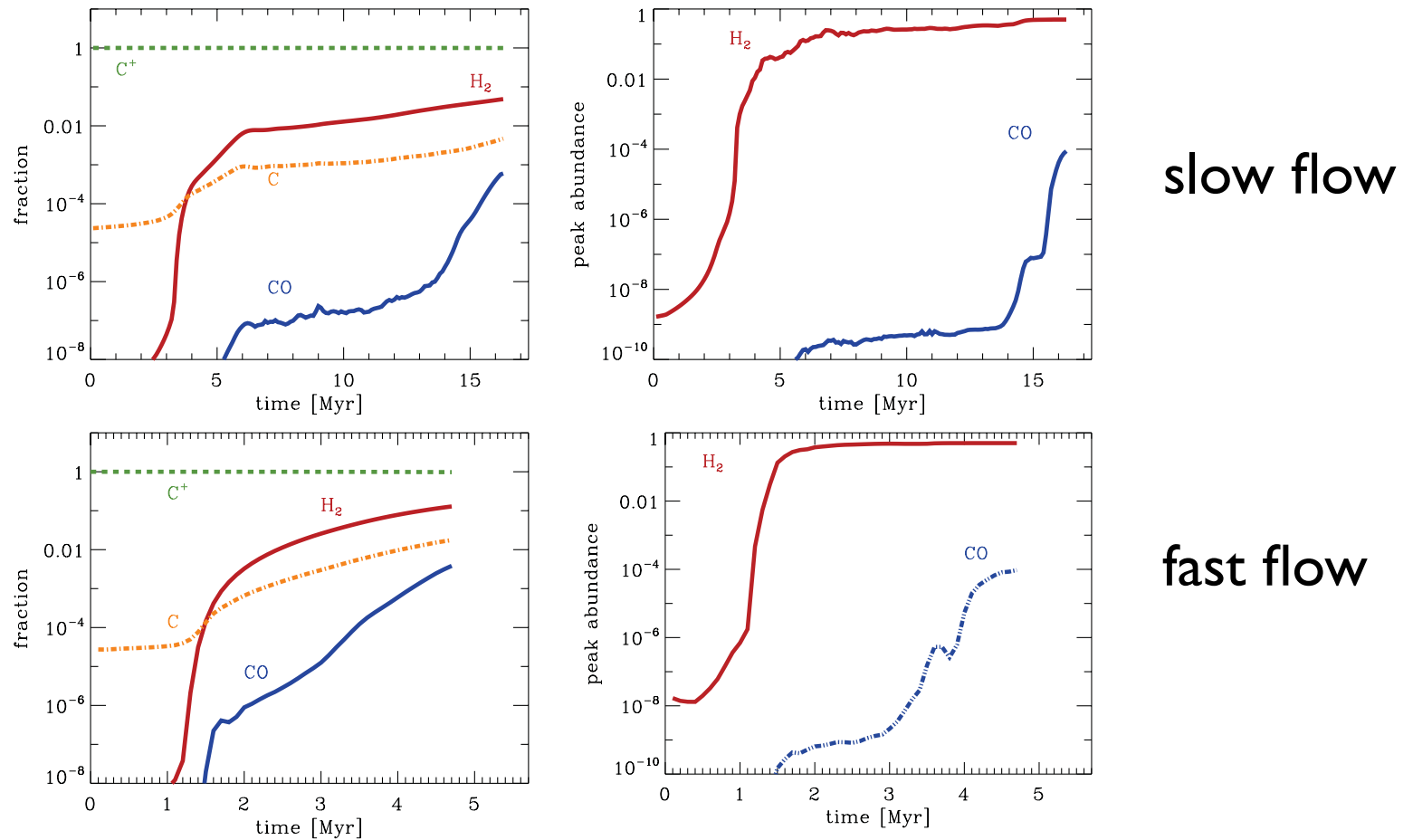


**Figure 5.** The gas temperature–density distribution in the flows at the onset of star formation.

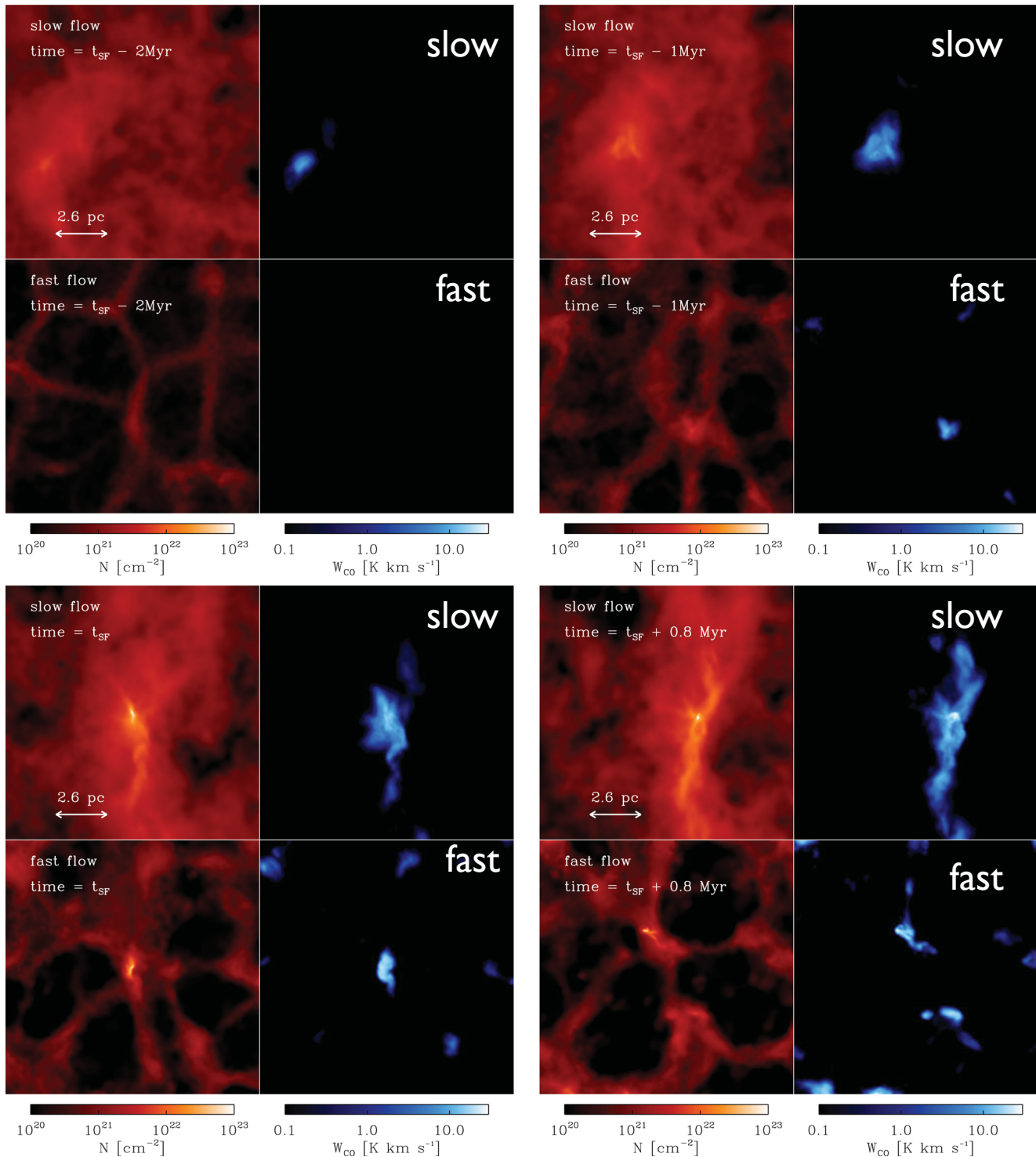
Clark et al. (2012, MNRAS, 424, 2599)

see also Pringle, Allen, Lubov (2001), Hosokawa & Inutsuka (2007)

# further evidence form detailed colliding flow calculations



**Figure 6.** Chemical evolution of the gas in the flow. In the left-hand column, we show the time evolution of the fraction of the total mass of hydrogen that is in the form of  $\text{H}_2$  (red solid line) for the  $6.8 \text{ km s}^{-1}$  flow (upper panel) and the  $13.6 \text{ km s}^{-1}$  flow (lower panel). We also show the time evolution of the fraction of the total mass of carbon that is in the form of  $\text{C}^+$  (green dashed line), C (orange dot-dashed line) and CO (blue double-dot-dashed line). In the right-hand column, we show the peak values of the fractional abundances of  $\text{H}_2$  and CO. These are computed relative to the total number of hydrogen nuclei, and so the maximum fractional abundances of  $\text{H}_2$  and CO are 0.5 and  $1.4 \times 10^{-4}$ , respectively. Again, we show results for the  $6.8 \text{ km s}^{-1}$  flow in the upper panel and the  $13.6 \text{ km s}^{-1}$  flow in the lower panel. Note that the scale of the horizontal axis differs between the upper and lower panels.



H<sub>2</sub> column

CO emission

fraction of CO dark gas will also change with metallicity and with ambient radiation field

summary



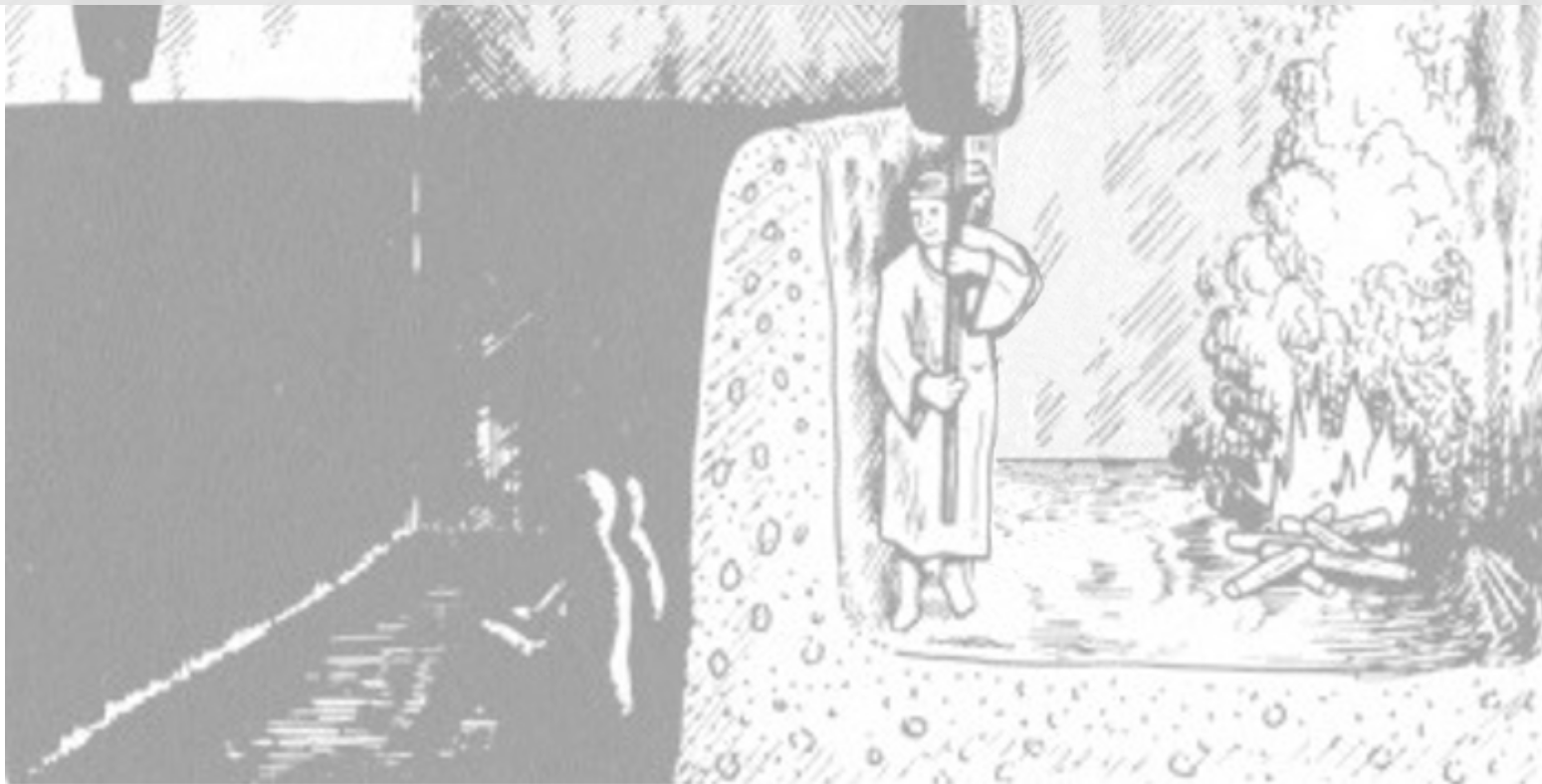
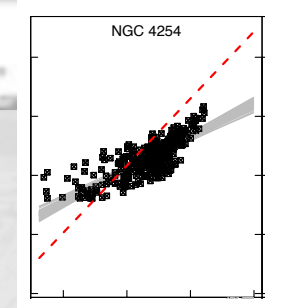
Star formation is intrinsically a multi-scale and multi-physics problem. Many different processes need to be considered simultaneously.



\* The Republic  
(514a-520a)

Star formation is intrinsically a multi-scale and multi-physics problem. Many different processes need to be considered simultaneously.

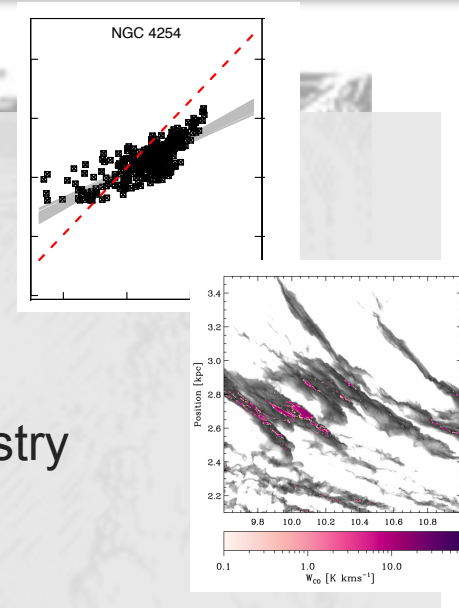
- hierarchical Bayesian statistics indicated galaxy to galaxy variations in the KS relation with typically sublinear slope  
→ *how much diffuse CO gas is there*



\* The Republic  
(514a-520a)

Star formation is intrinsically a multi-scale and multi-physics problem. Many different processes need to be considered simultaneously.

- hierarchical Bayesian statistics indicated galaxy to galaxy variations in the KS relation with typically sublinear slope  
→ *how much diffuse CO gas is there*
- detailed (M)HD calculations with time-dependent chemistry allow us to study the properties of CO-dark H<sub>2</sub> gas  
→ *im*

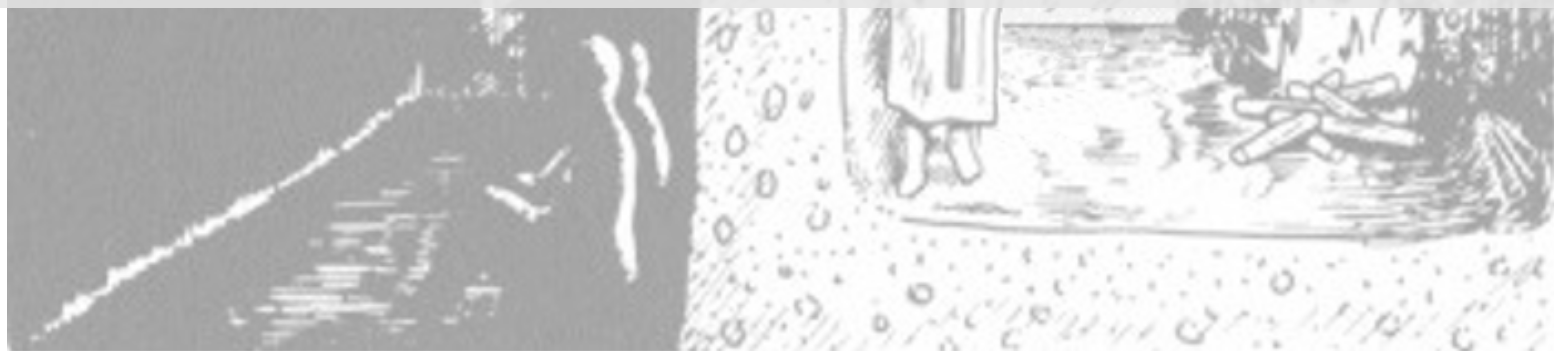
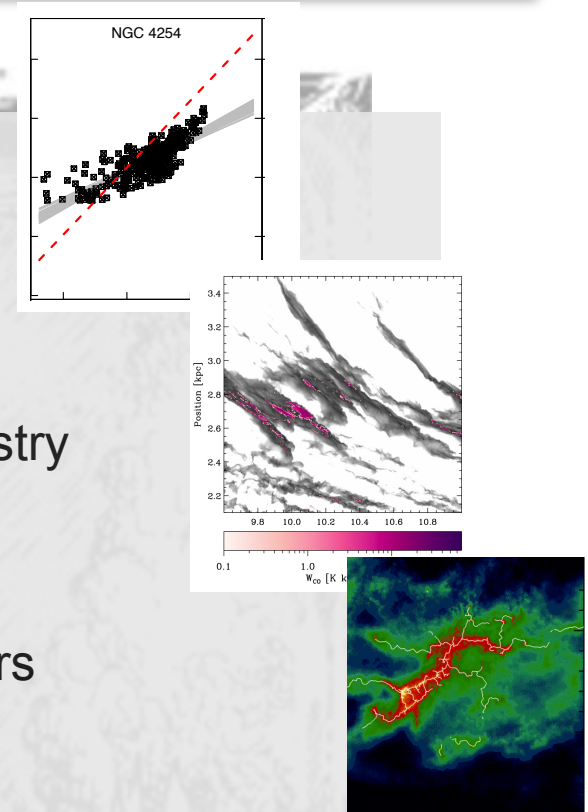


\* The Republic  
(514a-520a)



Star formation is intrinsically a multi-scale and multi-physics problem. Many different processes need to be considered simultaneously.

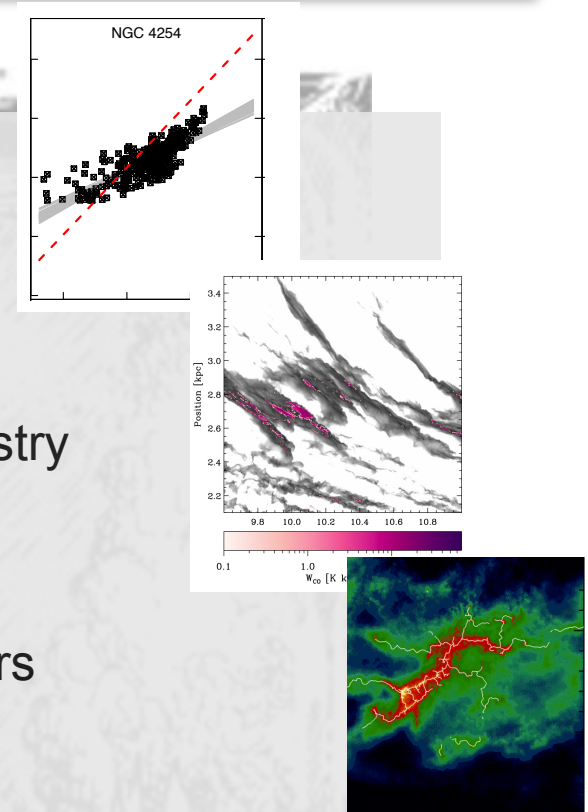
- hierarchical Bayesian statistics indicated galaxy to galaxy variations in the KS relation with typically sublinear slope  
→ *how much diffuse CO gas is there*
- detailed (M)HD calculations with time-dependent chemistry allow us to study the properties of CO-dark H<sub>2</sub> gas  
→ *implications for interpreting observational data?*
- molecular clouds are filamentary, but filament parameters (width, slope, central density) may vary significantly  
→ *what does it mean for star cluster formation?*





Star formation is intrinsically a multi-scale and multi-physics problem. Many different processes need to be considered simultaneously.

- hierarchical Bayesian statistics indicated galaxy to galaxy variations in the KS relation with typically sublinear slope  
→ *how much diffuse CO gas is there*
- detailed (M)HD calculations with time-dependent chemistry allow us to study the properties of CO-dark H<sub>2</sub> gas  
→ *implications for interpreting observational data?*
- molecular clouds are filamentary, but filament parameters (width, slope, central density) may vary significantly  
→ *what does it mean for star cluster formation?*
- next steps:  
***multi-physics simulations with Arepo and FLASH for comparison with existing survey data***



thanks